Master Thesis in Reservoir Physics

Low Salinity Waterflood in Combination with Surfactant/Polymer:
Effect of Brine Composition

Jon Endre Seljeset Mjøs

Centre for Integrated Petroleum Research

Department of Physics and Technology

University of Bergen

June 2014

Acknowledgement

The experimental work presented in this study has been carried out at the Centre of Integrated Petroleum Research (UNI Research CIPR) at the University of Bergen, during the period August 2013 to June 2014. I want to thank UNI Research CIPR for providing both research facilities and knowledge sharing from employees.

Additionally, I would like to express my gratitude towards my supervisor, Professor Arne Skauge, for his guidance and support during my work on this thesis.

Special thanks to my co-supervisors, Edin Alagic and Behruz Shaker Shiran. Their guidance during the experiments and throughout the writing process has been excellent.

Furthermore, I would like to thank Olav Eikrem and Adnan Al-Ajmi for the good discussions and teamwork exhibited during the experiments. The same gratitude goes to Håkon Færevåg. I would also like to thank all my fellow students for making my study an invaluable experience to me.

Finally, I would like to thank my family and friends for the support given, keeping up my spirit, motivating me. Special thanks to Ingvild Drønen for her support and positive presence throughout these years. Thank you!

Bergen, June 2014

Jon Endre Seljeset Mjøs

Abstract

The effect of low salinity water (LSW) on enhanced oil recovery has been known for decades. Although much research is done on the topic, a general agreement of the prevailing mechanism for the low salinity effect has still not emerged.

The present study compares the effect of LSW in secondary and tertiary mode in six Berea cores. Following tertiary mode LSW injection, low salinity surfactant polymer (LSSP) floods were conducted. In addition, measurements of density, pH, viscosity and interfacial tension was executed on the fluids used.

In secondary mode, aged and unaged cores were used for injection of synthetic seawater and diluted synthetic seawater (10%). The results show a higher production (1-12% OOIP) when injecting synthetic seawater compared to the diluted synthetic seawater (10%) in secondary mode. No fines or pH variation was observed during the floods.

In tertiary mode the cores were flooded with a sequence of brines with different composition (synthetic seawater without divalent ions, diluted synthetic seawater (10%) and 3000 ppm NaCl). Some enhanced production (5-9% ROIP) was observed when altering ion composition or reducing total salinity. The extra oil production was observed in some of the cores, but seems no to be reproduced in all parallel experiments. No fines or significant pH increase was observed during the floods.

Combining low salinity brine with surfactants and polymers yielded varying production, ranging from 11-32% ROIP. It was observed that the aged cores generally had a higher recovery compared to unaged cores.

Nomenclature

Variables

A	Area	[m^2]
A	Apparatus constant	[$K \cdot m^3/kg$]
AN	Acid Number	[mg KOH/g oil]
B	Atmospheric Pressure	[Pa]
BN	Base Number	[mg KOH/g oil]
a_0	Effective area per polar head group of surfactant	[m^2]
C, c	Concentration	[$kg \cdot m^{-3}$]
dp	Differential pressure	[mbar]
E	Electric potential	[mV]
E_A	Area sweep efficiency	dimensionless
E_D	Microscopic displacement efficiency	dimensionless
E_R	Recovery factor	dimensionless
E_V	Vertical sweep efficiency	dimensionless
E_{vol}	Volumetric displacement efficiency	dimensionless
F	Relative humidity	dimensionless
F	Faraday constant	[$96485\ C \cdot mol^{-1}$]
$I_{A\text{-}H}$	Amott-Harvey index	dimensionless
I_{USBM}	USBM index	dimensionless
h	Height	[m]
I	Ion Strength	[mol/L]
K	Absolute permeability	[m^2] (1 D = $0.98692 \cdot 10^{-12}$ m^2)
$k_{e,i}$	Effective permeability of phase *i*	[m^2] (1-D = $0.98692 \cdot 10^{-12}$ m^2)
$k_{end,i}$	End point permeability of phase *I*	[m^2] (1-D = $0.98692 \cdot 10^{-12}$ m^2)
k_{ri}	Relative permeability of phase *i*	dimensionless
L	Length	[m]
l	Effective length of HC chain	[m]
M	Mobility ratio	dimensionless
M^0	End point mobility ratio	dimensionless
m	mass	[kg]
N	Total reserves originally in place	[m^3]

N_s	Surfactant parameter	dimensionless
N_p	Produced reserves	[m^3]
N_vc	Capillary number	dimensionless
P	Pressure	[Pa] (1 mmHg = 133.322 Pa)
PV	Pore volume	dimensionless
Q	Flow rate	[$\mathrm{m}^3 \cdot \mathrm{s}^{-1}$]
R	Molar gas constant	[$8.314\ \mathrm{J} \cdot \mathrm{mol}^{-1} \cdot \mathrm{K}^{-1}$]
R, r	Radius	[m]
R_{RF}	Residual resistance factor	dimensionless
S	Saturation	dimensionless
S	Spreading coefficient	dimensionless
T	Temperature	[K] (0°C = 273.13 K)
T	Period	[s^{-1}]
t	Time	[s]
u	Darcy velocity	[$\mathrm{m} \cdot \mathrm{s}^{-1}$]
V	Volume	[m^3]
WC	Water cut	dimensionless
Δ	Difference	dimensionless
γ	Shear rate	[s^{-1}]
η	Viscosity (depended on shear rate)	[Pa·s] (1 Pa·s = 10^3 Cp)
θ	Contact angle	[°]
λ	Mobility	[$\mathrm{m}^2/\mathrm{Pa} \cdot \mathrm{s}$]
λ^0	End point mobility	[$\mathrm{m}^2/\mathrm{Pa} \cdot \mathrm{s}$]
μ	Viscosity	[Pa·s] (1 Pa·s = 10^3 Cp)
ρ	Density	[$\mathrm{kg} \cdot \mathrm{m}^{-3}$]
σ	Interfacial tension	[$\mathrm{N} \cdot \mathrm{m}^2$]
τ	Shear stress	[Pa]
ϕ	Porosity	dimensionless
v	Volume of hydrophobic chain	[m^3]
ω	Angular velocity	[rpm] [s^{-1}]

Subscripts

A	area
abs	absolute
b	bulk
c	capillary
c	core channel
D	microscopic
diff	differential
eff	effective
g	gas
i	component (phase)
i	initial
i	irreducible
ineff	ineffective
inj	injected
max	maximum
o	oil
pol	polymer
p	pore
p	produced
r	relative
r	residual
R	recovery
tot	total
V	vertical
vol	volumetric
w	water

Abbreviations

CDC	Capillary desaturation curve
CMC	Critical micelle concentration
COBR	Crude oil/brine/rock system
Ca^{2+}	Calcium ion
CIPR	Centre for Integrated Petroleum Research
CP	Cone & plate
DG	Double gap
DLVO	Deryaguin, Landau, Verwey and Overbeek
EOR	Enhanced oil recovery
FW	Fractionally wet
IOR	Improved oil recovery
IFT	Interfacial tension
HC	Hydrocarbon
HPAM	Hydrolyzed polyacrylamide
LSW	Low salinity water
LSSP	Low salinity surfactant polymer
MIE	Multicomponent ionic exchange
Mg^{2+}	Magnesium ion
MWL	Mixed wet large
MWS	Mixed wet small
NSO	Nitrogen, sulfur, oxygen
OOIP	Original Oil in Place
ppm	Parts per million
ROIP	Residual oil in place
RPM	Revolutions per minute
SARA	Saturates, aromatics, resins and asphaltenes analysis
SCAL	Special Core Analysis
SSW	Synthetic seawater
SW1	Synthetic seawater
SW2	Synthetic seawater without divalent ions
TDS	Total dissolved solids
WBT	Water breakthrough

Table of Contents

List of Figures

List of Tables

1 Introduction

The most applied method for oil recovery is injecting water into the reservoir for pressure support and sweep. The connate water in the reservoir has usually a different composition than the injected water. In later years, it has been found that the composition of the injection water is of importance for the total oil recovery. This has resulted in an increase in papers produced on the effect of low salinity brine on recovery, as observed in Figure 1.1.

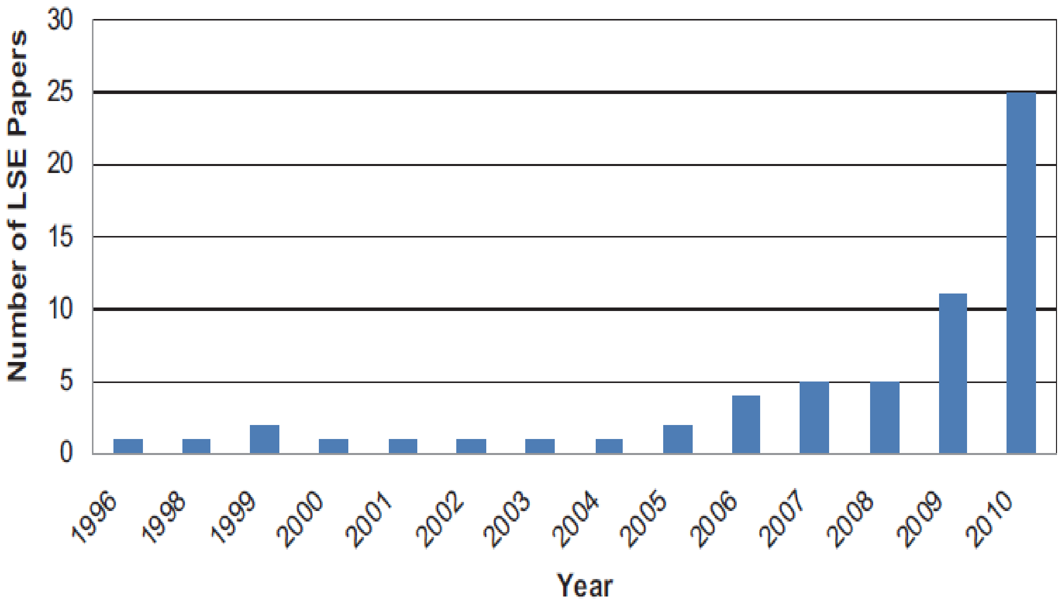

Figure 1.1: Publications regarding LSW submitted per year [1]

Conventional waterflood brines are seawater and/or aquifer water. The salinity of these fluids are high, ranging from 35 000 ppm to 300 000 ppm, respectively. By reducing salinity to under 6000 ppm, the brine is regarded as low salinity water (LSW) [2]. In studies on LSW, salinity usually ranges between 500 to 5000 ppm. Evidence of the low salinity effect (LSE) and its influence on recovery is discussed further in Chapter 3.

The benefit of combining the low salinity environment created with LSW with chemical additives such as surfactants and polymers is seen as an extension of the potential of LSW. The effectiveness of many chemical additives is dependent on the brine concentration, and are found to be more stable at low salt concentrations. In addition, surfactants that yield low interfacial tension (IFT) at low salinity are more readily available and less expensive compared to those which are constructed to endure high salinity conditions. The combination of LSW with surfactant and polymers is discussed in Chapter 3.2 and 3.3.

The present study compares the effect of low salinity brine in secondary and tertiary mode in six Berea cores. Following tertiary mode LSW injection, low salinity surfactant polymer (LSSP) floods were conducted. All experiments were executed under ambient temperatures. In addition, analysis of the fluids utilized in the experiments were carried out to give a greater insight to the experiments.

This thesis consists of seven chapters, the first one addressing basic fundamental principles in reservoir engineering. These concepts are important to understand as the terms will be applied in the following chapters. In the next chapter, emphasis is put on enhanced oil recovery including a literature study of the EOR mechanisms relevant for this thesis. This includes a summary of research done on the low salinity effect, its effect on field scale and the proposed mechanisms for the increased recovery by LSW. In addition, research combining the low salinity effect with surfactant and polymers is also included.

Chapter 4 discusses the experimental procedures and experimental setup used during the experimental work in this thesis. Result and discussion is found in Chapter 5, starting with basic fluid and rock properties followed up by waterflood experimental data. Conclusion and suggestions for further work are given in Chapter 6 and Chapter 7, respectively. All data gathered during the experiments are summarized in the appendices at the end of the thesis.

2 Fundamental Principles in Reservoir Physics

2.1 Porosity

Porosity is the void part of a rock`s total volume, unoccupied by rock grains and mineral cement [3]. Depending on the time of formation, the porosity can be divided into primary and secondary porosity. Primary porosity is created during deposition, and is dependent on the rock type, grain size, grain shape, sorting and packing. Secondary porosity is post-depositional alterations to the porosity, resulting from chemical reactions, like cementation, or fracturing of the formation.

The absolute porosity is expressed as the ratio between the total void volume and bulk volume.

$$\emptyset = \frac{V_{p_a}}{V_b} \tag{2.1}$$

Where Φ is porosity, V_{pa} is the absolute pore volume and V_b is the bulk volume. Depending on the pores interconnectivity, the absolute porosity is divided into effective and ineffective porosity.

$$\emptyset_{abs} = \emptyset_{eff} + \emptyset_{ineff} \tag{2.2}$$

Where φ_{abs} is the absolute porosity, φ_{eff} is the effective porosity and φ_{ineff} is the ineffective porosity.

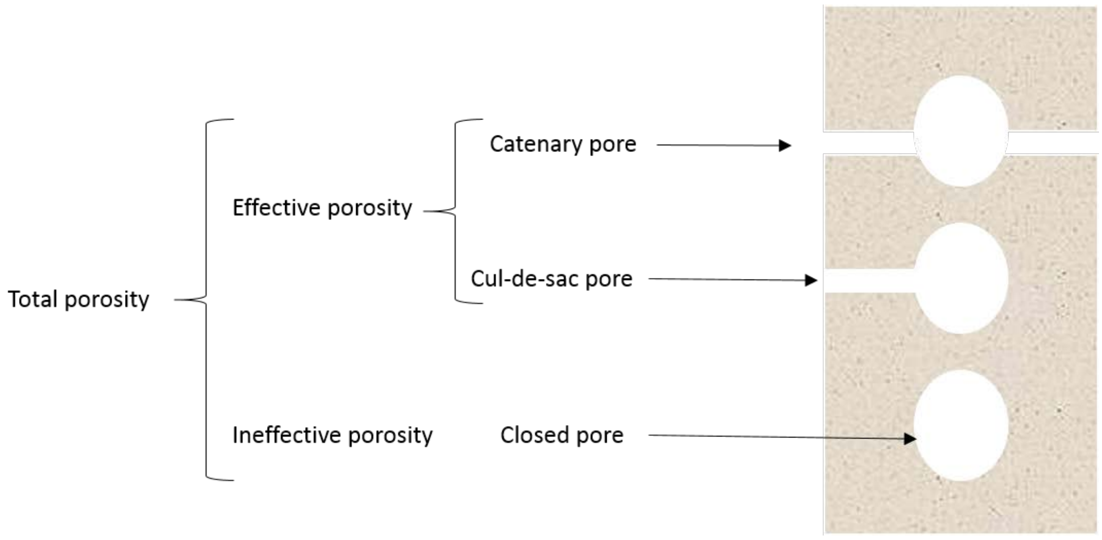

Figure 2.1: Three basic types of pores

Pores with no connectivity to other pores are part of the ineffective porosity. These pores have no capacity for fluid flow. Pores that constitute in the effective porosity are catenary and cul-de-sac pores (Figure 2.1), hence pores which fluid can flow in.

$$\emptyset_{eff} = \frac{V_{p,eff}}{V_b} \tag{2.3}$$

Where $V_{p,eff}$ is the effective pore volume and V_b is the bulk volume of the rock sample. The effective porosity depends on several factors, such as rock type, grain size, packing and orientation, cementation, weathering, leaching and type, content and hydration of clay minerals [3].

2.2 Permeability

Permeability is an expression for a porous medium´s capability to transmit fluids through its network of interconnected pores. Permeability is affected by many factors, among them porosity, tortuosity, grain size, grain shape and packing. Permeability is expressed by Darcy´s law [3]

$$u = \frac{Q}{A} = -\frac{K}{\mu} * \frac{dP}{L} \tag{2.4}$$

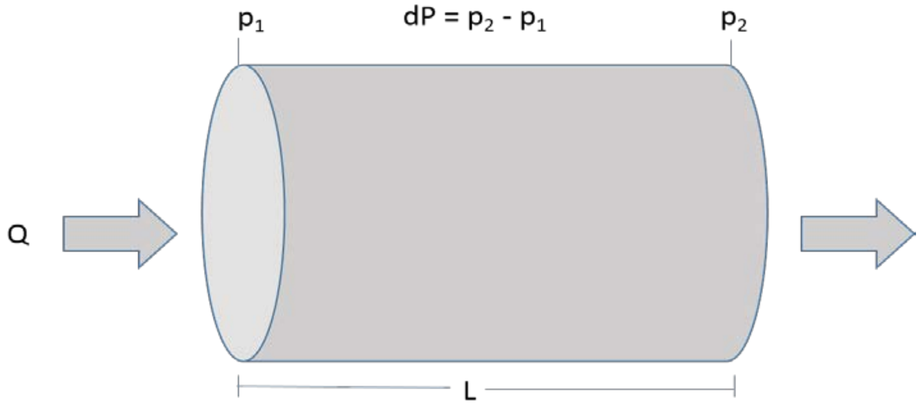

Figure 2.2: Fluid flow in porous media

Where u is the Darcy velocity, Q is the fluid flow rate, A is the cross-sectional area, k is the absolute permeability, μ is the fluids viscosity and $\frac{dp}{L}$ is the pressure gradient. This is illustrated in Figure 2.2. For Darcy´s law (2.4) to be valid, the following basic conditions has to be satisfied:

- 100% saturated with only one fluid
- Incompressible fluid
- Laminar and stationary fluid flow
- No chemical reaction between the fluid and rock
- Horizontal position of fluid flow (eliminating the force of gravity)

Permeability is regarded as a rock property if the rock is 100% saturated with one fluid. This is the absolute permeability, as expressed in equation (2.4), and is independent of fluid type. Permeability has the SI-dimension m^2, but is normally expressed in Darcy (1 Darcy=10^{-12} m^2).

If multiple fluids are flowing through the pores, the effective permeability of each fluid will depend upon their relative saturations. The fluids will hinder flow for each other, and the effective permeability is reduced compared to the absolute permeability. Hence, Darcy´s law in equation (2.4) needs to take each phase into account.

$$u_i = \frac{Q_i}{A} = -\frac{K_i}{\mu_i} * \frac{dP}{L} \tag{2.5}$$

Where *i* denotes the fluid phase. The relationship between absolute and effective permeability is given by the relative permeability. It expresses the ratio between the effective and absolute permeability.

$$k_{r,i} = -\frac{k_{e,i}}{K} \tag{2.6}$$

Relative permeability is a function of wettability, pore geometry, fluid distribution, saturation and saturation history [4].

2.3 Saturation

In a porous medium multiple fluids can be present at the same time. In a reservoir or core plug these are often oil, water and gas.

$$V_p = V_w + V_o + V_g \tag{2.7}$$

The saturation of a fluid is the fraction of fluid volume to the pore volume.

$$S_i = \frac{V_i}{V_p} \tag{2.8}$$

Where S_i is the saturation of fluid *i*, V_i is the volume of fluid *i* and V_p is the pore volume.

2.4 Residual Oil Saturation

When crude oil is displaced by water or gas, some of the oil will remain due to capillary trapping, caused by the tension between non miscible phases. The residual saturation is denoted S_{or}. There are several models which describe the residual oil saturation after water injection, but the following two models are the most acknowledged.

The pore doublet model

The pore doublet model takes into account a pore channel that splits into two channels. If one of the channels is narrower, then the wetting fluid will intrude this channel quicker due to capillary differences. This will lead to trapping of oil in the broad channel, as seen in Figure 2.3.

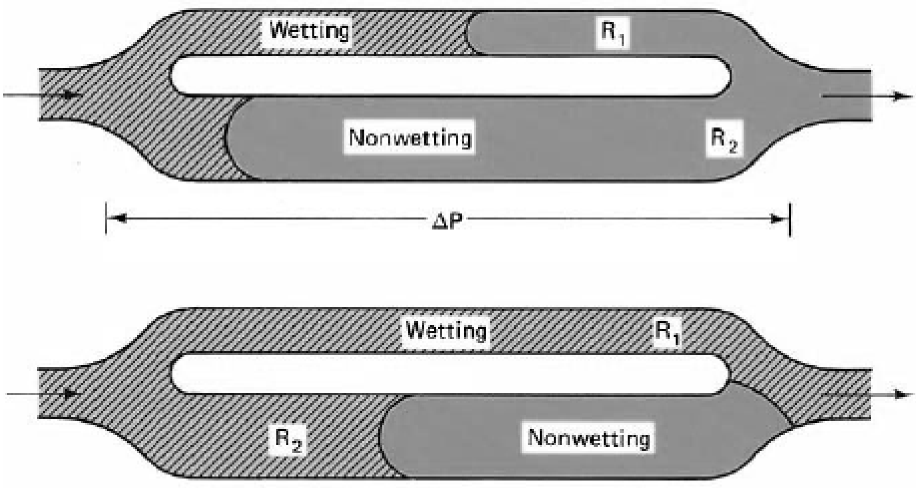

Figure 2.3 Trapping in a pore doublet model [5]

Snap-off model

In the snap-off model, oil is trapped due to the surface tension between oil and water. As the displacing water film increases in the pore, the oil film gradually becomes thinner, before it eventually snaps off and resides in the middle of the pore. When the oil is no longer continuous, it is trapped by capillary forces and is immobile.

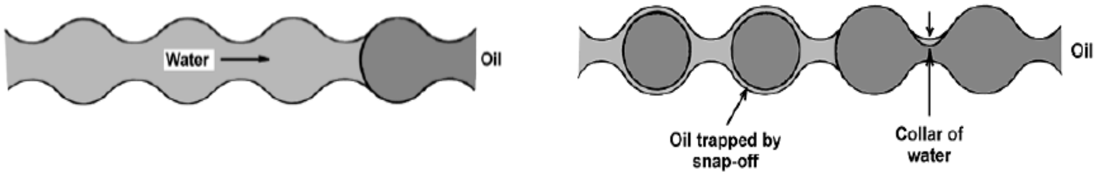

Figure 2.4: Trapping of oil by snap-off [5]

2.5 Fluid & Fluid Flow Properties

2.5.1 Ionic Strength

The ionic strength, I, of a solution is defined as

$$I = \frac{1}{2}\sum_{i=1}^{n}(c_i \cdot z_i^2) \qquad (2.9)$$

Where c_i is the concentration of the ion in solution, z_i is the charge of the ion and n is the sum of ionic species present in the solution.

2.5.2 pH

The pH is a measure of the acidity or basicity of an aqueous solution. It is defined as the negative logarithm of the concentration of the solvated hydrogen ion

$$pH = -log_{10}[H^+] \qquad (2.10)$$

The pH is non-negative, ranging from 1 to 14. The solution is regarded acidic if the solution has a pH less than 7, and basic or alkaline for pH greater than 7.

2.5.3 Density

The density, ρ, is defined as a substance´s mass per unit volume

$$\rho = \frac{m}{V} \qquad (2.11)$$

Where m is the mass of the substance, and V denotes the volume. In most cases, the density decreases with increased temperature [6].

2.5.4 Viscosity

Viscosity is a fluid`s internal resistance to flow. At low viscosity the fluid flows easy, whereas flow is reduced at higher viscosity. The dynamic shear viscosity is expressed as

$$\mu = \frac{\tau}{\dot{\gamma}} \qquad (2.12)$$

Where μ denotes viscosity, τ is the shear stress and $\dot{\gamma}$ is shear rate. The shear stress is defined as a tangential force acting upon an upper area plane, whilst the lower plane is at rest. If the material between the two planes starts to flow, a velocity gradient through the material will develop. This gradient is the shear rate [3]. This is illustrated in Figure 2.5.

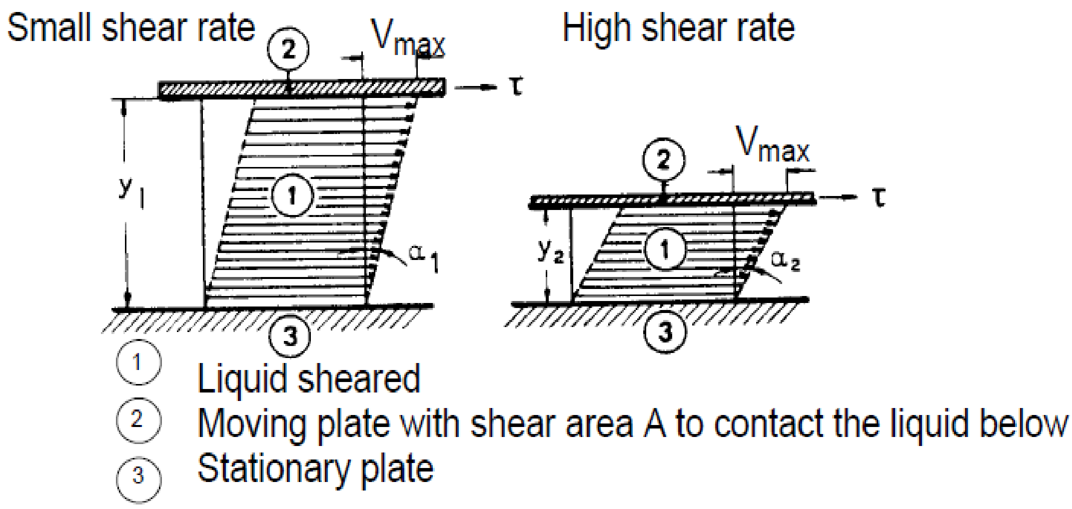

Figure 2.5: Flow between two parallell plates [7]

Depending on the viscosity behavior, fluids may be divided into Newtonian fluids and non-Newtonian fluids. In Newtonian fluids the viscosity is constant, independent of the shear stress rate, while non-Newtonian fluids are shear dependent. In ordinary conditions gases, water and many common liquids are regarded as Newtonian. Examples of non-Newtonian fluids are colloidal systems and polymer solutions.

2.5.5 Mobility

The mobility (λ) of a fluid is a defined as its relative permeability divided by its viscosity.

$$\lambda_i = \frac{k_{ri}}{\mu_i} \tag{2.13}$$

Where *i* denotes the fluid phase; oil, water or gas. Mobility ratio is defined as the mobility of the displacing phase divided by the mobility of the displaced phase, and is given for a waterflood as

$$M_{wo} = \frac{\lambda_{rw}}{\lambda_{ro}} = \frac{k_{rw}}{k_{ro}}\frac{\mu_o}{\mu_w} \tag{2.14}$$

To calculate the stability of a waterflood the endpoint mobility ratio is used and is denoted M°_{wo} , where ° indicates that the measurements are done at the endpoints S_{or} and S_{iw}. This parameter has a significant influence on the production behavior.

$$M^\circ_{wo} = \frac{\lambda_{rw}}{\lambda_{ro}} = \frac{k^\circ_{rw}}{k^\circ_{ro}}\frac{\mu_o}{\mu_w} \tag{2.15}$$

The endpoint mobility ratio assumes a plug-like displacement between the oil phase, at connate-water saturation before the flood front, and the water phase at residual oil saturation behind the front [8].

As illustrated in Figure 2.6 high mobility ratios (>1) are unfavorable as it yields early water breakthrough and a long tail production. The viscosity of the oil is much higher than the displacing water, thus the water will travel faster towards the production well.

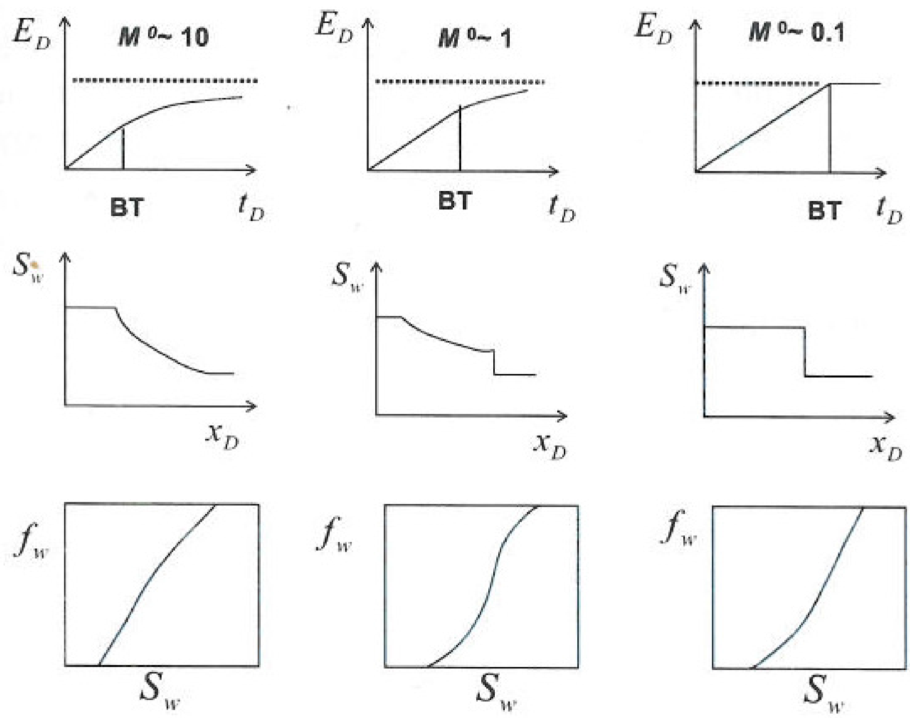

Figure 2.6: Effect of Mobility ratio on displacement efficiency [5]

Low mobility ratios (≤1) are optimal, meaning that the viscosity of the displacing water is higher than for the oil. This implies that the oil phase can move quicker through the reservoir rock as opposed to the displacing water phase. The water breakthrough will appear late in production and a small tail production occurs.

Despite ultralow M° values, the limit for production is the residual oil saturation, and the ultimate microscopic displacement efficiency is therefore defined as

$$E_D^{Max} = 1 - \frac{S_{orw}}{S_{oi}} \tag{2.16}$$

2.6 Capillary Pressure

Capillary pressure is the internal pressure difference over the interface of two immiscible fluids, the wetting fluid and the non-wetting fluid. The pressure difference is a consequence of electrostatic forces acting between the fluids. Capillary pressure is expressed by the Laplace-equation [3]

$$P_{c,ow} = P_{non-wetting} - P_{wetting} = p_o - p_w = \sigma_{ow}(\frac{1}{R_1} - \frac{1}{R_2}) \qquad (2.17)$$

For flow in a tube or a capillary, the Young-Laplace equation [3] is derived

$$P_c = p_o - p_w = \frac{2\sigma_{ow} cos\theta}{r} \qquad (2.18)$$

The Young-Laplace equation suggests that capillary pressure is a function of chemical composition of the fluid and rock, pore size distribution and the saturation of fluids. Although not specified in the equation (2.18), capillary pressure is also a function of saturation history due to hysteresis.

2.7 Drainage/Imbibition

The capillary pressure is important when observing pore filling. As observed in the Young Laplace equation (2.18), small pore radii results in high capillary pressure. In the opposite case, bigger pore radii gives low capillary pressure. This is decisive in pore filling sequences.

Imbibition refers to flow that leads to an increase in wetting phase saturation. During imbibition of a water-wet system, due to capillary pressure, the small pores will fill first. This is observed in the Young Laplace equation (2.18), where small pores needs the least pressure in the wetting phase to imbibe. Subsequent flooding will fill pores with increasing radii as the pressure in the wetting phase increases.

The process of decreasing the wetting phase saturation is referred to as a drainage process. For drainage processes, the non-wetting phase will fill the big pores first, and then pores with decreasing radii.

2.8 Capillary Number and CDC

The capillary number (N_{vc}) is a dimensionless number, expressing the ratio between the viscous forces and the capillary forces. There are many ways of defining the capillary number, and by Darcy`s law it can be expressed as

$$N_{vc} = \frac{u_w * \mu_w}{\sigma_{o/w}} \qquad (2.19)$$

Where u_w is the Darcy velocity of water, μ_w is the viscosity of water and $\sigma_{o/w}$ is the oil water interfacial tension.

Laboratory experiments have shown correlation between the capillary number and the residual oil saturation [9, 10]. Increasing the viscous force or reducing the capillary forces leads to mobilization of oil, resulting in a decrease in residual oil saturation. This relationship is represented by a capillary desaturation curve (CDC), illustrated in Figure 2.7.

From Figure 2.7, it is observed that normal waterfloods are usually in the range of low N_{vc}. As the magnitude of the capillary number increases a knee in the curve is observed, denoted the critical capillary number. Above this value the residual oil saturation starts decreasing. It is noteworthy that the critical capillary number is higher for the wetting phase opposed to the non-wetting phase.

The CDC is influenced by the wettability preference and pore size distribution (PSD) of the porous medium. The knee in the curve in Figure 2.7. will be less pronounced if the PSD is wide [3].

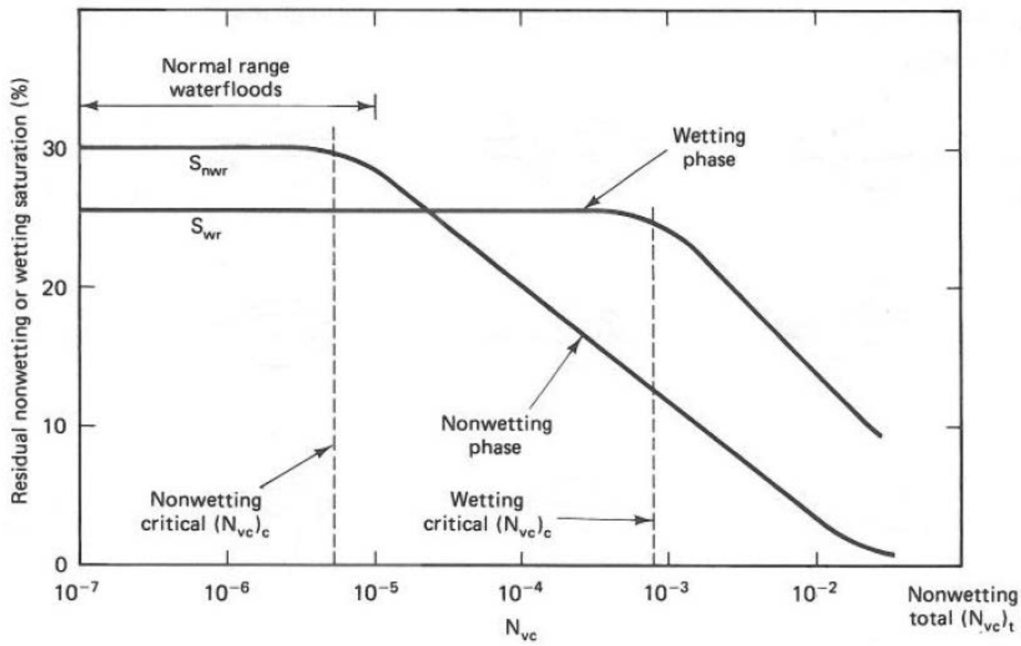

Figure 2.7: CDC wetting and non-wetting phase [11]

To achieve a reduction in residual oil saturation the parameters in equation (2.18) must be altered to increase the capillary number. This may be done by increasing the velocity of the water, increasing the viscosity of the water or decreasing the IFT between oil and water.

In a field perspective, increasing the Darcy velocity of water is not practical. This is due to capacity and pressure limitations in the injection equipment. Adding polymers may be an alternative, but reduction in injectivity limits the range.

The most convenient way of increasing the capillary number is by adding surfactants to the injection water. By lowering the interfacial tension between the oil and water, a significant increase in capillary number may occur, reducing the residual oil.

2.9 Wettability

Wettability of a solid can be defined as the tendency of one fluid to spread on, or adhere to, the solid surface in the presence of another immiscible fluid. Which fluid that will spread is determined by the spreading coefficient. The fluid with non-negative spreading coefficient will be the wetting phase, and spreads spontaneously at the surface. This is the fluid with the strongest adhesion to the solid. The driving force for spreading of fluid B at the A-C interface is given as

$$S_{B/A} = \sigma_{A/C} - \sigma_{A/B} - \sigma_{B/C} \tag{2.20}$$

Where $S_{B/A}$ is the spreading coefficient for fluid B spreading on A and σ is the interfacial tension between phases A, B and C. Wettability is often expressed by the contact angle (θ) between liquid-liquid or the liquid-gas interface and the solid surface. For a oil-water system the Young-Dupré equation is expressed as:

$$Cos\ \theta = \frac{\sigma_{o/s} - \sigma_{w/s}}{\sigma_{o/w}} \tag{2.21}$$

Where θ denotes the contact angle between the two immiscible fluids, and σ denotes the interfacial tension between the phases. The geometrical explanation is illustrated in Figure 2.8. The contact angle is always measured through the denser phase. The relationship between wetting angle and wettability is given in Table 2.1.

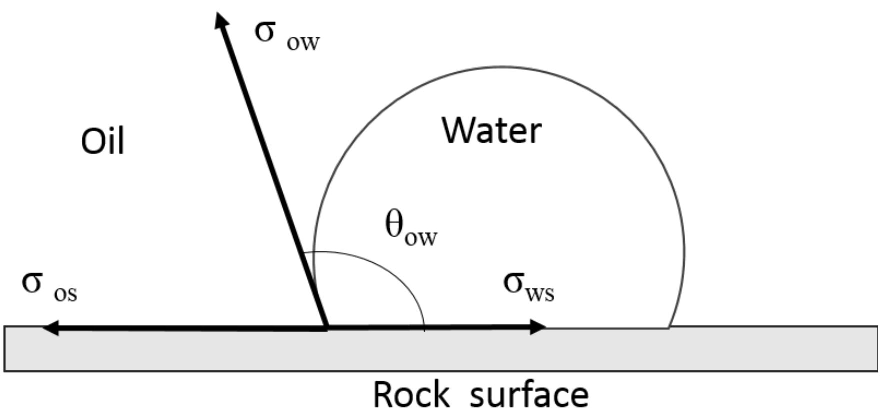

Figure 2.8: Oil/water/rock system at thermodynamic equilibrium state

Table 2.1: Wettability and contact angles [3]

Contact Angle (°)	Wettability preference
0-30	Strongly water-wet
30-90	Preferentially water-wet
90	Neutral Wettability
90-150	Preferentially oil-wet
150-180	Strongly oil-wet

Besides expressing the wettability by the contact angle, it is also common to use both the Amott-Harvey Index ($I_{A\text{-}H}$) and the US Bureau of Mines Index (I_{USBM}).

The Amott-Harvey Index is an empirical method based on studying spontaneous and forced imbibition processes. From special core analysis (SCAL) it is possible to obtain a curve representing capillary pressure as a function of water saturation. Based on this curve, a value ranging from -1 for strongly oil wet to +1 for strongly water-wet is given.

$$I_{A-H} = \frac{Spontaneus\ Water\ imb.}{Total\ Water\ imb} - \frac{Spontaneus\ Oil\ imb.}{Total\ Oil\ imb.} \qquad (2.22)$$

The USBM method is based on the same capillary curve as the Amott-Harvey method. It is a measure of the work required imbibe the fluids.

$$I_{USBM} = log\frac{A_1}{A_2} \qquad (2.23)$$

If $A_1 > A_2$ the wettability is defined as water wet. For the opposite case, the wettability is defined as oil-wet.

Skauge et al. [12] proposed that the intermediate wettability could be subdivided into three different sub-classes; mixed-wet-large (MWL), mixed-wet-small (MWS) and fractionally-wet (FW). Skauge et al. [12] proposed that different pore shapes can develop different wetting conditions. The existence of these wetting-classes was proved through experiments.

In a MWL system, the large pores tend to be oil-wet, while the small pores are water-wet. The water-wet pores have probably not been in contact with oil, and have not developed an affinity for it. In MWS systems, the small pores are oil wet, and the bigger pores are water-wet. For FW systems there are no correspondence between pore size and wettability, the oil films are found as spots that have adhered to the surface. This is illustrated in Figure 2.9.

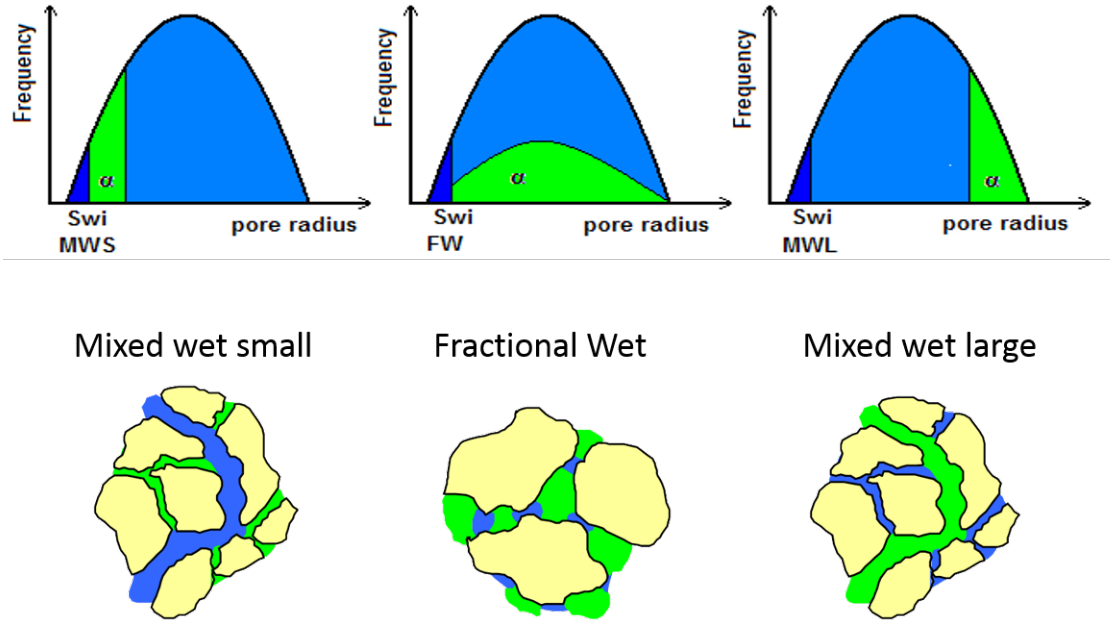

Figure 2.9: Illustration of the intermediate sub-classes, α is the fraction of oil-wet pores [12].

2.9.1 Effect of Wettability on Waterfloods and S_{or}

Wettability has long been known to affect waterflood behavior and recovery performance [13]. Generally, experimental data have shown that strongly water-wet cores exhibit higher recoveries than strongly oil-wet cores during waterflooding [14]. Wettability affects waterflood behavior by controlling the flow and spatial distribution of fluids in a porous medium [14].

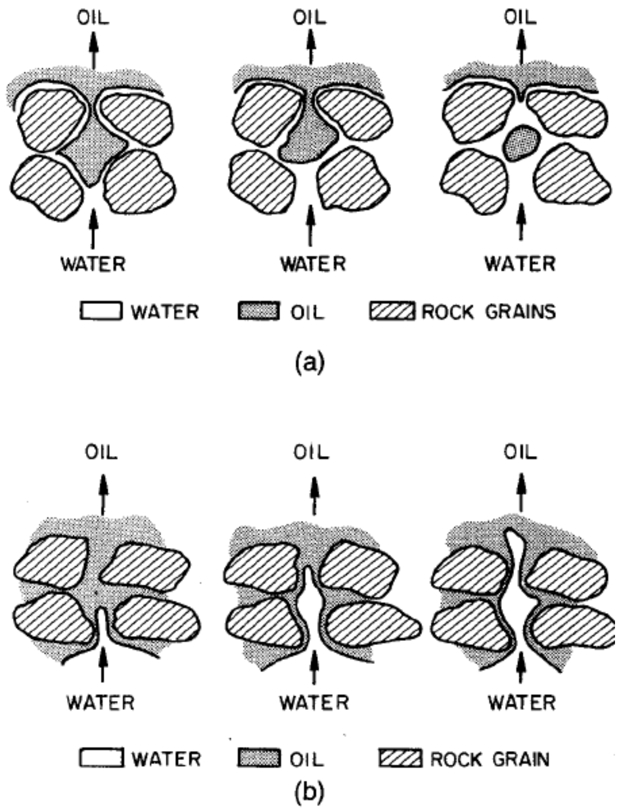

Figure 2.10: Water displacing oil from a pore during a waterflood: a) Strongly Water-wet b) Strongly Oil-wet [15]

During a waterflood in a strongly water-wet system, the water is imbibed into the smaller pores and oil is displaced into the larger pores. The displacement is such that the water phase maintains a fairly uniform front, resulting in a large fraction of the OOIP recovered before water breakthrough. After breakthrough, none or little oil is recovered and the water-oil ratio (WOR) increases rapidly [14, 16]. The remaining oil is capillary trapped as globules in the center of the core, as seen in Figure 2.10.

In oil-wet cores, the water breakthrough appears early and most of the oil is recovered in the tail production. This is primarily due to fingering and channeling of water through the big pores, leaving oil in the small pores and creavices. Figure 2.10 illustrates how the water invades the center of the pores, recovering oil by reducing the thickness of the oil film. Waterflooding in oil-wet systems are less efficient compared to water-wet, as less water imbibe spontaneously. The residual oil in oil-wet systems are typically found as continuous films over the pore surface, in pore throats or/and in big pockets of oil trapped by surrounding water [16].

In the transition between the two boundary conditions, strongly water-wet and strongly oil-wet, the trend observed is an earlier breakthrough and longer tail production. This is due to the facts that the system shifts towards more oil-wet conditions.

Skauge & Ottesen [17] summarized water flooding experiments from 350 North Sea reservoir cores. Their studies showed a minimum residual oil saturation for intermediate wetting systems, as displayed in Figure 2.11.

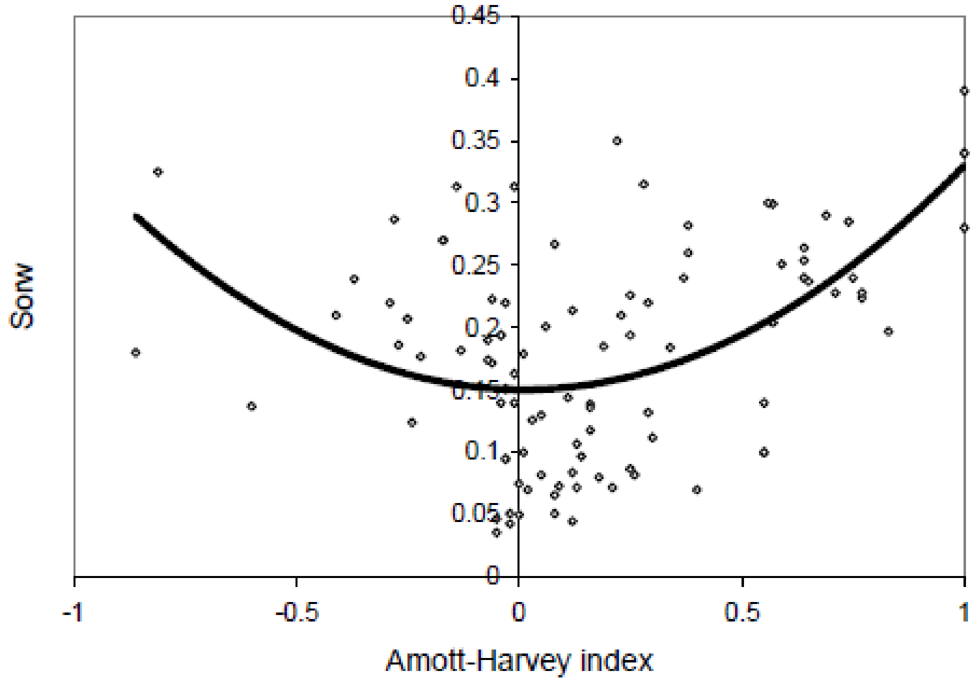

Figure 2.11: Residual Oil Saturation measuments for 30 North Sea reservoirs [17]

2.9.2 Effect of Wettability on Relative Permeability

The wettability state of the rock is a parameter that strongly determines the value of the relative permeability. Wettability affects relative permeability since it is a major factor in the control of flow, location and distribution of fluids in a porous medium. As the rock has an affinity for the wetting phase, adhesion will reduce the permeability of the wetting phase.

As mentioned, wettability effects the saturation distribution in the pore. For strongly water-wet cases, at S_{or}, the water will adhere to the pore walls letting the water flow in the water film. In the center of the pore, capillary trapped residual oil exists as globules acting as an obstacle for free water flow through the pores. Thus, the water relative permeability is reduced compared to the absolute water permeability.

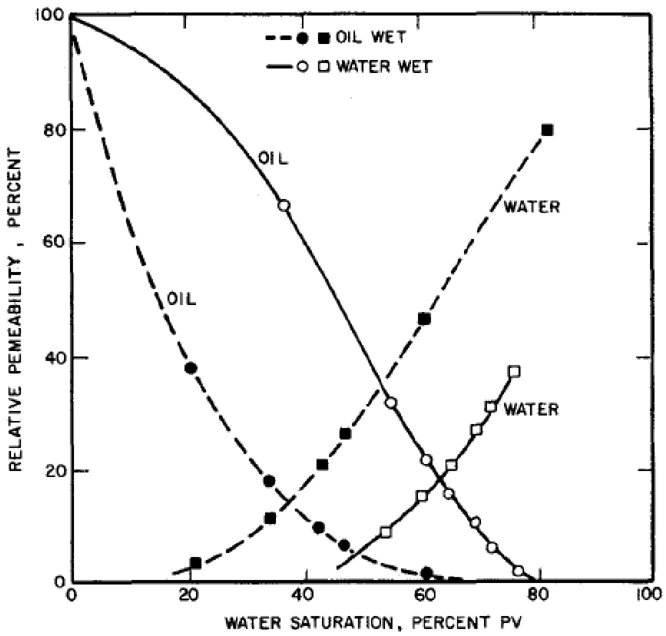

Figure 2.12: Steady State oil/water relative permeabilities [4]

In an oil-wet system, the distribution will be reversed as to the water-wet case, with water located in the center of the core and with oil adhering to the rock as seen in Figure 2.10. Naturally, the ease of flow will be higher for water in an oil-wet case compared to a water-wet case, as observed in Figure 2.11.

In order to predict wettability from relative permeability curves, Craig [18] proposed the following rule of thumb

Table 2.2: Wettability prediction, rule of thumb

	Water-wet	Oil-wet
S_{iw}	> 0.2 - 0.25	< 0.15
$S_{w,\ intersection}$	> 0.5	< 0.5
$K_{rw,or}$	< 0.3	> 0.5

The $S_{w,\ intersection}$ is the saturation at which oil and water permeabilites are equal (crossover saturation).

2.10 Wettability Alteration

Historically, all petroleum reservoirs were believed to be water-wet. This was based on the experience that all clean sedimentary rocks were water-wet and the fact that sedimentary rocks were deposited in aqueous environments. Later studies have shown that the wettability in reservoir rocks ranges from strongly water-wet to oil-wet state [12, 19-22].

Originally, all reservoir rocks are water-wet, but as migration of oil into the reservoir occurs the wettability of the rock may shift toward a more oil-wet state. As observed earlier, the degree of wettability alteration may be important prior to field implementation as production behavior may differ greatly depending on the wettability of the reservoir.

The degree of wettability alteration is dependent on multiple factors, such as crude oil composition, connate water (pH, salinity, and saturation), injected brine (pH and salinity) and lithology of the rock. Buckley et al. [21] studied several mechanism affecting wettability alteration by crude oils. Following are the main categories of crude oil/brine/rock (COBR) interactions identified in changing wettability

- Polar interactions – This mechanism predominates in the absence of a water film between the oil and solid. In the absence of a water film, the polar components in the oil have direct access to polar components on the solid surface, promoting wettability alteration. Parameters affecting the degree of wettability alteration is type of clay, type of cations, nitrogen content in the oil, and the ability of the oil to be a solvent for the polar components. (Figure 2.13 a)

- Surface precipitation – Depends mainly on the solvency of polar components in the oil. If the oil is a poor solvent for asphaltenes, the tendency of wettability alteration is enhanced. (Figure 2.13 b)

- Acid/base reactions – In the presence of water, both the solid and oil surface becomes charged. Polar functional groups on both the solid and in the oil can act as acids (giving away a proton and becoming negatively charged) and bases (gaining a proton and becoming positively charged). This may affect the stability of the water film or influence the degree of adsorption, leading to a wettability alteration. (Figure 2.13 c)

- Ion-binding – When Ca^{2+} is present, several interactions are possible:
    1. Oil – Ca^{2+} - Oil
    2. Mineral – Ca^{2+} - Oil, see (Figure 2.13 d)
    3. Mineral – Ca^{2+} -Mineral

    1 and 3 may limit the wettability alteration while 2 may promote it

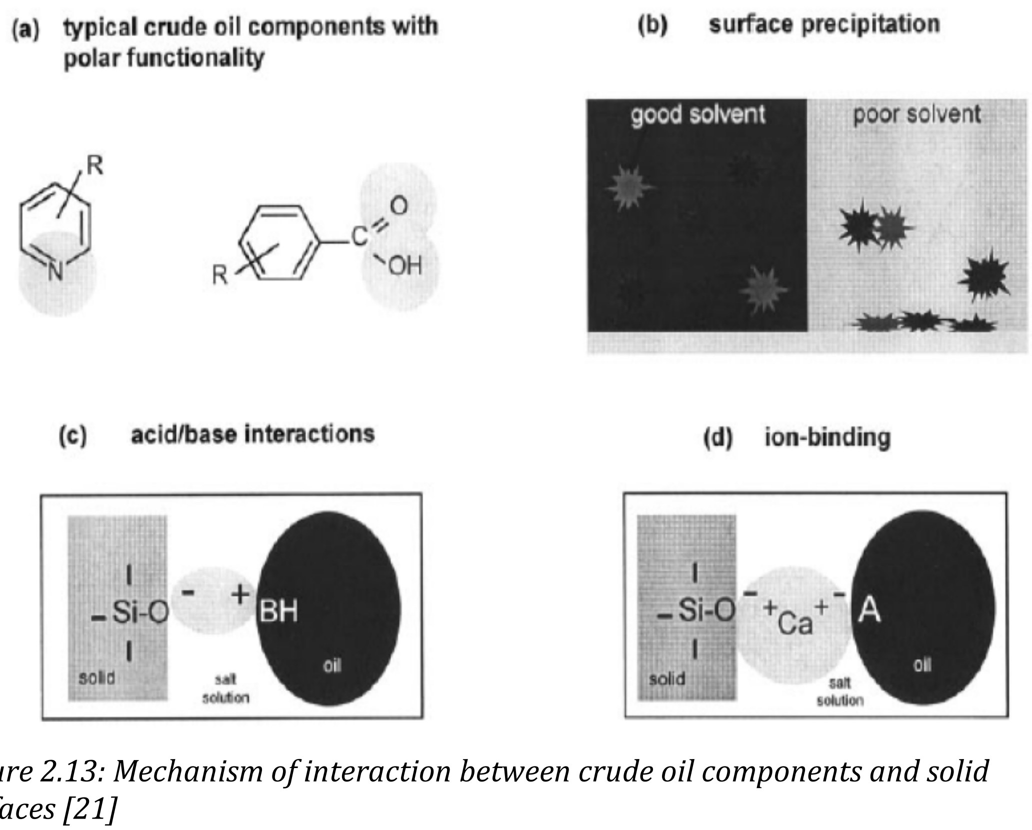

Figure 2.13: Mechanism of interaction between crude oil components and solid surfaces [21]

3 Enhanced Oil Recovery (EOR)

The demand for oil followed by high oil prices has driven the oil industry to seek for new methods to produce more from existing fields. These methods are referred to as improved oil recovery (IOR) methods. IOR processes are defined as all economic measures that are intended to improve the oil recovery factor and/or accelerate reserves [5]. This can be improved geological surveys, infill drilling, improved completion solutions, reservoir management, enhanced oil recovery (EOR) etc.

The lifespan of a reservoir may be divided into three different phases; primary, secondary, and tertiary recovery. Muskat [23] defines the "primary" production life (hence primary recovery) as to be from the moment of "field discovery and continuing until the original energy source for oil expulsion are no longer alone able to sustain profitable producing rates." Although this definition limits primary recovery to production by the natural drive of the reservoir, some definitions also include the use of artificial lifts. The natural drive of the reservoir may produce the oil by mechanisms as expansion drive, solution gas drive, gas cap drive and water drive. As a result of these mechanism the pressure in the reservoir drops, and they are therefore known as pressure depletion mechanisms.

Muskat defines secondary recovery as the injection of fluids after the reservoir has "reached a state of substantially complete depletion of its initial content of energy available for expulsion or where the production rates have approached the limits of profitable operation" [23]. The most common mechanism of secondary production is by gas or water injection. By injecting fluids into the reservoir the pressure is maintained and the injected fluid will displace the oil.

Lake [11] defined EOR as "oil recovery by the injection of materials not normally present in the reservoir". Methods with purpose to maintain pressure as waterflooding and gasflooding are therefore not considered as EOR measures. Although much attention is on EOR as a tertiary method, this definition doesn't limit EOR to a phase. When production from the reservoir is no more economical with conventional methods, EOR methods may be used to extract more of the oil at an economical manner. Thermal methods and injection of chemicals as polymers, surfactants or low salinity water are among the EOR methods used to increase oil recovery.

Oil recovery is the ratio between produced reserves and oil originally in place and is given by [5]

$$E_R = E_D * E_A * E_V = E_D * E_{vol} = \frac{N_p}{N} \tag{3.1}$$

Where

- E_R is the recovery factor
- E_D is the microscopic displacement efficiency
- E_A is the areal sweep efficiency
- E_V is the vertical sweep efficiency
- E_{vol} is the volumetric displacement efficiency
- N_p is the produced volumes
- N is the total cumulative reserves originally in place

The two parameters which EOR methods has greatest impact on is the microscopic and volumetric displacement efficiency.

$$E_{vol} = \frac{Volume\ of\ contacted\ fluid}{Total\ fluid\ volume} \tag{3.2}$$

$$E_D = \frac{Volume\ of\ displaced\ fluid}{Volume\ of\ contacted\ fluid} \tag{3.3}$$

The aim for EOR methods are therefore to increase the volume that is contacted by the injection fluid, and increase the amount of displaced oil in the pores. The use of surfactants mobilizes oil that has been capillary trapped by reducing the interfacial tension between oil and water. By mobilizing the oil, more oil is produced from the pores that has been in contact with the surfactant. It will therefore increase the microscopic displacement efficiency, hence the recovery factor. This will be further discussed in chapter 3.2.

The most well-known method for increasing the volumetric displacement efficiency is polymer injection. By injecting a more viscous fluid, the displacement front will stabilize and sweep of the reservoir is increased.

This study will look into the effect of low salinity brine injection in combination with injection of polymer and surfactant. Other EOR methods will therefore not be discussed further.

3.1 Low Salinity Waterflooding

Waterflooding has been the most used method for extracting oil from reservoirs for over a century. The first waterflood was performed in 1865 in Pennsylvania, as water accidentally entered the reservoir [18]. In the 1880s, waterflooding was used primarily as pressure maintenance, but as the effects of waterflooding on recovery got more well-known the practice increased. In the 1920s waterflooding had become a common oilfield practice [8]. Although practiced for a long time, it was not only before early 1950s that the applicability of waterflooding was understood.

Traditionally the water injected has been from the most convenient source (seawater, produced formation water), and little attention has been given to the composition of the injected water.

In 1967, Bernard G. [24] investigated the effect on recovery injecting freshwater relative to injecting seawater. Experiments showed an increase in recovery using freshwater instead of seawater, both as secondary and tertiary mode, but only if accompanied by a big pressure drop across the cores. Experiments injecting different salinities of sodium chloride was also executed, showing that increased recovery was only observed for salinities lower than 1 wt % NaCl.

Studies of low salinity increased in the 1990s, following the work of Morrow et al. [20, 25-31]

Jadhunandan and Morrow [25] studied the effect of wettability on waterflood recovery for crude-oil/brine/rock systems. By investigating fifty Berea corefloods at slow-rate water injection, they concluded that recovery is at its maximum on weakly water-wet cores, corresponding to 0.2 on the Amott-Harvey Index. Mechanisms that were demonstrated to effect wettability was aging temperature, initial water saturation and crude oil and brine composition.

Yildiz and Morrow [28] confirmed the work of Jadhunandan [32] observing an increase in oil recovery on Moutray crude oil by injecting 2% $CaCl_2$ compared to injecting 4% NaCl + 0,5% $CaCl_2$. Later, the opposite effect was observed by Yildiz and Morrow [20] on Prudhoe bay oil by injecting brine with the same properties. The conclusion was therefore that the effect of the brine composition must be specific to the crude oil. Yildiz and Morrow[20], as Jadhunandan and Morrow [25], experienced that the aging conditions are decisive on recovery performance.

Tang & Morrow [26] performed spontaneous water imbibition and water flooding tests to examine the impact salinity of injected brine and connate water has on oil recovery. Berea cores were saturated to S_{wi} with Dagang crude oil (DG) and modified synthetic Dagang reservoir brine (DG RB) before aging at elevated temperatures. They observed that when injecting water with same composition as the connate water (referred as standard case), an increase in recovery was seen with decrease in salinity. It was also observed that waterflood recoveries increased in extent with increased spontaneous imbibition recovery. This was surprising as it contradicted to prior studies [25]. Further experimentation with varying injected brine salinity and varying connate water salinity showed increased recovery with decrease in salinity, but in a less extent than for the standard case.

Tang & Morrow [27] continued their work, studying the influence of brine composition on COBR interactions. By firing at 800°C and acidizing some of the Berea cores, it was also possible to study the effect of fines migration. From their studies, it was evident that fines mobilization played an important role on the effect of low salinity. Their experiments showed an increase in spontaneous imbibition and waterflooding recovery on unfired Berea cores with decrease in salinity, consistent with prior studies [26]. For the unfired Berea cores, the behavior was different. The cores showed no sensitivity to salinity, and the recovery from spontaneous imbibition was lower than for unfired cores. It was also observed that Bentheimer and Clashash, sandstones with less clay content than Berea, were less sensitive to salinity. These results raised the discussion about the impact of clay in sandstones on recovery.

Tang and Morrow [27] discovered that refined oils gave no effect in increased recovery. This giving an indication that adsorption of polar components in crude oil is necessary to give an effect in low salinity brine injections. This observation was as expected and consistent with previous studies [20, 28, 32]. Another observation was that when no connate water was present (core 100% saturated with crude oil), no effect of low salinity injection was noticed. Both observations were later noticed by Sharma and Filoco [33]. This lead to Tang and Morrow postulating that the presence of clay, crude oil and initial water saturation were necessary for the LSE.

Sharma and Filoco [33] experienced an increase in production with decreased salinity of the brine on Prudhoe Bay oil. The salinities of the connate water and the injected brine were in this case the same, and coincided with the research of Tang & Morrow [26, 27]. Further investigation showed that injection with different salinity brines (0.3%, 3% and 20% NaCl) at a fixed connate water salinity (3%) gave no response in increased recovery. However, increased recovery was experienced when altering the connate water salinity, with a fixed injection brine. Hence, the increased recovery that was previously observed had to be an effect of the connate water composition and not the composition of the injected low salinity brine. Based on these results, they suggested that the observed increase in recovery was due to wettability alteration from a water-wet state to a mixed-wet state when salinity decreased.

Zhang & Morrow [29] extended the study of connate water saturation, looking into the impact of variation in initial water saturation (S_{wi}). The experiments were executed on a reservoir core and Berea cores with permeability ranging from 60 to 1100 mD. Three types of crude oil (Minnelusa, CS Crude and "crude A") was utilized in combination with reservoir brines (CS RB, Minnelusa RB) and its dilutions. Based on their observations it was concluded that sandstone properties are the most significant factor in improving recovery by injection of low salinity brine. The experiments showed an increase in recovery factor with increase in S_{iw}. Cores with low permeability, 60 mD to 140 mD, showed little effect of low salinity injection. According to Zhang & Morrow, this was due to the presence of chlorite and not due to the low permeability of the cores. In the reservoir core, the response to tertiary injection of low salinity was positive, leading to an incremental recovery of 27% compared to the secondary high salinity flood.

Wickramathilaka et al. [34] studied the effect of salinity on oil recovery by spontaneous imbibition. By testing the imbibition potential of different types of cores, they discovered an increase in oil recovery in Berea and RS reservoir cores with decrease in salinity and brine composition. This was observed both in secondary and tertiary imbibition mode. Al-Aulaqi et al. [35] also experienced the same trend. By studying i) imbibition of cores with constant connate water salinity and varying injection brine and ii) imbibition of cores with varying connate water salinity and constant injection brine, they experienced an increase in recovery with decreasing salinity. Observing the changes in the Amott-Harvey index (0.19 to 0.5), gave an indication of more water-wet state by decreasing the salinity in both cases.

Nasralla et al. [36] studied the efficiency of oil recovery by low salinity brine injection in Berea sandstone cores. The experiments were run with low salinity brine in secondary and tertiary modes, using brines of different compositions. The highest recovery experienced (22%) occurred when injecting deionized water, with a decrease in recovery with increase in salinity. Although efficient in a secondary mode, no effect of low salinity brine was seen in tertiary mode.

Ashraf et al. [37] investigated the effect of wettability in Berea sandstone cores as LSW was used as a secondary recovery process. The experiments were conducted on four different wettabilities; water wet, neutral-wet, neutral-wet TOW (towards oil-wet) and oil-wet. The trend observed was that in all cases recovery increased with reduction in salinity of the invading brine. The highest ultimate recovery was observed for core plugs with neutral with conditions (I_{A-H} = 0.12).

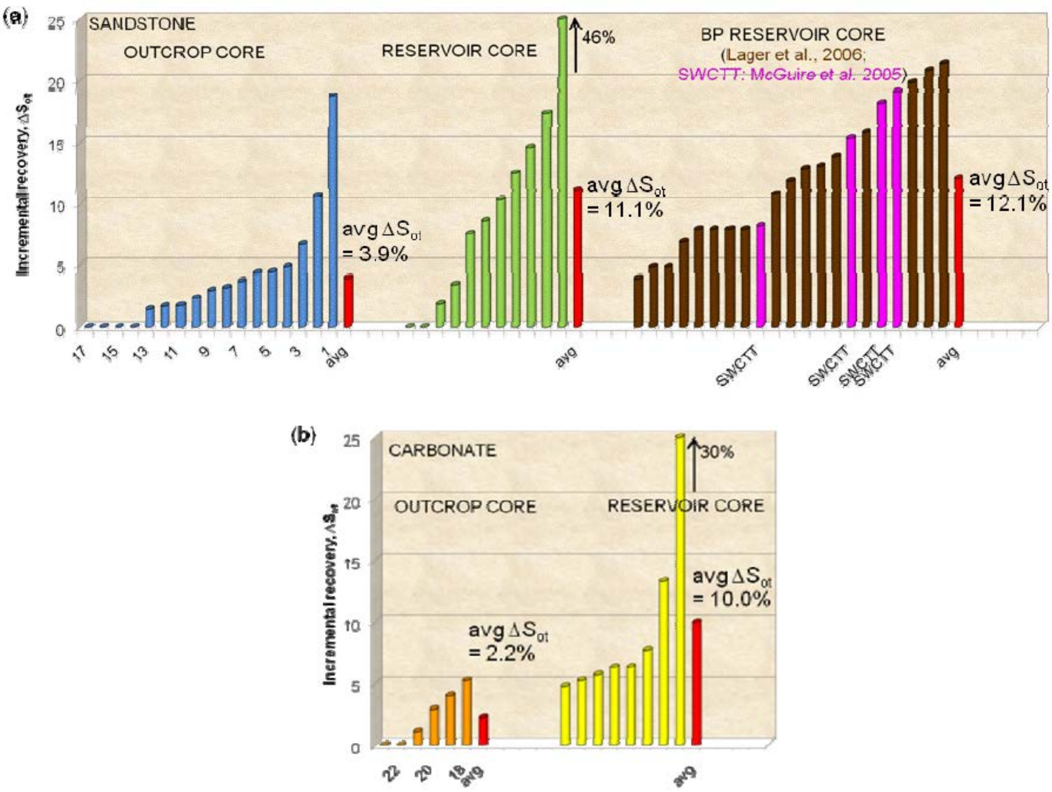

Figure 3.1: Incremental tertiary recovery by LSW in a) sandstone and b) carbonate [38]

Winoto et al. [38] performed secondary and tertiary injection of low salinity brine on outcrop and reservoir rocks. Figure 3.1 illustrates their results on recovery in tertiary mode for outcrop and reservoir cores as well as the results obtained by Lager et al. [39] and McGuire et al. [40]. For sandstone, their studies showed a greater average response to low salinity brine in reservoir cores (11.1%) compared to outcrop cores (3.9%). This was also experienced for the carbonate cores.

Although much research concur with the results of Tang & Morrow [27], there are also reports of increased recovery without the presence of clay minerals. Al-Aulaqi et al. [35] studied the effect of brine salinity and temperature in reservoir sandstone cores. They experienced an increase in oil recovery with decreasing salinity of sodium chloride in Berea cores and reservoir sandstone. As no clay was present in the reservoir sandstone, this conflicted with previous theory postulated by Tang and Morrow [27]. Al-Aulaqi et al. proposed that the existence of negatively charged silica surface was enough to promote a wettability alteration towards a more water-wet state, resulting in enhanced oil recovery.

There have also been reports of little or no effect of low salinity brine on recovery. Thyne & Gamage[41] experienced no incremental recovery for Minnelusa reservoir core plugs. This behavior was also confirmed by Thyne & Gamage [42], where they studied the effect of low salinity waterflooding for 26 fields in the Minnelusa Formation. By comparing recovery data from fields treated with low salinity brine compared to high saline brine, they concluded that there were no incremental benefit of using low salinity brine. This behavior could be attributed to the lack of mobile clay, as experimental studies in Berea cores with the same oil and water showed incremental production.

Shiran & Skauge [43] studied the effect of wettability on low salinity brine recovery. The study was performed in Berea and Bentheimer cores, with different wettability states. From literature, it was expected that the clay content in Berea cores and the oil-wet character of the Bentheimer cores would make them good candidates for low salinity effect. However, experimental data showed no or little increase on oil recovery in the Bentheimer and Berea cores when low salinity brine was injected as a tertiary recovery mode.

Rivet et al. [44] conducted 21 different tertiary waterfloods using brines of different composition in Berea and sandstone reservoir cores. They experienced that although low salinity brine gave an effect on most of the cores, in some cases where the wettability was not altered, and no incremental production was seen.

Loahardjo et al. [45] also experienced a lack in response by injection of low salinity brine in tertiary mode. Nineteen outcrop sandstones cores were screened for low salinity effect, whereas four cores showed no response to low salinity brine. All cores met the screening criteria postulated by Tang and Morrow [27] (presence of clay, crude oil and initial water saturation), pointing out the complexity of LSE.

3.1.1 Observed Effects of LSW on Field Scale

As the amount of positive experimental results from low salinity waterflods amplified, the interest from oil companies, and implementation on field scale increased.

Webb et al. [46] performed a log-inject-log field test measuring the residual oil saturation (S_{or}) in the near wellbore after low salinity brine injection. To begin with it was injected 0.1 to 0.15 pore volumes of high salinity water to reach the baseline residual oil saturation. This was followed by a sequence of three different water injections with decrease in salinity and a high salinity flood for calibration purposes. In all three logging sections a decrease in Sor with low salinity brine injection was experienced. The results coincided with laboratory results, showing a 25-50% decrease in S_{or}.

In the North Sea, the Snorre field was seen as a prospect for increased recovery by low salinity brine injection. Through laboratory and field tests Skrettingland et al. [47] got results showing little or no potential injecting low salinity brine. This behavior was also experienced in laboratory tests. The reason was believed to be the natural wetting of the formation, being already optimal (neutral-wet to slightly water wet). Under these conditions seawater injection was already efficient.

Lager et al. [48] demonstrated the effect of injecting low salinity brine into an Alaskan reservoir. By using a single injector and two production wells, they monitored the production data, observing changes in behavior during low salinity injection. The produced water was also sampled for ionic analysis. Additionally, the reservoirs response to low salinity brine injection was confirmed by a single well chemical tracer test. They experienced a change in chemical composition simultaneously as the drop in WOR occurred. In Figure 3.2, the increased production is illustrated.

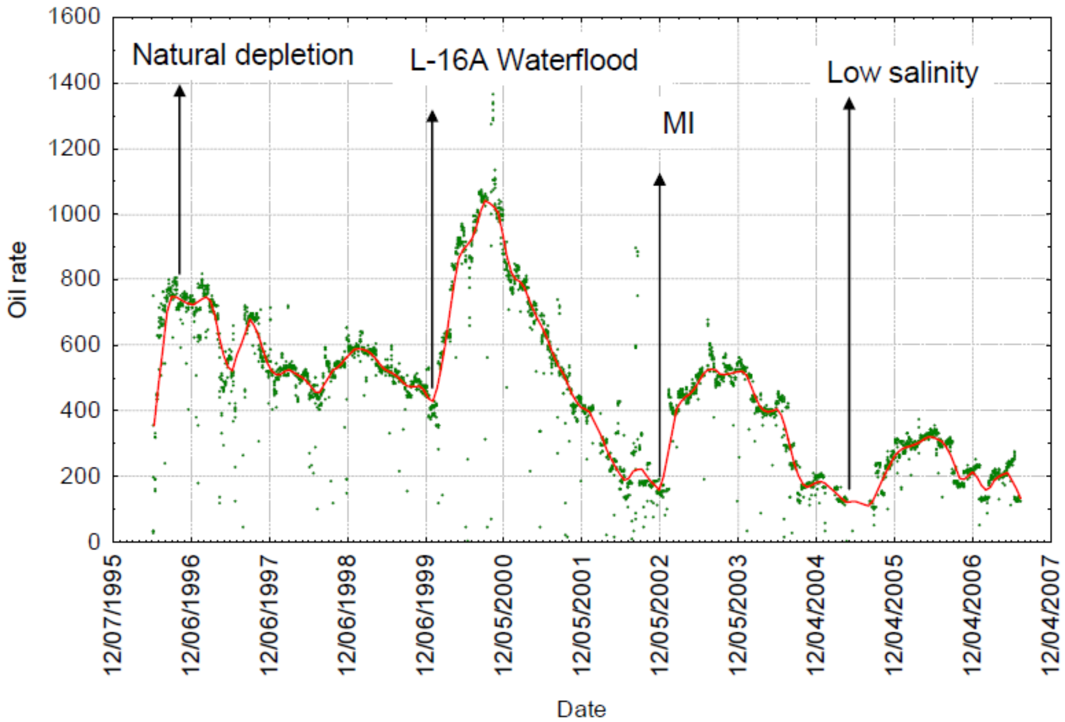

Figure 3.2: The effects of LS injection on oil rate [bbls/day] [48]

In 2010, Seccombe et al. [49] published a paper describing a comprehensive inter-well field trial on the Endicot field, North Slope Alaska. This was the first British Petroleum (BP) operated tertiary reduced-salinity EOR pilot. By monitoring the changes in watercut and ionic composition at the producer, the researchers could detect the EOR responses. Three months after the low salinity water injection had commenced a reduction in watercut and water salinity was observed in the production well. The result was an incremental oil recovery of around 10% of the total pore volume in the swept area. These results concurred with previous studies of low salinity effects on the Endicot field [50].

In all studies [46-50] correlation between field and laboratory tests was experienced, showing the importance of laboratory tests prior to field implementation.

3.1.2 Proposed Mechanisms

Laboratory and field experiments have shown the potential of LSW. The mechanisms behind the LSE is still not fully understood due to the complex nature of crude oil-brine-rock (COBR) interactions. Still, some mechanism are more accepted than others, and following are the proposed main mechanisms

- Fines migration
- pH variation
- Wettability alteration
- Multicomponent ionic exchange (MIE)

Fines Migration

As mentioned, Tang & Morrow [27] observed that the amount of clay present in the core affected the sensitivity of low salinity flooding. In addition to observing the recovery from the cores, an effluent analysis was performed. Production of fines, mainly kaolinite, was observed in the effluent. This behavior was ascribed to partial stripping of mixed-wet fines from pore walls during flooding.

Tang & Morrow explained this behavior with the DLVO (Deryaguin-Landau-Verwey-Overbeek) theory. The DLVO theory explains the stability of colloids in aqueous dispersions and describes the forces between charged surfaces interacting through a liquid medium [51].

The DLVO theory is expressed as the sum of the attractive van der Waals forces and the electrostatic repulsion.

$$\emptyset_{net} = \emptyset_A + \emptyset_R \tag{3.4}$$

The electrostatic repulsion is an effect of the electric double layer of counterions surrounding an object in liquid.

The electric double layer explains the structure of ions in a solvent close to a charged solid, like a clay mineral. It consists of two layers. The inner layer , called the Stern layer, contains strongly bound counterions. The outer layer contains ions that are in Brownian motion in the adjacent liquid. The thickness of the double layer, called the Debye length, depends on the electrolyte concentration and ion valency. Low magnitude of one of the two latter leads to a thicker double layer.

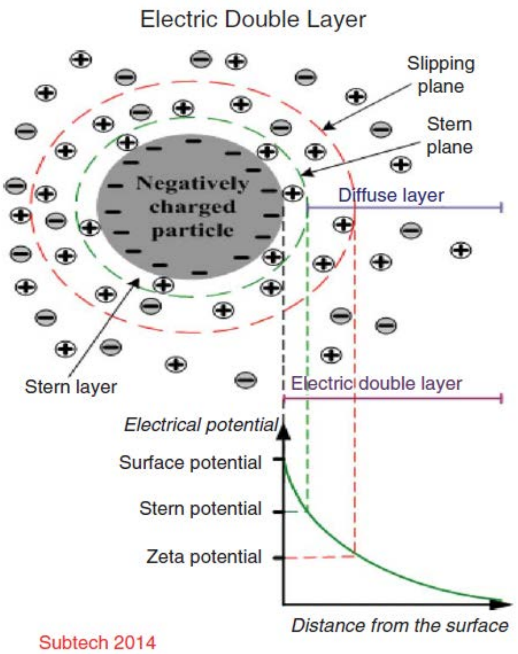

Figure 3.3: Illustration of the electric double layer [52]

Reducing the salinity of the injected brine results in an expansion of the double layer and an increased tendency of stripping fines. By mobilizing fines, Tang & Morrow [27] concluded that increase in recovery came as a result of either wettability alteration or diversion of flow.

Presence of high salinity brine has no effect on clay, and clay retains its oil-wet nature while in contact with high salinity brine. Whencontacted by low salinity brine, the clay will be destabilized and the fines will be stripped from the pore walls (Figure 3.4 b) This will lead to a wettability change towards a more water-wet condition, which is consistent with previously published results [25, 28, 31, 32]. It was also proposed that detachment of fines which had oil attached to it could increase the recovery (Figure 3.4c). As mentioned, the detachment of fines can also result in blockage of pore throats, resulting in a diversion of flow. This hypothesis was supported by a noticeable reduction in permeability when reducing the salinity of injected brine [27] .

Although Tang & Morrow [27] observed production of fines, other research have shown that fine production in the effluent is not essential to observe enhanced oil production with low salinity injection [30, 35, 39]. The recent discoveries of the effect of low salinity brine in carbonate also support this [53-57]. Carbonates are clay free, ruling out the effect of clay swelling and fines migration being the primary mechanism for the low salinity effect. This suggests that although fine migration may be an effect in increased oil recovery with low salinity injection in sandstone, it is not the primary mechanism.

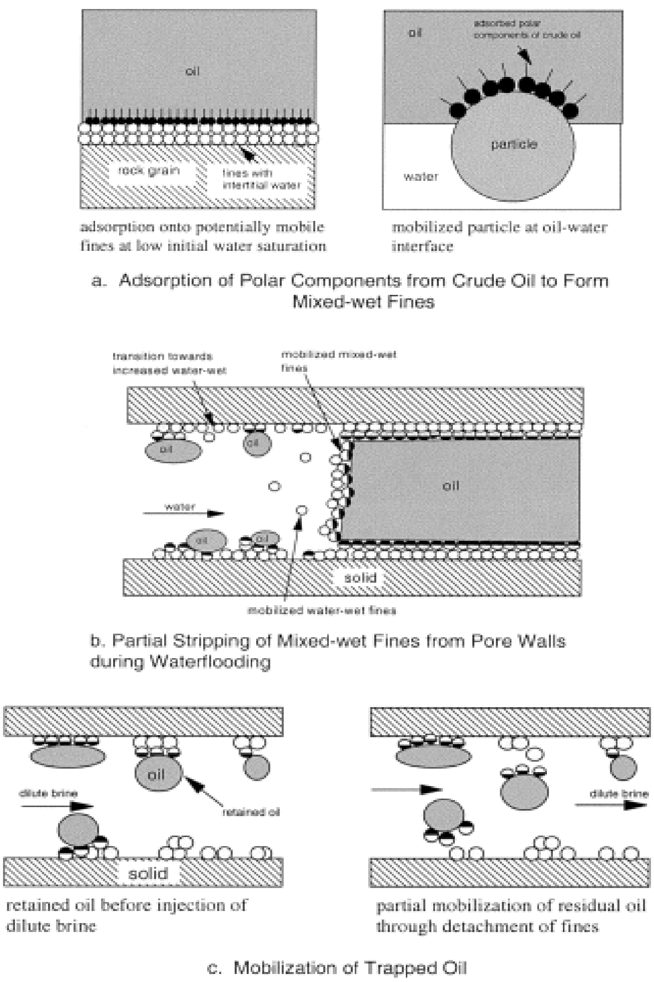

Figure 3.4: Role of potentially mobile fines in crude/oil/brine interactions and increase in oil recovery with decrease in salinity [27]

pH variation

A high pH in the effluent during LSW flooding have been noticed in many laboratory experiments [27, 39, 40]. There are two proposed mechanisms influencing the change in pH; carbonate dissolution and cation exchange. The dissolution of carbonate is given in equation (3.5) and (3.6), showing an excess of OH- will occur when carbonate is dissoluted, inducing an increase in pH. Kinetically, this is a slow reaction and depends on the amount of carbonate material present.

$$\mathrm{CaCO_3(s)} \leftrightarrows \mathrm{Ca^{2+}\ (aq)} + \mathrm{CO_3^{2-}\ (aq)} \qquad (3.5)$$

$$CO_3^{2-}(aq) + H_2\mathrm{O} \leftrightarrows HCO_3^-\ (aq) + OH^-(aq \qquad (3.6)$$

Cation exchange is a reaction between cations in solution and cations attached to clay minerals. By substituting cations on the clay surface with H^+ ions in the solution, the pH of the effluent increases. The affinity of several ions for clay sites is [58]:

$$Li^+ < Na^+ < K^+ < Rb^+ < Cs^+ < Mg^{2+} < Ca^{2+} < Sr^{2+} < Ba^{2+} < H^+$$

Cation exchange is a process much faster than carbonate dissolution and is dependent on the cation exchange capacity (CEC), which is specific for a given rock. CEC is a measure of to which degree clay can adsorb and exchange cations. CEC is mainly influenced by the clay texture (surface area, solubility of clay, organic matter), the relative concentration of the cations in place and pH.

McGuire et al. [40] proposed that low salinity waterfloods worked like an alkaline waterflood. This implying that the high pH, which was observed in the effluent, could have changed the wettability of the reservoir and cause saponification, reducing the interfacial tension between oil and water. This hypothesis is controversial as it has been shown that a high acid number (>0.2) is needed to create enough surfactants to sufficiently reduce the interfacial tension [59]. This contradicts the theory of McGuire et al. [40] as the corefloods that gave the best response to injection of low salinity brine were of very low acid number.

Lager et al. [39] concluded that high pH could not be the reason for increase in oil recovery with low salinity brine due to proton buffering (desorption of proton H^+ from oxides and organic matter), and the presence of CO_2 in the reservoir. This conclusion has later been supported by Jerauld et al. [60].

Wettability Alterations

Wettability alterations towards more water-wet state or oil-wet state has been proposed to be the cause of increased oil recovery with low salinity waterflooding. The degree of wettability alteration is strongly dependent on the stability of the water film between the mineral surface and the oil phase. The stability of the water film is dependent on the disjoining pressure.

Disjoining pressure (Π) is the force acting between two interfaces separated by a thin film. The disjoining pressure is a result of three different forces; electrostatic interactions, van der Waals interactions and hydration forces. The disjoining pressure quantifies the driving force for spontaneous thickening. If the disjoining pressure is positive, the two interfaces will repel each other and the film is stable. However, if the disjoining pressure is negative the interfaces will attract each other and the film is unstable. This will promote a wettability alteration towards less water-wet state [12].

Buckley et al. [21] experienced through adhesion tests that high salinity brines had more stable films and were less prone to wettability alteration. This giving indications that low salinity brine could be expected to be more susceptible to modification of the wettability towards a more oil-wet state. This concurring with the conclusion of Sharma & Filoco [33].

Studies concurring with the results of Buckley and Sharma & Filoco has later emerged. Sandengen et al. [61] interpreted relative permeability and capillary pressure data from secondary injection of high and low salinity water. Based on their results they concluded that the wettability shifted towards a more oil-wet state, increasing the recovery.

Fjelde et al. [62] performed low salinity waterflood experiments with the objective of describing the brine-rock interactions at high and low salinity on North Sea sandstone reservoir cores. This was done by studying recovery data and analyzing the ion concentrations and pH of the effluent. By history matching production and differential pressure data they were capable of simulating relative permeability (k_r) and capillary pressure curves (P_c). They noted that while the high salinity waterflood gave a close to piston-like displacement, the low salinity waterflood produced for a longer time. This giving an indication of a less water-wet state occurring during low salinity waterflood. These indications were later supported by k_r and P_c curve estimations showing a more water-wet state during flooding with formation water compared to diluted formation water. In addition, modeling of cation-exchange showed that the concentration of divalent cations on the clay surfaces were higher during injection of low salinity brine. As mentioned earlier, divalent ions may lead to a more oil-wet surface due to increased adsorption of acidic oil components by cation binding.

Although the general perception is that mixed-wet wettability is the optimum for increased recovery [16, 17, 19, 25, 63], a lot of research have shown an increase in recovery with increased water wetness during low salinity brine injection.

As previously mentioned, Tang & Morrow [26, 27] performed waterflood and imbibition tests in Berea cores, studying the influence of connate and invading brines on wettability and oil recovery.

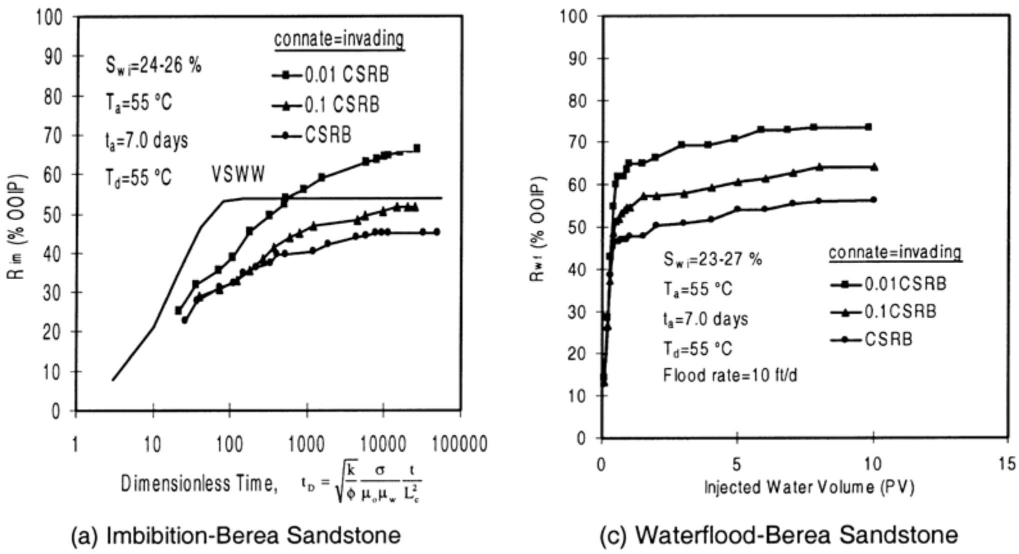

Figure 3.5: Recovery of CS crude oil by spontaneous imbibition and waterflooding with changing brine composition [27]

Based on their experiments, as illustrated in Figure 3.5, they concluded that water wetness and/or oil recovery increased with decrease in salinity. Multiple authors have later verified this conclusion [29, 30, 34, 35, 44].

Ligthelm et al. [64] investigated the influence of LSW on reservoir wettability. The study showed an alteration towards a more water-wet state when the cores were flooded with low salinity brine. They proposed that the wettability alteration was caused by an expansion of the double layer between the clay and the oil interface leading to organic material release. As low salinity brine was injected into the core, the electrostatic repulsive forces emerged maintaining a high disjoining pressure. This leading to a shift towards water-wetness, and increased recovery.

Alotaibi et al. [65] performed wettability studies using low salinity brine in sandstone cores. By studying the contact angle and zeta potential of the effluent they concluded that wettability of COBR systems depended on the salinity, temperature and the rock mineralogy. Although low salinity brine altered the wettability of Berea sandstone towards a water-wet state, the same system changed the wettability for the Scioto sandstone towards a neutral wet state. This behavior was explained by the key role of rock mineralogy.

Agbalaka et al. [66] performed coreflood studies on outcrop cores studying the effect of low salinity waterfloods compared to high salinity waterfloods and the role of wettability in any observed recovery benefit. A benefit of utilizing low salinity brine was experienced as reduction in residual oil saturation was observed. Studying the Amott-Harvey index they also observed an increase in water-wetness with decrease in salinity.

Proofs of wettability alteration on a field wide scale was given by Vleder et al. [67], studying the Omar field in Syria. Observing the production over time gave indications of wettability alterations due to the observation of dual steps in water cut development. This was later supported by analyzing SCAL, NMR and spontaneous imbibition experiments on core material and log-inject-log tests in an analogue field. They estimated an incremental recovery due to LSW injection to 10-15% of the Stock Tank Oil Initially in Place (STOIIP).

It is important to note that wettability conclusions based on imbibition test and waterfloods only provide an indication of the probable wettability, and does not give an exact answer.

It is also important to note that both wetting alteration towards oil-wet or water-wet state with increased recovery is plausible. Depending on the initial wetting state of the system, increase and decrease in production can be expected when altering the wettability. Referring to the studies of Skauge [17], intermediate wetting systems gives the highest recovery, as observed in Figure 2.11.

In the case of an initial weakly oil-wet system, an increase in water wetness may lead to an increase in recovery. This is also the case if the system is initially weakly water-wet and the alteration is towards a less water-wet state.

Multicomponent ionic exchange (MIE)

The rock surface has naturally occurring exchange sites. Under steady state chemical conditions, the composition will be in equilibrium with the resident formation brine. If there occurs a change in brine composition, the exchanger readjust its composition in order to reach equilibrium [68]. This readjustment was observed by Lager et al. [39], being the fundament for proposing multicomponent ionic exchange (MIE) as the primary mechanism for the low salinity effect. By analyzing the effluent after flooding North Slope cores with low salinity brine, Lager et al. observed a decrease in Ca^{2+} and Mg^{2+} concentration. The concentration dropped lower than the initial injected brine concentration, giving evidence for strongly adsorption of Ca^{2+} and Mg^{2+} to the rock matrix. This behavior had earlier been reported by Valocchi et al. [69].

This led to the proposal that MIE was responsible for the increase in oil recovery. Studies had shown that additional oil production increased with content of kaolinite in the formation due to the oil-wet nature of the kaolinite surface [13, 60]. On an oil-wet surface, multivalent cations at the clay surface will bond with the polar component (resins and asphaltenes) present in the oil, forming organo-metallic complexes. Injecting low salinity brine induces an expansion of the electrical double layer, which allows multivalent ions to be accessible for a multicomponent ion exchange process. This process replaces the complex ions on the clay surface with uncomplex ions, leading to a change in wettability towards more water-wet conditions.

According to the extended DLVO theory [70] and Sposito [71], there are eight mechanism that leads to adsorption of organic matter onto clay minerals. Among those, only four are strongly affected by cation exchange occurring during low salinity brine injection; cation exchange, cation bridging, ligand bonding and water bridging.

Cation exchange is regarded as the primary mechanism, and occurs when molecules containing quaternized nitrogen or a heterocyclic ring replace exchangeable metal cations initially bound to the clay surface. Cation bridging is a weak adsorption interaction between polar functional groups and exchangeable cations on the mineral surface.

Ligand bonding refers to the direct bond formation between a multivalent cation and a carboxylate group. This leads to a detachment of organo-metallic complexes (RCOO-M; where M represent the multivalent cation) from the mineral surface. Ligand bonding is a bonds stronger than both cation exchange and bridging.

If the exchangeable cation is strongly solvated (i.e Mg^{2+}) water bridging will occur. It involves the complexation between the water molecule solvating the exchangeable cation and the polar functional group of the organic molecule.
All these mechanism are illustrated in Figure 3.6.

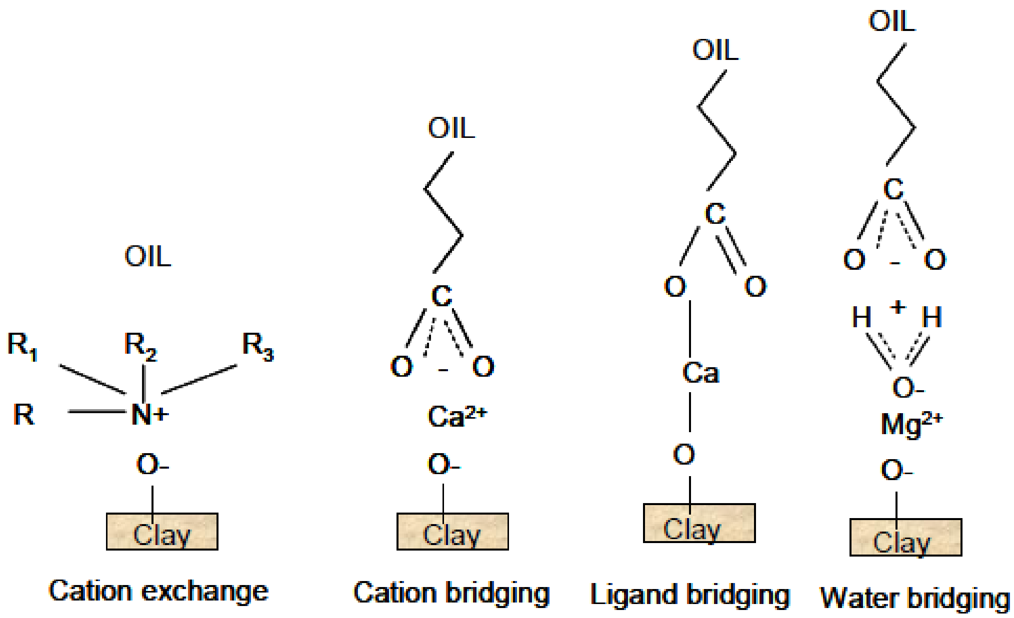

Figure 3.6: Illustration of oil-wettability mechanism [50]

To test and confirm these mechanisms, Lager et al. [39] executed a low salinity injection experiment on cores where multivalent ions had been replaced by Na^+. By doing so, all active components related to MIE were removed.

After flushing the cores sufficiently with brine containing NaCl, the cores were flooded until S_{wi} with dead crude oil and aged. A high salinity waterflood consisting of NaCl at reservoir temperature (102°C) resulted in an oil recovery of 48%. Continuing the flooding sequence with low salinity NaCl and a low salinity flood containing Ca^{2+} and Mg^{2+} gave no increase in recovery. This was as expected.

In the initial high salinity flood, the recovery was expected to be high due to the absence of oil adsorption caused by ligand formation and multivalent cation bridging and exchange. The subsequent low salinity NaCl flood showed no increase in recovery as all the mobile oil had been displaced in the primary flood and no organo-metallic complexes were present. As the rock surface only contained non-complexable monovalent ions, Na^+, no production by injecting low salinity brine containing Ca^{2+} and Mg^{2+} was experienced. Lager et al. [39] argued that these evidences showed that MIE must be an important mechanism in low salinity flooding. This mechanism has later been supported by Lee et al. [72].

3.2 Surfactants

Surface-active agents, abbreviated surfactants, are amphiphilic molecules that are active at the interface between two immiscible phases. Amphiphilic molecules are molecules that are dual in nature, meaning that it consists of two parts, a hydrophilic and a lipophilic segment. The hydrophilic moiety is referred to as the "tail", while the lipophilic segment is the "head-group".

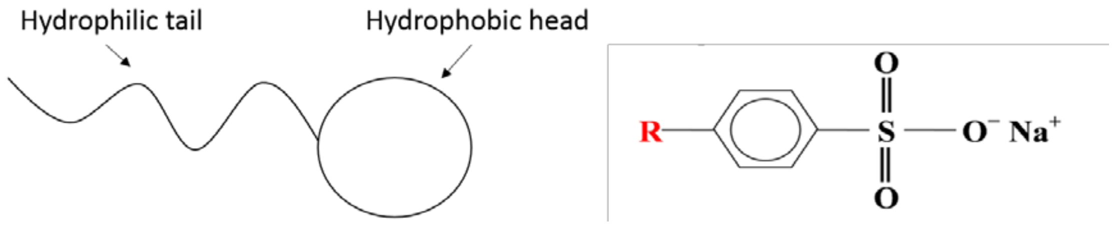

Figure 3.7: Illustration of a surfacant molecule (left), molecular formula for the surfactant sodium alkyl benzene sulphonate (with the tail to the left, and sulphonate as the head)

Surfactants are distinguished upon their polar moieties and is classified into four different groups [51, 73].

Anionic surfactants contains a negatively charged component on the lipophilic head group. This component is often a salt or an acid, most commonly sulphates, sulfonates, phosphates or carboxylates. To establish electroneutrality inorganic metals (most often sodium) is used. When the anionic surfactant is dissolved in the aqueous phase, the surfactant dissociate into a cation and a monomer. Anionic surfactants are the most frequently used surfactant, due to its good reservoir properties and low cost.

Cationic surfactants contains a positively charged salt. Cationic surfactants have little impact on recovery from oilfields due to retention. The positive nature of the polar group give rise to reactions with clay and silicates (often found in sandstone) and the surfactant adsorbs to the surface.

Non-ionic surfactants contains no polar group, and the lipophilic moiety is often present by a chemical specie as alcohol, ether or epoxy group. Since the head group has no charge, non-ionic surfactants are less sensitive to salinity opposed to the two ionic groups. However, the solubility in water decreases with temperature [74]. Non-anionic surfactants are relatively cheap, and are mainly used as co-surfactants.

Amphoteric surfactants can be anionic or cationic depending on the pH of the solution.

The main effect of adding surfactants to a solution is reduction of the interfacial tension between two immiscible phases. Many other mechanisms can reduce the interfacial tension, but surfactants are special in that way that only small concentrations are needed to reduce the interfacial tension significantly.

When surfactants are added to a mixture of two immiscible phases, for instance oil and water, the monomers will orient themselves at the interface with the hydrophilic segment in the water phase and the lipophilic segment in the oil phase. Addition of more surfactants will further lower the interfacial tension between oil and water. At a point the monomers will start to self-aggregate, and the concentration where this occurs is called the critical micelle concentration (CMC).

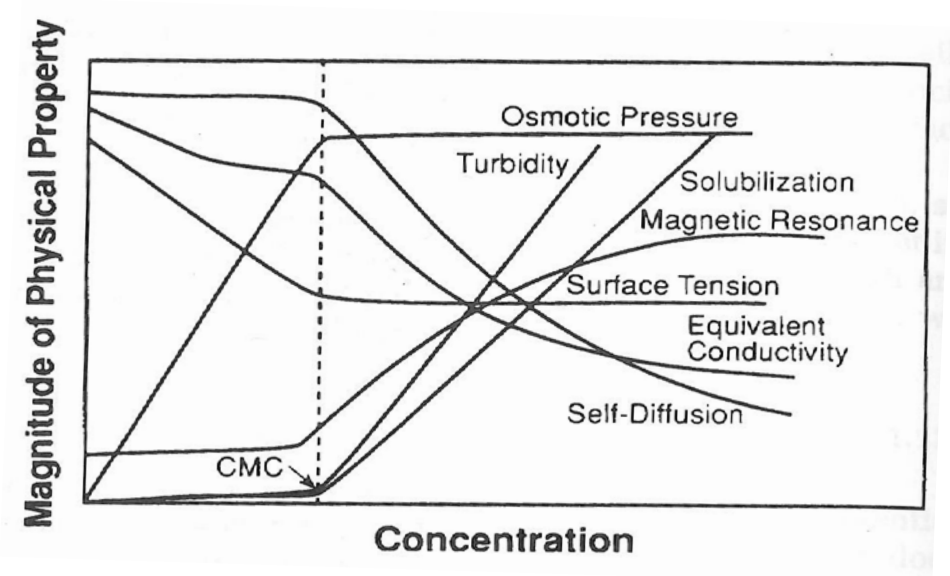

Figure 3.8: Parameters affected by CMC [51]

At CMC, the interface between the phases is full and an additional increase in surfactant concentration will not decrease the interfacial tension between the phases further [75]. CMC is therefore the concentration where the interfacial tension is at the lowest. Factors that affects the CMC are the length of the hydrophobic chain and its branching, the valence of the counterion and the effective size of the polar head group.

McBain [76] showed that CMC could be discovered by multiple means. His experiments showed changes in conductivity, interfacial tension and osmotic pressure around CMC. Later also changes in turbidity and other colligative properties have been seen to change close to CMC [75, 77].

As mentioned, at CMC the surfactants will aggregate into micelles. In an aqueous solution, the surfactants orient themselves with their lipophilic segment toward the center of the structure, while the hydrophilic segment are in contact with the water. To be able to predict the type of aggregate structure that is most likely to occur, Israelachvili [78] introduced the dimensionless surfactant parameter (N_s).

$$N_s = \frac{v}{la_0} \qquad (3.7)$$

Where v is the volume of the hydrophobic chain, l is the effective length of the hydrocarbon chain and a_0 is the effective area per polar head group. The effective head group area, a_0, is not generally calculable a priori and depends not only on the physical size of the head group, but also on its state of hydration, ionization, ionic environment etc. [51].

Spherical micelles:	$N_s < 0.33$
Infinite cylinders:	$0.33 < N_s < 0.5$
Flexible bilayers, vesicles, lamellar structures:	$0.5 < N_s < 1$
Planar bilayers:	$N_s \sim 1$
Inverted cylinders and micelles:	$N_s > 1$

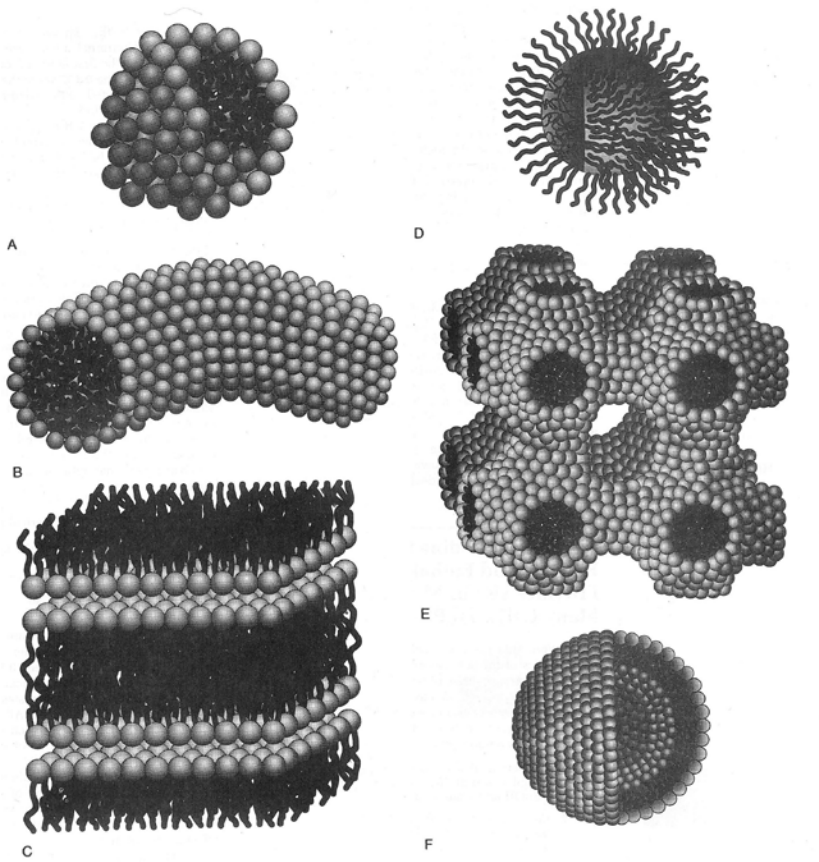

Figure 3.9: Amphiphilic aggregate structures a) spherical micelle b) cylindrical micelle c) planar bilayers d) inverted micelle e) bicontinuous structures f) vesicles [77]

3.2.1 Phase Behavior

The surfactant phase behavior is strongly affected by the salinity of the brine. Winsor [79] defined in 1954 three types of microemulsions that can emerge in a surfactant-oil-brine system. The theory was later adapted to surfactant flooding [80, 81].

A microemulsion is an isotropic solution containing substantial amounts of both a strongly polar component (usually water) and a strongly apolar component that are stabilized thermodynamically by an amphiphilic additive [77]. Microemulsions must consist of at least three components; water, oil and surfactant, although other components such as dissolved salt or co-surfactants may also be present [51].

Winsor type I microemulsion are termed oil in water microemulsions (Figure 3.10). These microemulsions occurs at low brine salinity exhibiting good surfactant solubility in the aqueous phase and poor solubility in the oleic phase. Therefore, two phases will occur: an excess oil phase and a microemulsion phase that contains brine, surfactant and solubilized oil. The solubilized oil occupies the core of the micelles.

Winsor type II microemulsions are referred to as water in oil microemulsions (Figure 3.10). Type II occurs at higher salinities as higher electrostatic forces drastically decrease the surfactants solubility in the aqueous phase. This leads to formation of an excess brine phase and a microemulsion phase containing swollen micelles of surfactant with solubilized brine. Opposed to the Windsor type I microemulsion, the micelles are inverted, with brine at their cores.

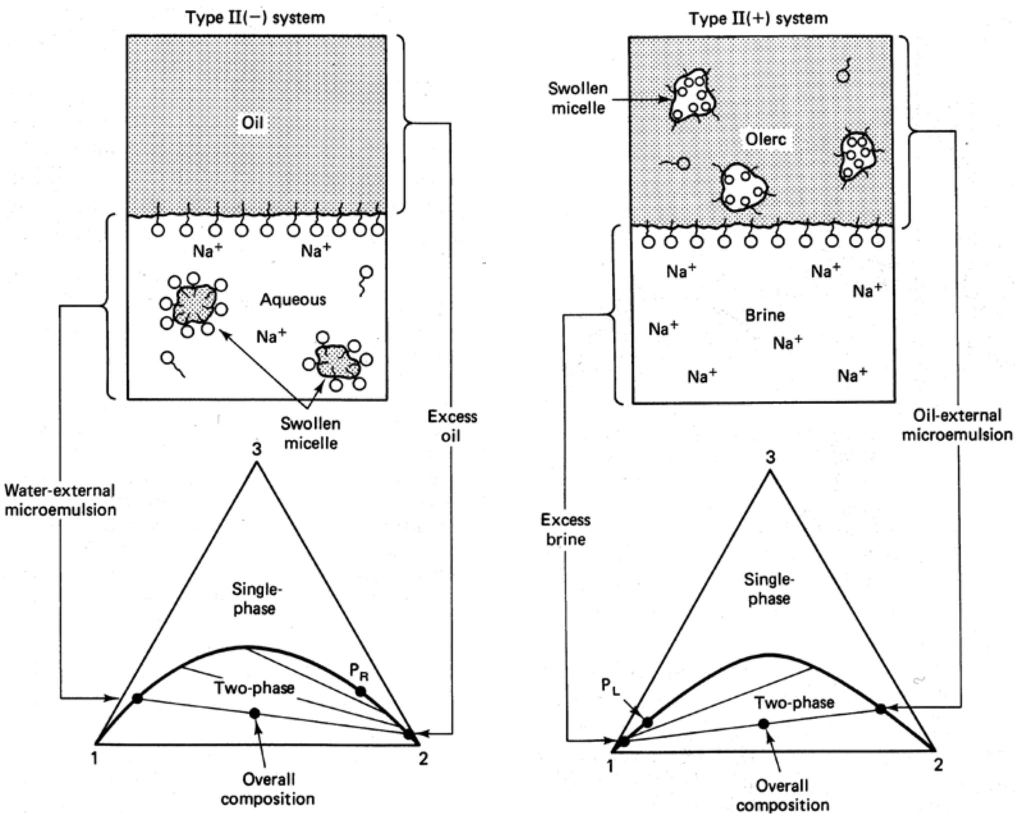

Figure 3.10: Schematic representation of Winsor type I (II-) and Winsor type II (II+) [11]

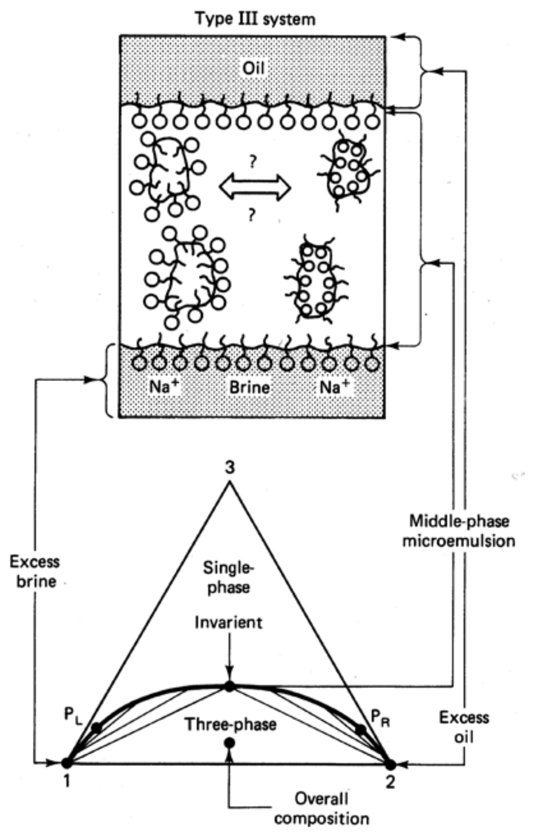

Figure 3.11: Schematic representation of Winsor type III [11]

In between Winsor type I and type II salinities there must be a continuous change in systems. At intermediate salinities a third microemulsion phase occurs, Windsor type III. This is illustrated in Figure 3.11. An overall composition within the three-phase region separates into excess oil and brine phases, and into a microemulsion phase whose composition is represented by the invarient point. Experimental studies have shown that lowest interfacial tensions are obtained at these conditions [3].

Although salinity is a significant parameter in surfactant-oil-brine interactions, other parameters also contribute to shifts in phase environment, such as [11]:

- Type of salt
- Varying concentration and type of alcohol
- Ratio between water and the oleic phases
- Type of oil
- Pressure
- Temperature

3.2.2 Low Salinity Surfactant Flooding

As salinity is an important parameter in surfactant flooding, increased interest in the use of surfactants in combinations with low salinity brine has grown.

In 2010, Alagic & Skauge [73] presented a new hybrid EOR process combining the effect of low salinity brine injection with surfactant flooding. By performing coreflood experiments on outcrop sandstone cores, they experienced a recovery of 90% of OOIP when injecting anionic surfactants in a tertiary mode. This behavior was confirmed in three experiments. They also reported that the effect of surfactant injection as a tertiary recovery mechanism was significantly reduced when no prior pre-flush of low salinity brine was done. The increased effect of surfactants was attributed to destabilization of oil layers caused by change in brine salinity and simultaneous mobilization of residual oil at low IFT. During surfactant flooding the surfactants formed a Windsor type I microemulsion, giving low retention. This in combination with high recoveries promotes this hybrid EOR method as an economical attractive method.

Alagic et al. [82] executed core displacement tests on aged and unaged Berea cores, testing the effect of low salinity surfactant flooding. The studies confirmed the results of Alagic & Skauge [73], showing high incremental recoveries for both unaged and aged cores. The highest effect was seen on the aged cores, in both low salinity flooding and combined low salinity with surfactant flooding. This indicating that less water-wet cores could have more unstable oil layers with larger degree of continuous oil.

Spildo et al. [83] continued the work of Alagic et al.[73, 82] studying the effect of low salinity brine at reduced capillarity. The experiments were executed on Berea sandstone cores using brines with total dissolved solids (TDS) of 36 393 ppm (SSW) and 3002 ppm (LSW). The cores were first pre flushed with SSW to establish S_{or}, followed by a LSW flood to create a low salinity environment. Marginal production was seen injecting LSW in a tertiary mode. The cores were then injected with a low salinity surfactant solution. During flooding, a Windsor type I system developed, exhibiting good recoveries and low retention. In conclusion, Spildo et al. [83] claimed that reduction of interfacial tension in low salinity waterfloods generates an increase in oil recovery which exceeds the expected performance of injecting a solution with the same reduction in interfacial tension but without the low salinity contribution.

Johannessen & Spildo [84] furthered their study on combining surfactants with low salinity injection. Their experiments using syntethic seawater (SSW), 43% diluted SSW (Optimal salinity surfactant) and 7% diluted SSW showed insignificant response to low salinity brine on Berea sandstone cores compared to SSW alone. Injecting surfactants in tertiary mode gave higher oil recoveries for 7 % SSW than what would be predicted by the capillary number relationship. It was also observed that moderate reduction in IFT under low salinity conditions gave the same oil recovery as ultralow IFT gave for higher salinities. In addition it was observed that flooding in low salinity environment had less retention compared to higher salinities, making it more economical feasible.

Studies regarding the effect of low salinity surfactant flooding has mainly been done on Berea cores. In 2012, Riisøen [85] conducted four coreflooding experiments evaluating the effect of low salinity surfactant injection on oil recovery in aged Bentheimer sandstones. The effect of low salinity alone was marginal on Bentheimer, concurring with the studies of Shiran & Skauge [43]. However, combining low salinity brine with surfactant flooding resulted in a significant increase in oil recovery, giving incremental recoveries of 8-26% OOIP.

3.3 Polymers

Polymers are long chained molecules with repeating units (monomers) linked by covalent bonds. By adding polymers to the injection water, the viscosity is increased resulting in more favorable mobility ratio. For EOR purposes, researchers distinguish between two types of water-soluble viscosity enhancing polymers; biopolymers and synthetic polymers.

Biopolymers are biological polymers formed through fermentation processes. Historically, the two types of biopolymers primarily used are Xanthan and Sclergoglucan polymers.

Synthetic polymers are formed in laboratories, and are therefore cheaper and can be produced in larger quantities than biopolymers. They have emerged to become the predominant and preferred polymer type for use in commercial oilfield conformance-improvement operations. This is because of the inherent chemical and biological stability of synthetic polymers, along with injectivity and cost [8].

The most widely used synthetic polymers are acrylamide polymers, mainly polyacrylamide (PAM) and partially hydrolyzed polyacrylamide (HPAM). Due to the slightly positively charge of pure polyacrylamide in acidic or neutral pH environment, polyacrylamide tends to adsorb onto reservoir rock surfaces, especially sandstone. Therefore, in sandstone, HPAM is most often favored.

The structure of HPAM is flexible, and the viscofying effect is dependent on many factors. In brines of low salinity, electrostatic repulsion between the negatively charged carboxylate groups results in a relative stiff rodlike molecule, providing a strong viscofying effect. Increasing the salinity of the brine, leads to a coiled structure of the molecule with lower viscofying power. In particular, divalent ions like Mg^{2+} and Ca^{2+} strongly reduce viscosity of a HPAM solution [86].

The Carreau model explains the behavior of polymer solutions at pure shear flows where the velocity gradient (or shear rate) is orthogonal to the direction of flow [3].

At low shear rates the molecules rotate at a constant angular velocity without significant conformation change. Hence, the viscosity remains constant and the regime of flow is Newtonian. With increase in shear rate, the macromolecules start to deform and/or orient themselves in the direction of flow. This results in a decrease in viscosity. At high shear rates all the macromolecules are oriented in the flow direction and does not affect the viscosity of the polymer solution. The viscosity is low, and flow is back to Newtonian.

In a porous medium, the shear rate will depend on the solution velocity and on the properties of the media (porosity, permeability). In order to predict the efficiency of a polymer flood one has to deal with averaged values [3]. Chauveteau [87] defined the active porous medium shear rate as:

$$\dot{\gamma} = \alpha \frac{4 * u}{(8 * \varphi * k)^{1/2}} \tag{3.8}$$

Where α is constant related to pore geometry and type of porous media. According to Stavland [88] α=2.5 for Berea cores.

3.3.1 Low Salinity Polymer Flooding

Ayirala et al. [89] conducted a cost-performance analysis on the effect of low salinity and polymer flooding applications on offshore projects. The conclusion was that the use of low salinity brine reduced the operating costs of offshore polymer floods. A change from high salinity to low salinity brine was anticipated to contribute to a 5-10 times reduction in polymer consumption due to less retention at low salinities. This, in combination with the increased effect of low salinity brine on recovery, suggested low salinity polymer as more cost-effective compared to seawater polymer flooding.

Kozaki [90] conducted experiments investigating the effect of low salinity polymer injection in sandstone cores. The experimental data showed an increase in recovery injecting low salinity brine compared to injecting high salinity brine. The low salinity polymer floods were performed in secondary mode and in tertiary mode following a high salinity flood. The result in both cases showed a reduction in residual oil saturation by 5-10% over that of the secondary high salinity waterflood. It was also noticed that the ultimate recovery was achieved with less pore volumes of injection than in waterfloods.

Mohammadi & Jerauld [91] demonstrated the benefit of combining polymer with low salinity water for enhanced oil recovery. Simulating the effects of low salinity polymer injection in secondary and tertiary processes, they demonstrated an enhancement in oil recovery and timing of the low salinity waterflood. This behavior was attributed to the improvement in fractional flow behavior when injecting polymers. Their results also showed a significant reduction in polymer consumption when using low salinity brine compared to high salinity brine, improving the cost-efficiency of low salinity waterfloods.

Opposed to the previous studies of Mohammadi & Jeruald [91] and Kozaki [90], Shiran & Skauge [92] studied the effect of low salinity polymer after establishing a low salinity environment in the porous media. By conducting coreflooding experiments on outcrop Berea cores, they experience a very high total oil recovery combing low salinity water and polymer flooding. The results were reproducible. The oil recovery by polymer injection was improved significantly when the low salinity environment had been established at S_{wi} rather than S_{or}, i.e. low salinity brine injected as a secondary mechanism opposed as a tertiary. The importance of the initial wettability was also noticed, as intermediate-wet cores responded better than water-wet cores.

4 Experimental Procedures and Equipment

4.1 Chemicals, Fluids and Core Material

4.1.1 Core Material

The cores used in these experiments were Berea Sandstone cores. The homogenous nature of the Berea cores neglects the effect of heterogeneities caused by sedimentation usually present in reservoir rock cores. The cores are therefore ideal for studying physical and chemical aspects of oil production. Cores J1-J4 were cut from the same batch while C1-C2 were cut from another batch of Berea Sandstone. The measured parameters for the cores are given in Table 5.8.

Figure 4.1: Berea cores used in the experiment, C1 and C2 are the two cores to the right

Based on X-ray diffraction data, Churcher et al. [93] studied the mineral fraction in different outcrop sandstones. Based on apparent rock properties between the Berea sandstone used in this experiment and in Churcher et al. [93], it is possible to assume similar mineral composition.

Table 4.1: Mineral fraction in 400 mD Berea Sandstone 400

	Quartz	Feldspar	Dolomite	Kaolinite	Illite
Mineral fraction [%]	87	5	1	6	1

4.1.2 Brines

The ionic composition, salinity and ionic strength for each of the brines are given in Table 4.2. The brines were put on a magnetic stirrer for a day after mixing the salts and distilled water together. It was later filtered through a 0.45 µm vacuum filter from the PALL company to remove unwanted particles.

Table 4.2: Brine ion composition and salinity

	Concentration (ppm)			
Ion	SSW	SSW w/o Ca^{2+} & Mg^{2+}	10 % diluted SSW	NaCl
Na^{+}	11146	11146	1115	1180
Ca^{2+}	470	0	47	
Mg^{2+}	1329	0	133	
Cl^{-}	20136	15424	2014	1820
HCO_3^{-}	139	139	14	
SO_4^{2-}	2742	2742	274	
K^{+}	349	349	25	
TDS	**36311**	**29800**	**3622**	**3000**
I [mmol/L]	**721**	**522**	**72**	**51**

From now on, SSW and SSW w/o Ca^{2+} and Mg^{2+} will be denoted as SW1 and SW2.

4.1.3 Oil Types

The oil types used in these experiments were Marcol 152, a North Sea crude oil and a dilution of the North Sea crude oil (40% octane, 60% Crude oil). The octane was from Sigma-Aldrich.

A high viscosity mineral oil, Marcol 152 from ExxonMobil, was used to establish S_{wi}. Using a mineral oil with high viscosity (63 cp at 23°C) is favorable when the goal is to achieve lowest possible S_{wi}. Aging cores at low S_{wi} increases the impact of wettability alteration[31]. The oil was also used to measure the effective oil permeability at S_{wi}.

The crude oil in the study is from a North Sea field. Oil from the same field was analyzed by Bøe [94]. In the study the acid number (AN) and base number (BN) was analyzed as well as the crude oil composition (SARA analysis). The results are given in Table 4.3 and Table 4.4.

Table 4.3: Acid and base number of the crude oil [94]

Acid Number [mg KOH/g oil]	**Base Number [mg KOH/g oil]**
2.84 ± 0.01	0.95 ± 0.01

Table 4.4: Crude oil composition [94]

Saturate [wt.%]	**Aromatic [wt.%]**	**NSO [wt.%]**	**Asphaltenes [wt.%]**
55.0	38.0	6.2	0.7

According to Buckley [95], oil with either high AN or high BN, but not both, appear to be most active in altering wetting by ionic interactions. As the oil used in this experiment has a significantly higher acid number compared to the base number, it is expected to be a good wettability altering agent.

4.1.4 Preparation of Polymer

For polymer injection hydrolyzed polyacrylamide (HPAM) was prepared. Aspects which were important to take into consideration under preparation was unnecessary exposition to air, iron contamination, shear degradation, sample homogeneity and creation of microgels.

First, a stock solution was prepared. The mother solution had a concentration of 5000 ppm in 0.3 wt. % NaCl. To prepare this, 540 grams of pre-filtered 0.3 wt. % NaCl was added to a beaker. The beaker was put on a magnetic stirrer, and the speed was adjusted to achieve a vortex extending 75% of the vertical length of the beaker. It was important to have a beaker with sufficient wide diameter to achieve a good mixing of the polymer solution.

The activity of HPAM is approximated to be around 90%. The final concentration in ppm is therefore:

$$C_{polymer} = \frac{10^6 * W_{poly} * 90}{W_{poly} + W_{brine}} \qquad (4.1)$$

3 grams of HPAM was added to the NaCl solution. To achieve best possible mixing the HPAM was added to the shoulder of the vortex. Addition of HPAM had to happen slowly to avoid lumps, which dissolves badly. After 2 hours of mixing, the rotation speed of the magnet was reduced, and kept overnight at low rate. The viscosity of the solution was then measured using a cone & plate geometry on a Malvern Kinexus rheometer.

It was of interest to find the best suited polymer solution for polymer injection. The stock solution was diluted with 0.3 wt.% NaCl to 1000 ppm, 600 ppm, 300 ppm and 100 ppm HPAM solutions. The solutions were put on magnetic stirrers at low rate over night to achieve homogenous distribution in the solution. The viscosity of the solutions were then measured using a cone & plate n the Malvern Kinexus rheometer. Afterwards, the solutions were filtered, and viscosity measured again.

4.1.5 Preparation of Surfactant

The preparation of surfactants was done by mixing 1 wt. % surfactant with 3000 ppm NaCl low salinity brine. The surfactants used are XOF 25S and XOF 26S, both sodium alkyl benzene sulphonate surfactants from Huntsman. The percentage of active matter in the surfactants were 25.6% (XOF 25S) and 24.5% (XOF 26S). The general molecular structure is given in Figure 3.7

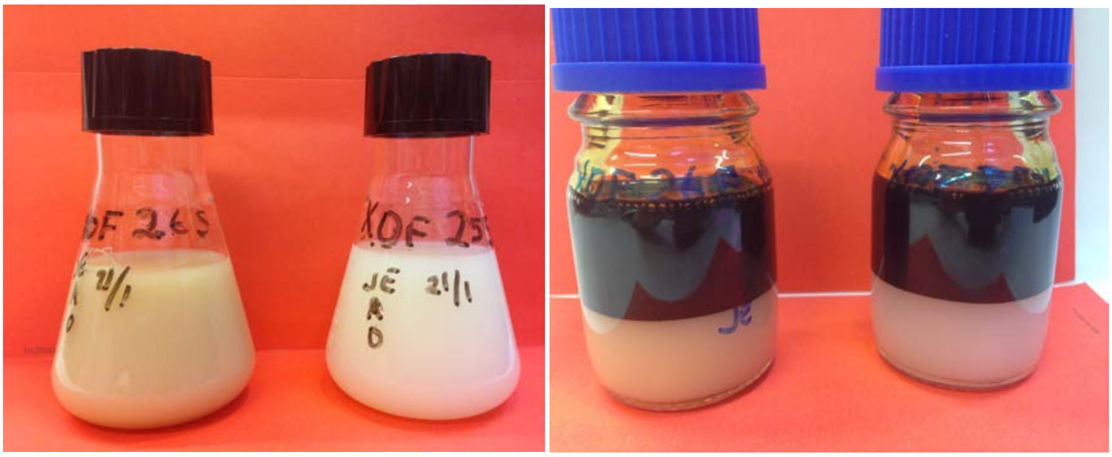

Figure 4.2: Left: Surfactant samples, XOF 26S (left) and XOF 25S (right) Right: Surfactant samples in equilibrium with oil, XOF 26S (left) and XOF 25S (right)

To study formation of gels, mixtures containing 50 wt.% surfactant and 50 wt.% diluted North Sea oil was made. The samples were left to equilibrate for a couple of days. Figure 4.2 shows the oil and surfactant solution in equilibrium. No Winsor type III phase was observed in neither surfactant solutions. Viscosity measurements were done on pure samples and samples which had been in equilibrium with oil. Little difference was observed in viscosity indicating low formation of gels. Formation of gels is unfavourable as it can hinder the transport efficiency of the surfactant flood and oil bank through the reservoir [96]. Unpublished work at UNI Research CIPR have shown that the surfactants used in this experiment are stable up to 2.5 wt.%.

To choose which surfactant to use in the LSSP experiments, interfacial tension measurements were done on pure and equilibrated samples.

4.2 Core Preparation and Waterflooding

4.2.1 Core Preparation

The length of the six cores in this study was in the beginning measured to calculate the bulk volume of the cores. Later the cores were mounted in Exxon core holders with a confining pressure of 22 bar. The confining pressure was achieved by injecting water on the outside of the sleeve, preventing fluids bypassing the core. The core holders were weighed and later vacuumed until they reached a sufficient low vacuum pressure (<1.5 Torr).

4.2.2 Porosity Measurements

The cores were saturated using a Quizix pump at constant pressure delivery, set at five bar. The constant pressure delivery continued until the injected volume stabilized and remained constant. The porosities were obtained by two different methods. First, by using the Quizix pump it was possible to record the injected volume into the cores. Thus, the injected volume is equal the pore volume of the cores, as given equation (4.2)

$$V_p = V_{w,injected} \tag{4.2}$$

By recording the weight difference of the core holder with dry core and saturated core, the porosity of the cores were determined. The two methods showed approximately equal estimations. The cores were then left for a week at ambient temperature and pressure to reach ionic equilibrium.

4.2.3 Permeability Measurements

After the porosity measurements, the cores were flooded with synthetic seawater (SW1) at five different rates, measuring the differential pressure over the core for each step. The rates were checked twice, to ensure that the flow followed Darcy's law. The cores were flipped to measure the absolute permeability of the rock in the other flooding direction.

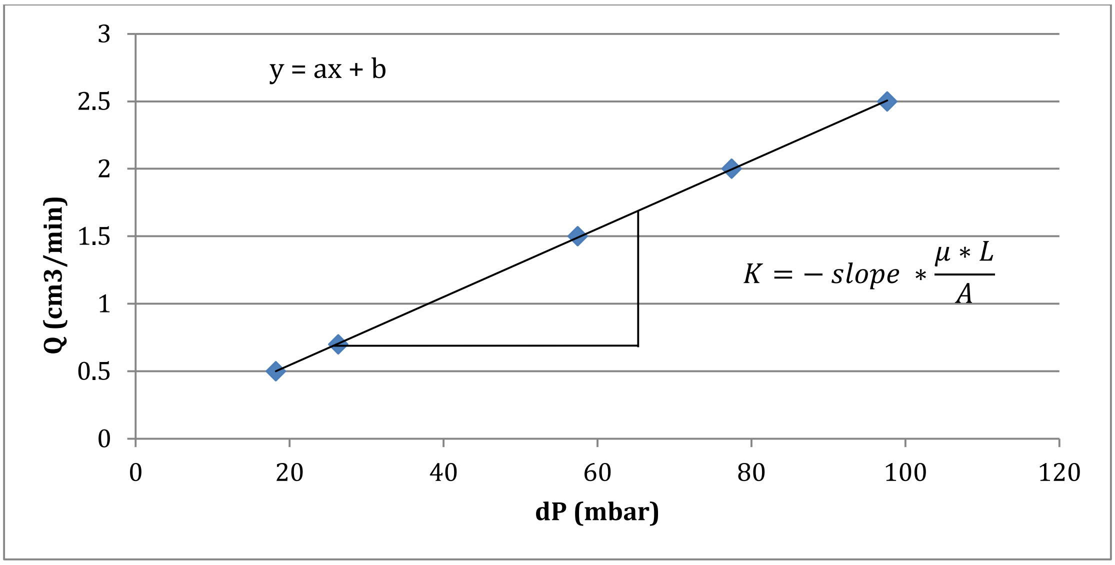

Figure 4.3: Illustration of permeability calculations

As observed in Figure 4.3 the permeability was estimated by plotting the differential pressure against injection rate. By knowing the viscosity, length of core and cross sectional area in combination with the slope of curve, the permeability was calculated. It is possible to use this method using only two reference points, but using more points yields a higher certainty of measurement. This method was also used for endpoints effective permeabilites later in the experiments.

4.2.4 Drainage

Following the permeability measurements, the core was flooded with Marcol 152. This was done to attain initial water saturation. To reduce end effects, the core was flooded in both directions. By following the same procedure as in 4.2.3, the oil permeability at initial water saturation was given.

4.2.5 Aging (Wettability Alteration)

After drainage, the Marcol 152 was displaced by injecting a North Sea crude oil. Before injecting, the crude oil was filtered through a 0.5 µm filter to remove solids. Changing oil from Marcol 152 to North Sea crude oil, increases the probability of changing the wettability due to the polar components in the North Sea crude oil. Afterwards it was attempted to measure the permeability of the crude oil, but this was not possible due to lack of stability in the pressure readings.

Before putting the cores in the heating cabinet, the cores were dismounted from the Exxon core holders and mounted into Reslab core holders, as seen in Figure 4.4. To obtain a change in wettability, the cores were put in the heating cabinet for a total of four weeks. It was first tried to age cores J1 and J2 for two weeks, but as only a little change in the effective endpoint oil permeability was observed, it was decided to age for two more weeks. Cores J3 and J4 aged four consecutive weeks.

Figure 4.4: Cores in heating cabinet

The heating cabinet was then set to 110°C. To avoid damage to the cores or gas precipitating out of the oil, the confining pressure was set to 27 bar. A backpressure regulator was used to increase the boiling point of the fluids, to preventing boiling during aging. While in the heating cabinet, the cores were refilled with filtered North Sea crude oil each week to accelerate the aging process.

After four weeks, the temperature was gradually reduced. At 50°C the cores were flooded with filtered North Sea crude oil to remove potential asphaltene or resin precipitation from the cores. At ambient temperature, the core was flooded with two pore volumes (PV) diluted North Sea crude oil to obtain a better mobility ratio. The diluted oil was injected at different rates, measuring the differential pressure over the core to obtain the effective permeability of oil at S_{wi}. This was used as measure for wettability alteration.

4.2.6 Waterflooding

The waterflood experiments consisted of four different flooding sequences, as summarized in Table 4.5.

Table 4.5 : Waterflooding sequences

	Flooding Sequence			
Core	1.	2.	3.	4.
J1	SW1	SW2	10 % SSW	3000 ppm NaCL
J2	SW1	SW2	10 % SSW	3000 ppm NaCL
J3	10 % SSW	SW2	3000 ppm NaCl	
J4	10 % SSW	SW2	3000 ppm NaCl	
C1	SW1	4.5 % SSW		
C2	4.5 % SSW			

The sequence used for J1 and J2 will from now on be referred as sequence 1. The sequence used for J3 and J4 will be Sequence 2. The sequences for the cores C1 and C2 will be name sequence 3 and 4, respectively. The experimental setup was as seen in Figure 4.5

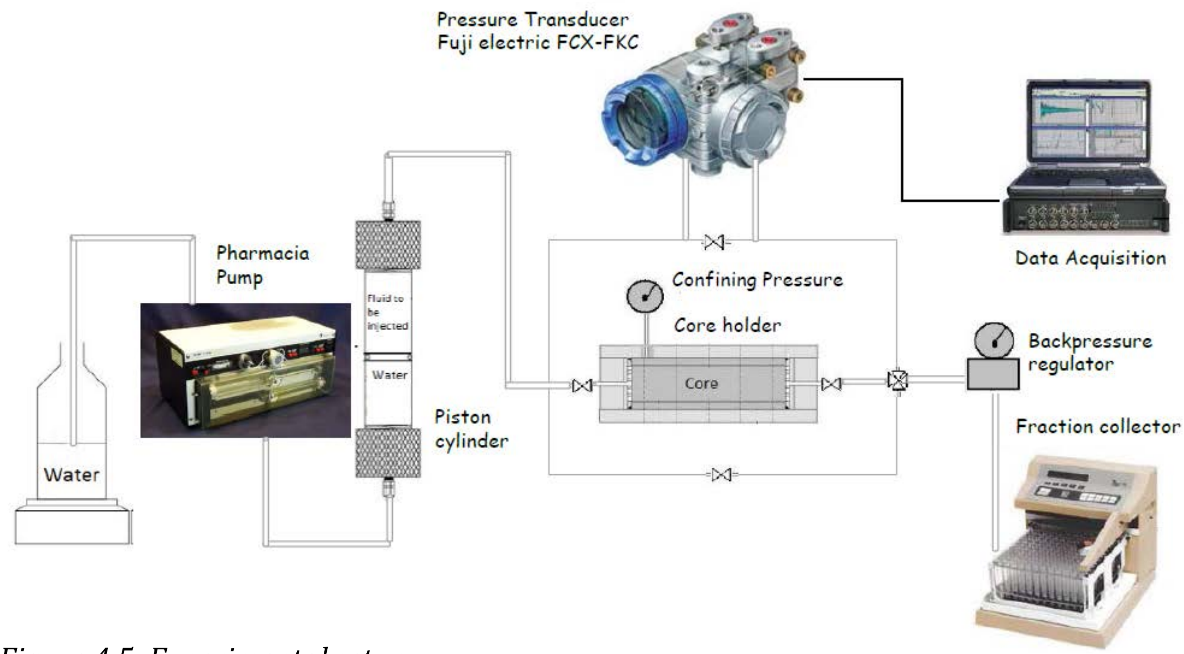

Figure 4.5: Experimental setup

Sequence 1

Sequence 1 consists of a high salinity secondary flood, and a low salinity tertiary recovery sequence. In the first flood, SW1 displaced the oil. The injection was first done at a low rate (0.1 mL/min) until no oil production was observed for approximately one PV. When a state of no oil production was reached, the rate was increased to 0.5 ml/min and later to 1 ml/min. To minimize end effects, the injection rate was increased in steps at the end of each flooding sequence. Before each increase in rate, the effective water permeability was measured by reducing the rate and measuring the differential pressure. Differential pressure was recorded automatically under the whole flooding. At the end of the SW1 waterflood, effective water permeability was measured.

The tertiary low salinity flood was initiated at $S_{or,SW1}$. The low salinity floods were executed in a similar manner as for the SW1 waterflood, including permeability measurements before every increase in rate. Collecting the effluent in tubes made it possible to do pH analysis with regards to production time. The pH measurements were not done in situ.

Sequence 2

The experimental setup and procedure was as for sequence 1, but contrary to sequence 1 the initial secondary recovery flood was by low salinity brine. Tertiary mode is executed in same way as the secondary mode, following the flooding sequence given in Table 4.5.

Sequence 3

The experimental setup was as in Figure 4.5 , but instead of collecting oil in a fraction collector an Amott cell was used. The core was first injected with SW1 as a secondary recovery method, injecting at low rate and increasing the rate when no production was observed from the core. The production was then continued with diluted SSW (4.5%) as a tertiary method, at three different rates. The differential pressure was recorded during the whole experiment.

Sequence 4

The experimental setup was equal to sequence 3. The core was injected with 4.5 % diluted SSW at low rate (0.1 ml/min) until no production was observed. Injection was continued with increased rates of 0.5 ml/min and 1 ml/min. Differential pressure was recorded during the experiment.

4.2.7 Low Salinity Surfactant Polymer (LSSP) Waterflood

The low salinity surfactant polymer (LSSP) waterflood was initiated at $S_{or,LSW}$. Cores C1 and C2 had prior to the LSSP waterflood been injected with 3000 ppm NaCl to achieve similar initial conditions. The experimental setup was equal as for the prior experiments, given in Figure 4.5. The flooding sequence is summarized in Table 4.6, with proposed injected volumes of each fluid. During the experiments, deviations from the proposed injected volumes for the waterfloods occurred as the cores were flooded until no more oil production was observed. In the LSSP experiment for core J4 there was a malfunctioning of the pump, resulting in varied injection rate.

Table 4.6: LSSP flooding sequences

	Flooding Sequence				
	1st	2nd	3rd	4th	5th
Fluid	XOF 26S	300 ppm HPAM	3000 ppm NaCl	600 ppm HPAM	3000 ppm NaCL
PV injected	1	1	2	1	2

As seen from table Table 4.6, polymer were injected in two stages with different concentration. The polymer was injected to give mobility control, increasing the volumetric sweep and therefore the area in which surfactants may act in.

4.2.8 Volume Estimations

In some cases the produced volumes could be difficult to estimate as they were small. The tubes were also of plastic, thus oil-wet, and the interface between oil and water would curve, evidently showing higher produced values compared to actual production. In order to estimate the produced volumes, the volumes were compared to reference tubes of known volume. The reference tubes were prepared by gravimetric determination.

Preparation was done by first placing a known volume of water into plastic tubes and noting the total weight. The tubes were then filled with oil of different volumes and by knowing the weight and density of the oil in the tubes, the oil volumes could be calculated. For comparison with the actual production, pictures were taken.

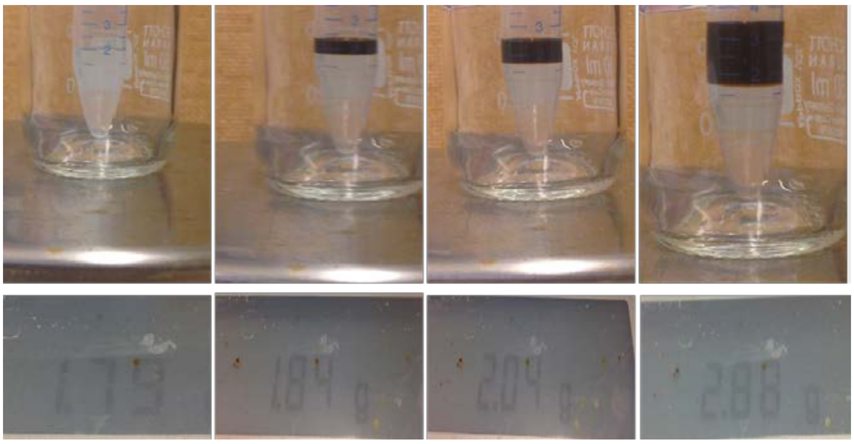

Figure 4.6: Illustration of reference tubes

4.3 Equipment

In this section the apparatus used during the experiments will be described with emphasis on setting, principle, procedure and uncertainties in the apparatus.

4.3.1 Rheometer

To measure the viscosity of fluids, the Malvern Kinexus rheometer (Figure 4.7) was used. It is a rotational rheometer, which means that it relates the force needed to turn an object in a fluid to the viscosity of the fluid. The uncertainty in measurements were estimated to be 5% of measured value. For the purpose of the experiments, double gap and cone & plate geometry were used.

Figure 4.7: Malvern Kinexus Rheometer

The double gap geometry (Figure 4.8) was used for the diluted oil, surfactant and water samples, as it is ideal for low viscous samples. This is due to the double gap´s high surface area, giving high sensitivity in readings. The double gap geometry works by placing a pre-defined volume of test fluid into the cup, and measuring the torque needed to obtain a certain rotational speed. The torque is proportional to the shear stress in the fluid, and can easily be converted to viscosity. This is done by equation (4.3).

$$\eta = \frac{\tau}{\dot{\gamma}} \qquad (4.3)$$

Where μ denotes the viscosity, τ is the shear stress and $\dot{\gamma}$ is shear rate.

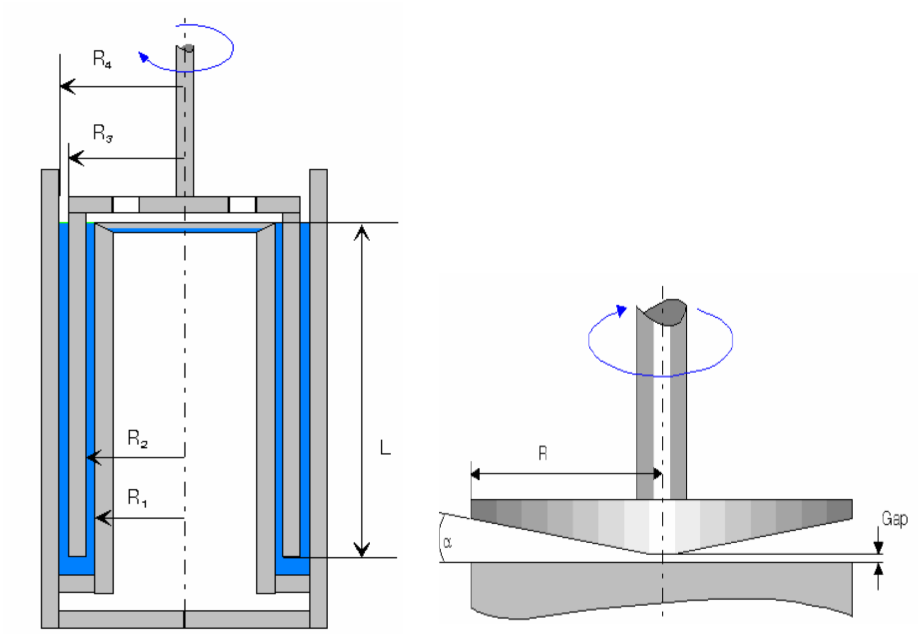

Figure 4.8 Illustration of a double gap geometry (left) and a cone & plate geometry (right) [97]

For the polymer, the cone & plate geometry (Figure 4.8) was the best-suited geometry. This geometry is ideal, as it only needs small samples and gives a constant shear rate along the complete gap. The diameter of the cone used was 40 mm with an angle of 4°. Equation (4.4) expresses the viscosity measured in a cone & plate geometry [97].

$$\mu = \frac{\tau}{\dot{\gamma}} = \frac{3M\alpha}{2\pi * R^3 * \omega} \qquad (4.4)$$

Where M is the torque, ω denotes the angular velocity, R is the radius and α is the cone angle.

Depending on the measurement, the values obtained at low and high shear rates may not be accurate or reproducible. This may be related to the sensitivity of the geometry chosen, i.e. that the shear stress is too low to measure, or due to turbulent flow caused by high shear rates.

As the shear rate during the waterfloods are unknown, apparent viscosities were calculated. The apparent viscosity is used in capillary number calculations.

4.3.2 Spinning Drop Tensiometer

The spinning drop method is an experimental method for obtaining the interfacial tension between two immiscible fluids. By injecting drops of the less dense fluid into a capillary tube filled with the denser fluid, and spinning the tube at a certain rate, it is possible to obtain the interfacial tension (σ) by Vonnegut's expression [98].

$$\sigma = \frac{(\Delta\rho)\omega^2 r_m^3}{4} \tag{4.5}$$

Where $\Delta\rho$ is the density difference between the liquids, ω is angular velocity and r_m is the radius. When the length of the drop is much greater than the radius, the droplet can be assumed as a cylinder with hemispherical ends. The bigger the ratio between the length and the radius, the more correct Vonnegut's expression is. With increased spin the droplet will elongate as the centrifugal forces increases. The droplet will stop elongating when the centrifugal forces and the interfacial tension reaches equilibrium.

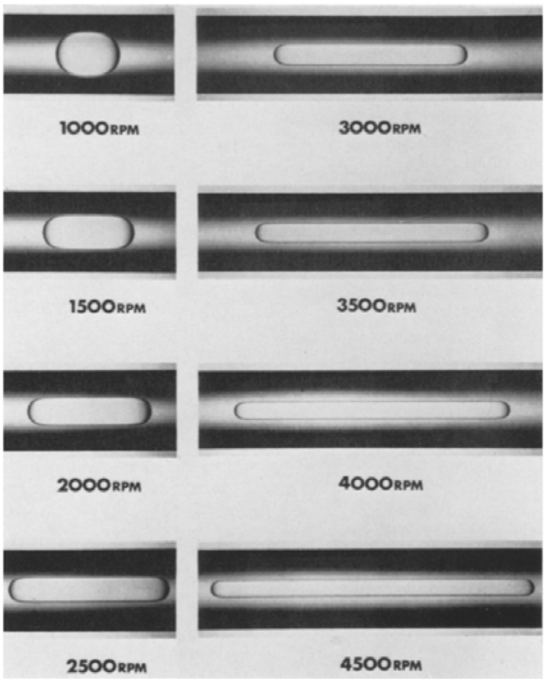

Figure 4.9 Picture of droplet at different angular velocities [99]

The spinning drop method is an ideal method for measuring the interfacial tension in surfactant systems as it is developed to measure very low IFT. The apparatus used in the experiment, shown in Figure 4.10, was a Spinning Drop Tensiometer SITE100 from Kruss GmbH.

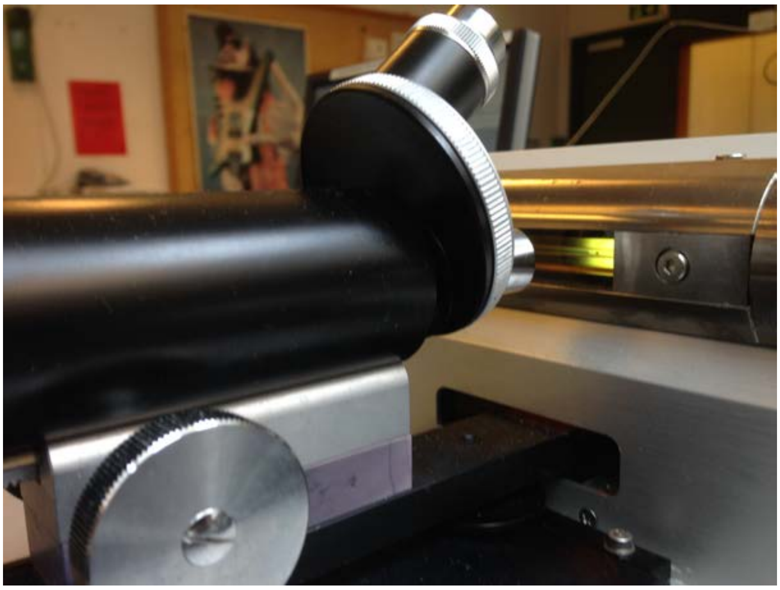

Figure 4.10: Spinning drop tensiometer

Measurements were done using a camera, a spinning drop tensiometer and the software DSA2. The camera was connected to a computer, delivering images for interfacial tension calculations. Before starting the experiments the camera was calibrated using a 0.688 mm wide needle submerged in the tube, filled with only the heavy phase. The needle was then removed, and to avoid bubbles in the heavy phase, the rotational speed was set to 5000 RPM.

Further the oil was injected into the tube, afore enclosing it and spinning at different rates. For each change of rate, equilibrium had to be reached before measurements were done. DSA2 required input on the density of the fluids before using equation (4.5). All experiments were executed at 23°C.

The highest uncertainty in the measurements of IFT are found in measurement of the radius. This is observed in equation (4.5), as the radius is cubed. The total uncertainty in all the measurements was estimated to be ± 20% of the absolute values obtained.

4.3.3 Densitometer

For density measurements, an Anton Paar K.G. DMA 60 Densitometer and a DMA 602 density-measuring cell were used. The measuring cell was connected to a water bath operated by a Heto Birkerød temperature controller.

The densitometer is connected to a hollow tube that is filled with the sampling fluid. By oscillating the tube, the frequency of the oscillation is recorded and is related to the density of the fluid. The oscillating frequency changes depending on the density of the fluid, decreasing with increasing density.

Figure 4.11: Densitometer

To execute the experiment, the sampling fluid was injected inside the hollow tube with a syringe. The hollow tube was flushed thoroughly with the sampling fluid, ensuring that no other fluids were present. While the syringe was held kept in position, the other end was enclosed with a rubber plug. When the temperature was constant, the time periods were recorded.

Equation (4.6) was used to calculate the density. Parameters including an * denotes a pure solvent.

$$\rho - \rho^{*} = \frac{1}{A}\left(T^{2} - T^{*2}\right) \qquad (4.6)$$

Where T is the time period, A is apparatus' constant and ρ is the density of fluid.

The apparatus constant can be calculated by measuring the time period for two fluids with known density. For simplicity it is convenient to use air and water.

The density of air is given as a function of temperature (T), relative air humidity (F) and atmospheric pressure (B).

$$\rho_{air} = 0.46464 \frac{B - 0.08987 \cdot F}{T} \cdot 10^{-3} \qquad (4.7)$$

The apparatus constant is dependent on temperature, thus it is necessary to measure an apparatus constant for each temperature measured. The total uncertainty in all of the measurements were estimated to be ± 10^{-4} g/ml.

4.3.4 pH Measurements

The pH measurements were conducted using a Hach Lange pH-meter with accuracy of ±0.01 pH. Prior to conducting the pH-measurements, the pH-meter was calibrated using three fluids of pH 4, 7 and 10. The percent calibration slope was 92.8.

After calibration, the probe was placed in the solution. The probe was stirred gently, ensuring a homogenous solution during measurements. In between measurements, the probe was cleaned with distilled water and dried using fine paper.

Figure 4.12: Hach Lange H160 portable pH-meter

An electrochemical cell for pH measurement always consists of

- An indicating electrode
- A reference electrode
- An aqueous sample

While the indicating electrode is directly proportional to pH, the reference electrode is independent of pH. If all three parts are in contact with each other, a potential can be measured between the indicating electrode and reference electrode.

The potential is dependent on pH of the sample and its temperature [100]. Nernst equation (4.8) expresses the relationship between the measured potential E [mV], pH and the temperature [K].

$$E\ (T) = \ E^{O}(T) - \frac{RT}{F} \times\ pH \qquad (4.8)$$

Where R is the molar gas constant, T is the temperature and F is the Faraday constant. The Hach Lange pH-meter had a built in thermometer, giving the pH directly.

4.3.5 Other Experimental Equipment

Experimental equipment used:

- Fuji electric FCX-FKC - The apparatus was used to measure the differential pressure over the core. The maximum span limit was 5000 mbar. A voltage signal was sent from the apparatus to the computer were the signal was converted to pressure readings. The uncertainty of the readings were 0.04% of full range. (Figure 4.13 A)

- Exxon core holder – The cores were held in rubber sleeves inside the core holder, forcing the flow through the core. It was important that the sleeve was tight to the core, preventing flow going around the core as well as preventing fluid used for confining pressure to invade the core. (Figure 4.13 B)

- Pharmacia LKB-Pump P-500 – The Pharmacia pump delivered constant flow rate from 1 ml/h to 500 ml/h. (Figure 4.13 C)

- Back pressure regulator(BPR) –The BPR was used during production and aging of the cores. The BPR was set to 8 bar. (Figure 4.13 D)

- Foxy Jr. Fraction collector - Was used to collect the effluent during production. The time setting of the collector was dependent on the rate. (Figure 4.13 E)

- Vacuum ejector from Edwards - Was used to evacuate the air from the cores before porosity measurements. To measure the pressure during vacuuming a Granville-Philips 275 mini-Convetron was utilized. (Figure 4.13 F)

- Cellstar collection tubes from Greiner Bio-one – 15 ml tubes were used to collect the effluent. It is estimated that the uncertainty in the reading of the tube values are 0.25 mL. (Figure 4.13 G)

- Digitron 2004T thermometer – Was used to measure the temperature during experiments. The resolution of the thermometer is 0.1° in the range of measurements. (Figure 4.13 H)

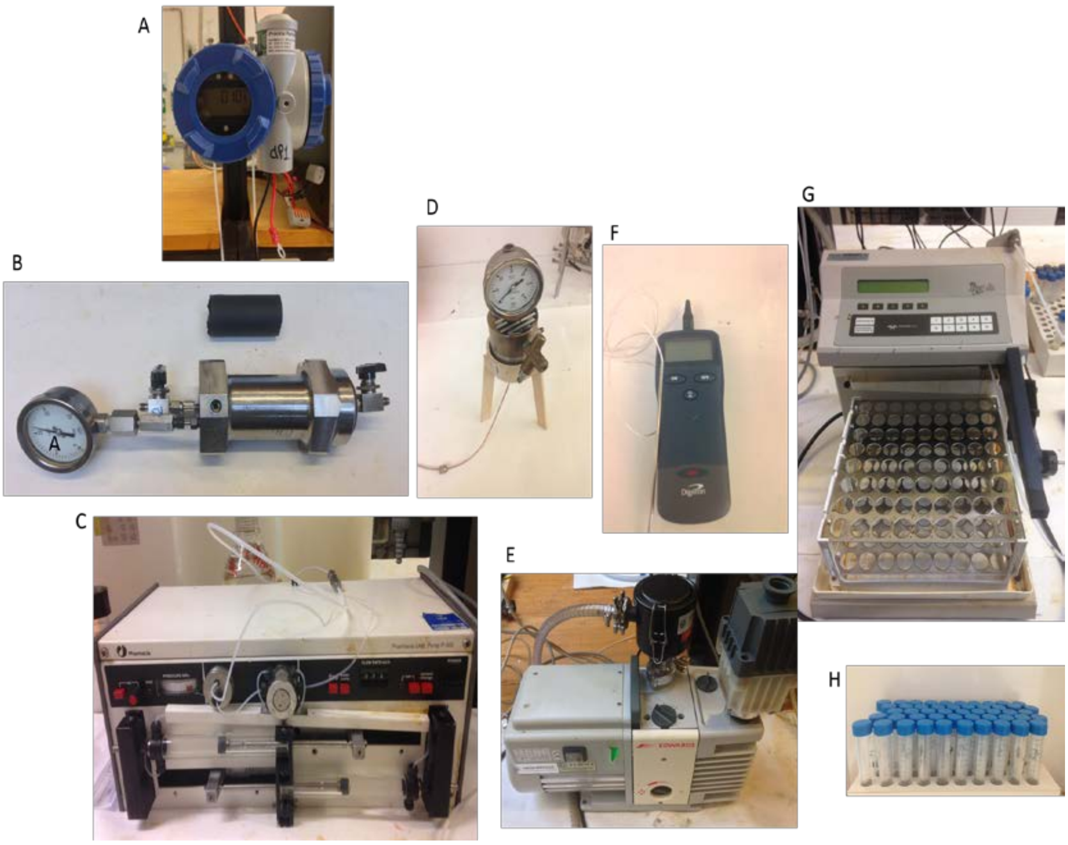

Figure 4.13: Experimental equipment

5 Results and Discussion

The objective of this research was to study the effect of LSW injection on recovery in Berea sandstone cores, concentrating on the effect brines with different ionic compositions and salinities had. Following the LSW injection a low salinity surfactant polymer (LSSP) flood was executed.

An explanation of the flooding sequences is given in 4.2.6 .

5.1 Fluid and Rock Properties

5.1.1 Density Results

All densities measured are given in appendix A.4 and only densities used during experiments are given in Table 5.1. The density measurements showed as expected [5] a decreasing tendency with increasing temperature. In addition, the density of diluted North Sea crude oil (NSCO) and the low salinity brine were as expected lower than their respective mother solutions. The densities were used as inputs in the IFT measurements.

Table 5.1: Density measurements, with uncertainty ± 0.001

T (°C)	ρ_{NSCO} [g/ml]	$\rho_{diluted\ NSC}$ [g/ml]	ρ_{SW1} [g/ml]	$\rho_{3000\ ppm\ NaCL}$ [g/ml]
23	0.8999	0.8115	1.024	0.9986

5.1.2 Interfacial Tension

IFT measurements were done for surfactants XOF 26S and XOF 25S in contact with diluted North Sea crude oil. Experiments were done on pre-equilibrated and pure samples of surfactant. As observed in The uncertainty is estimated to be 20% of measured value.

Table 5.2 and Table 5.3, surfactant XOF 26S gave the lowest interfacial tension and was chosen to be used in the LSSP experiment. The uncertainty is estimated to be 20% of measured value.

Table 5.2: First contact interfacial tension

T [°C]	σ_{XOF26S} [mN/m]	σ_{XOF25S} [mN/m]
23	$2.4*10^{-2} \pm 0.005$	$5.8*10^{-2} \pm 0.012$

The interfacial tension was also measured on samples of surfactant and oil which had been pre-equilibrated.

Table 5.3: Interfacial tension of pre-equilibrated surfactant-oil system

T [°C]	σ_{XOF26S} [mN/m]	σ_{XOF25S} [mN/m]
23	$1.6*10^{-2} \pm 0.003$	$4.7*10^{-2} \pm 0.009$

5.1.3 Viscosity Results

The viscosity of brine, surfactant and oil samples were measured with constant shear rate, while for polymer solutions the shear dependency was checked. Besides the polymer solutions, all values are measured at $100s^{-1}$. The apparent viscosity was calculated for the polymers, and the viscosity generated is given at $16\text{-}18s^{-1}$. It was chosen to use 300 ppm and 600 ppm HPAM in the LSSP experiment.

Table 5.4: Viscosity of different brines, the uncertainty is 5% of measured value

T [°C]	$\mu_{SW1\ SW1}$ [cp]	$\mu_{1/10\ SSW}$ [cp]	μ_{SW2} [cp]	$\mu_{3000\ ppm\ NaCl}$ [cp]
23	1.01 ± 0.05	1.04 ± 0.05	0.99 ± 0.05	0.93 ± 0.05

Table 5.5: Viscosity of oil used in experiment, DC was collected as effluent at $S_{wi,}$ the uncertainty is 5% of measured value

Core	T [°C]	μ_{DC} [cp]	μ_{CO} [cp]	$\mu_{Marcol\ 152}$ [cp]
J1	23	2.64 ± 0.13	33.31 ± 1.67	63.12 ± 3.16
J2	23	2.69 ± 0.13	33.31 ± 1.67	63.12 ± 3.16
J3	23	3.34 ± 0.17	33.31 ± 1.67	63.12 ± 3.16
J4	23	3.31 ± 0.17	33.31 ± 1.67	63.12 ± 3.16

Table 5.6: Polymer (HPAM) viscosity at different concentrations, the uncertainty is 5% of measured value

T [°C]	$\mu_{p,100\ ppm}$ [cp]	$\mu_{p,300\ ppm}$ [cp]	$\mu_{p,600\ ppm}$ [cp]	$\mu_{p,1000\ ppm}$ [cp]
23	2.26± 0.11	5.25 ± 0.26	11.64± 0.58	22.02± 1.01

Table 5.7: Surfactant viscosity, the uncertainty is 5% of measured value

T [°C]	$\mu_{XOF\ 26S}$ [cp]	$\mu_{XOF\ 26S\ equil}$ [cp]	$\mu_{XOF\ 25S}$ [cp]
23	1.16 ± 0.09	1.20 ± 0.09	1.18 ± 0.09

5.1.4 Rock Properties

Table 5.8: Rock properties

Core ID	Length [cm]	Diameter [cm]	Bulk Volume [cm³]	Pore volume [cm³]	Porosity [%]	Absolute Permeability [mD]	S_{wi} [%]
	±0.01	±0.01	±0.2	±0.2	±0.2		±0.1
J1	6.38	3.83	73.59	18.16	25.53	414 ± 20	26.2
J2	6.34	3.83	74.04	16.94	23.19	374 ± 15	21.9
J3	6.32	3.83	72.69	17.01	23.39	370 ± 15	24.0
J4	6.30	3.83	72.53	16.59	22.87	331 ± 13	24.1
C1	6.29	3.79	71.05	15.59	21.90	367 ± 15	23.7
C2	6.48	3.80	73.34	16.06	21.90*	309 ± 12	22.7
*It is assumed that C1 and C2 has equal porosity							

From Table 5.8 it is observed that both porosity and absolute permeability measurements differs between the core. The range of the absolute permeability measurements are in the range of 300-400 mD, and for cores J1-J4 it seems like there is some consensus between the porosity and measured permeability values. Due to leakage during porosity measurements of C2, it is assumed that cores C1 and C2 have equal porosity as they are cut from the same batch.

5.2 Production Profiles

Production profiles for all waterflood experiments are given in Figure 5.1 to Figure 5.6. Important production parameters for secondary water injection mode are summarized in Table 5.9, Table 5.10 and for tertiary mode in Table 5.13. More detailed experimental data is found in the appendix.

Pressure was measured continuously and recorded every second. The pressure data has later been averaged to simplify the input in the curves. The averaging has been done in the add-on TDMS Reader in MATLAB Compiler Runtime. Abrupt changes in the pressure profiles are due to changes in rate. Three rates have been used; 0.1 ml/min, 0.5 ml/min and 1 ml/min.

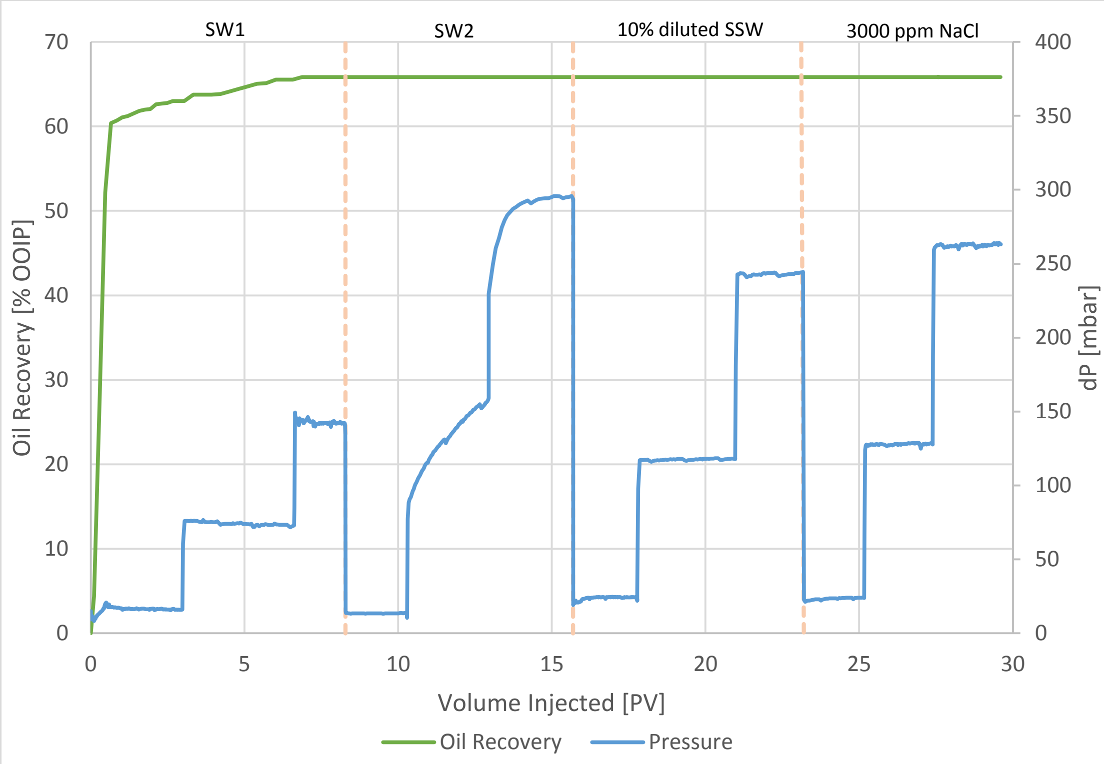

Figure 5.1: Oil recovery curve obtained from coreflood experiments in Berea core J1. The blue curve represents the differential pressure over the core, while the green curve represents the total recovery of OOIP

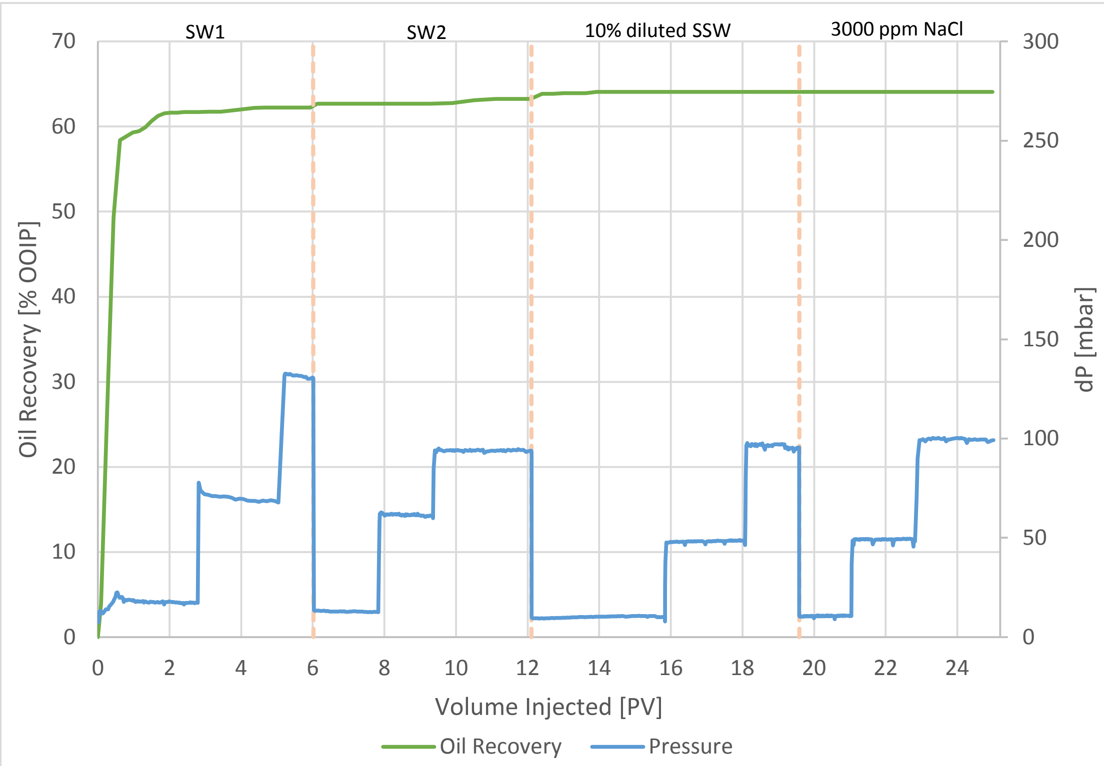

Figure 5.2: Oil recovery curve obtained from coreflood experiments in Berea core J2. The blue curve represents the differential pressure over the core, while the green curve represents the total recovery of OOIP

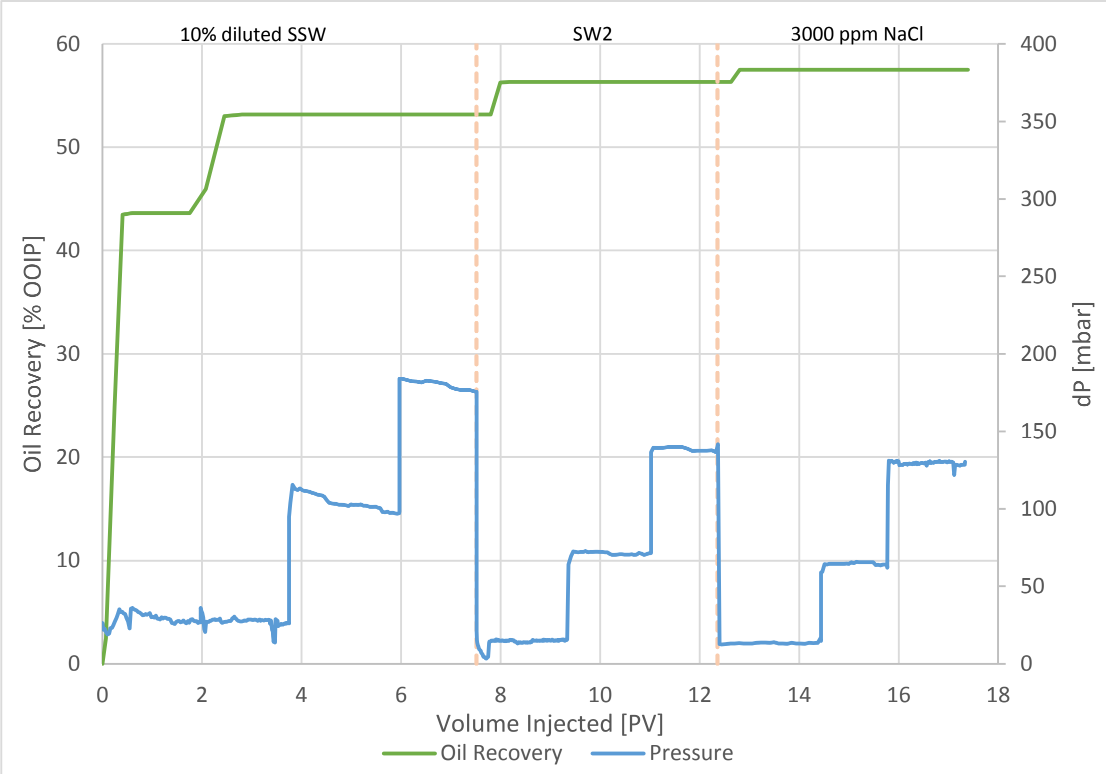

Figure 5.4: Oil recovery curve obtained from coreflood experiments in Berea core J3. The blue curve represents the differential pressure over the core, while the green curve represents the total recovery of OOIP

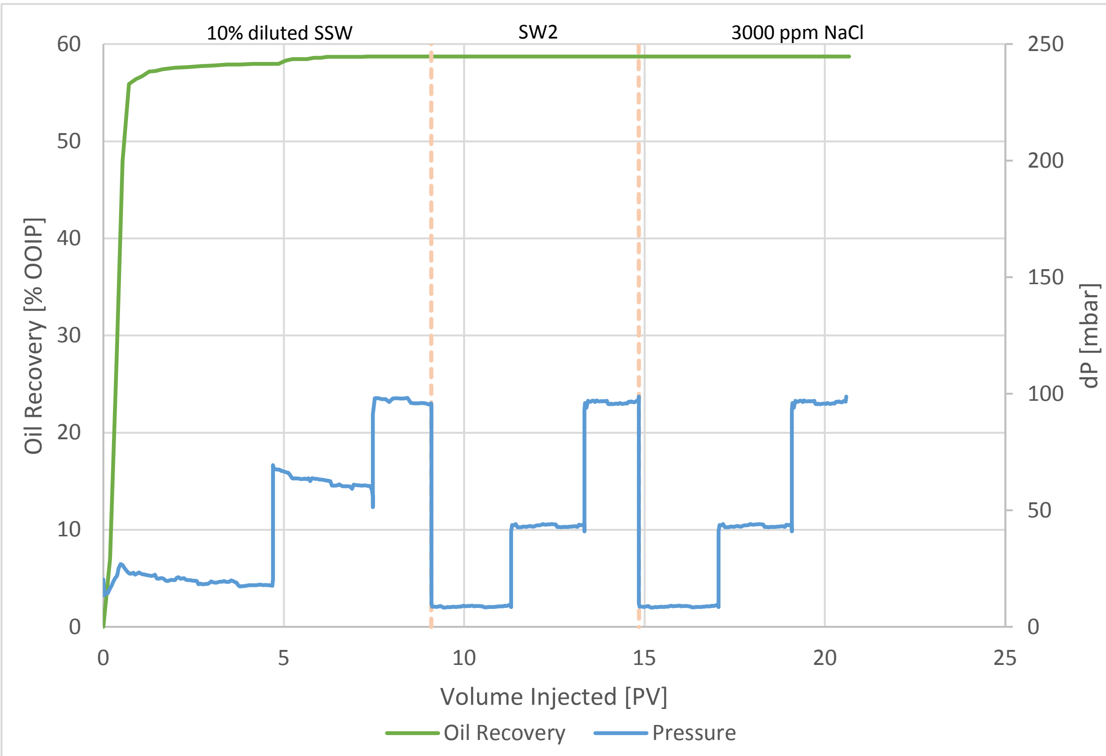

Figure 5.3: Oil recovery curve obtained from coreflood experiments in Berea core J4. The blue curve represents the differential pressure over the core, while the green curve represents the total recovery of OOIP

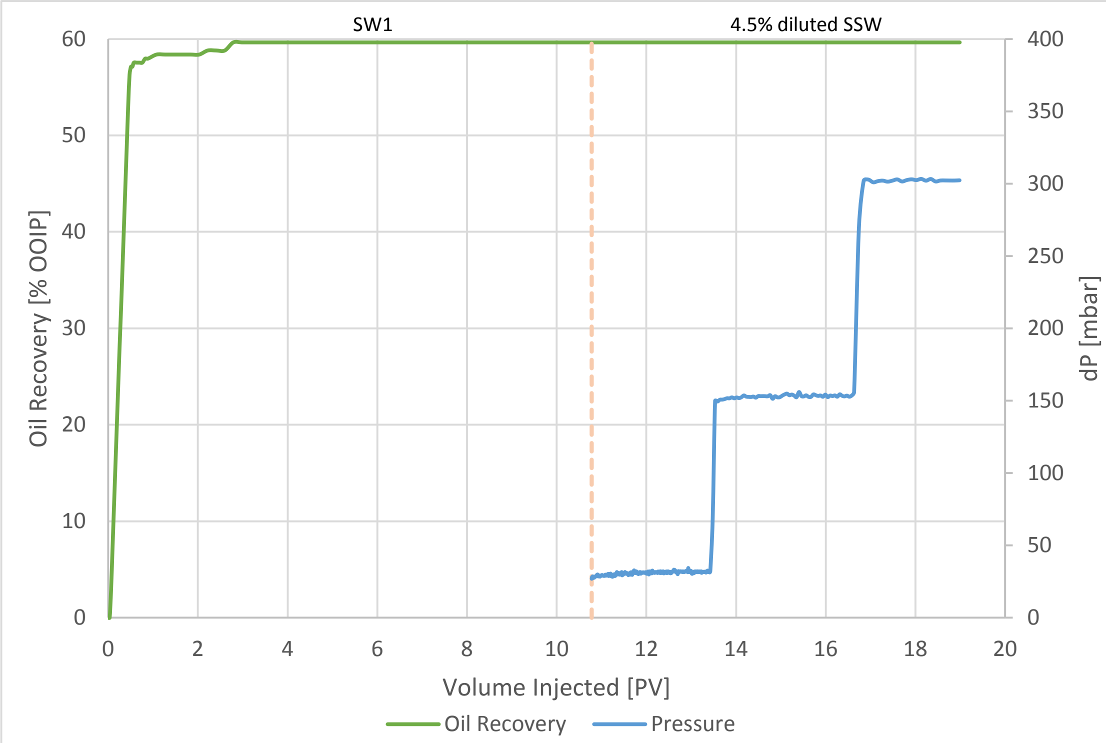

Figure 5.5: Oil recovery curve obtained from coreflood experiments in Berea core C1. The blue curve represents the differential pressure over the core, while the green curve represents the total recovery of OOIP

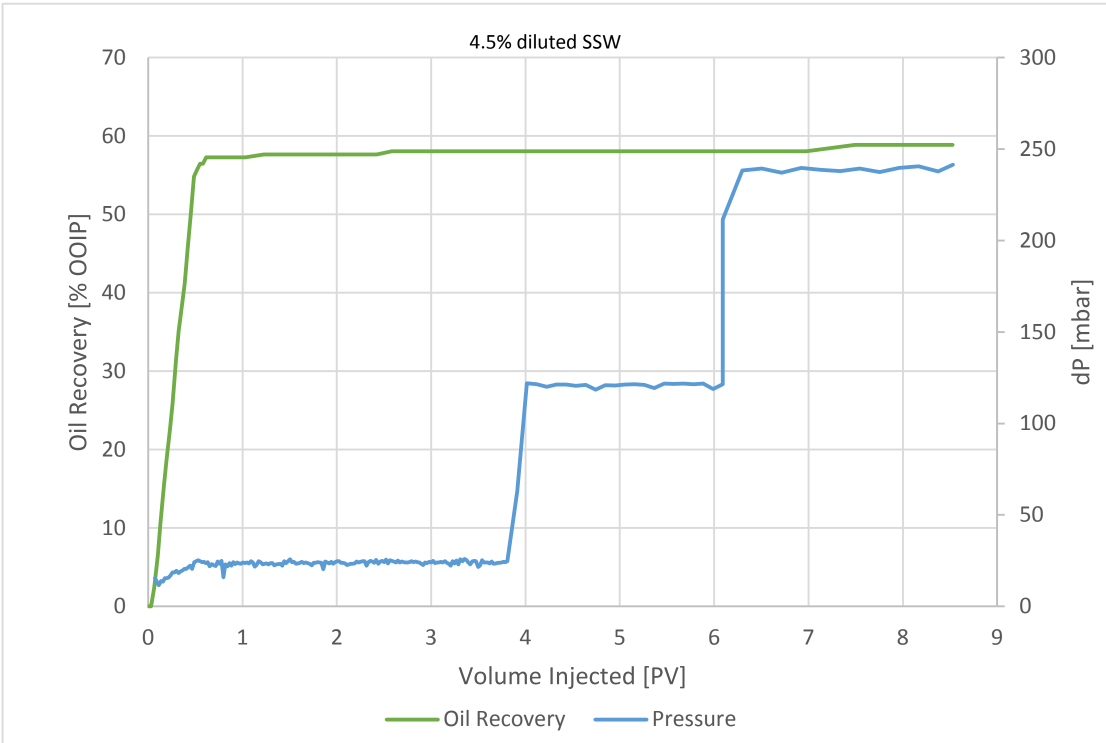

Figure 5.6: Oil recovery curve obtained from coreflood experiments in Berea core C2.. The blue curve represents the differential pressure over the core, while the green curve represents the total recovery of OOIP

5.3 Secondary Mode Waterflooding

5.3.1 Secondary Synthetic Seawater (SW1) Waterflood

Three cores were flooded with SW1, whereas two of the cores (J1-J2) were aged and the other unaged (C1). The waterfloods were executed in accordance with sequence 1 and 3 in 4.2.6. The purpose of the SW1 injection is to establish a conventional waterflood in which low salinity flooding can be investigated in tertiary mode. Important experimental data is summarized in Table 5.9.

Table 5.9: Experimental data from SW1 secondary mode

Core ID	WBT [PV]	WBT [% OOIP]	SW1 Recovery [% OOIP]	$S_{or,SW1}$ [% PV]	K_{rw} ($S_{or,SW1}$)
	± 0.01	± 2.0	± 2.0	± 1.0	± 0.01
J1	0.66	60.40	65.86	25.17	0.16
J2	0.61	58.39	62.25	29.04	0.19
C1	0.54	57.54	59.64	30.78	0.10

5.3.2 Secondary Low Salinity Waterflood (LSW)

For LSW in secondary mode, two aged cores (J3-J4) and one unaged core (C2) was investigated. Studying the effect of LSW injection contrary to SW1 injection in secondary mode may give an indication on which stage in production LSW may be most beneficial. The flooding procedures in sequence 2 and 4 in 4.2.6 were followed in these experiments. Important data gathered is summarized in Table 5.10.

Table 5.10: Experimental data from LSW secondary mode

Core ID	WBT [PV]	WBT [% OOIP]	LSW Recovery [% OOIP]	$S_{or,LSW}$ [% PV]	K_{rw} ($S_{or,LSW}$)
	± 0.01	± 2.0	± 2.0	± 1.0	± 0.01
J3	0.41	43.49	53.16	35.58	0.14
J4	0.62	55.89	58.72	31.31	0.29
C2	0.52	55.65	57.78	31.75	0.12

5.3.3 Observations

Based on the waterfloods done in secondary mode, indications of wettability alteration on the aged cores may be observed. Studies of waterflood characteristics such as production profiles, water breakthrough (WBT) and endpoint water permeabilities may indicate to which degree the wettability has been altered [82]. These characteristic may only serve as an indication of the wettability state.

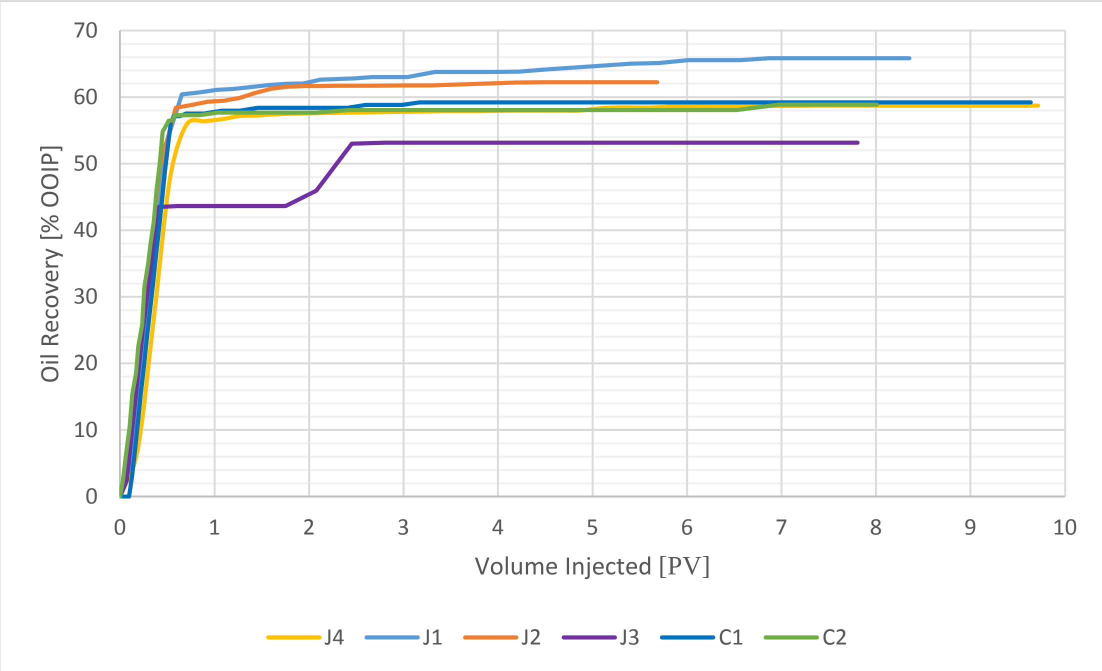

Figure 5.7: Experimental recovery data for secondary mode injection

Summarized from 2.9, oil-wet systems have earlier breakthrough and longer tail production compared to water-wet systems. A comparison of the aged and unaged cores, for both SW1 and LSW, shows little difference in WBT saturations, except for J3. As expected, it is notable that the aged cores have higher tail production compared to the unaged cores. It is of interest that the aged cores injected with SW1 has the longest tail productions. This can be observed in Figure 5.7. A comparison of endpoint water relative permeabilities in Table 5.9 and Table 5.10 shows an increase in water permeability for aged cores compared to unaged cores. This is in accordance with previous studies [4] stating that the affinity for water decreases with increased oil wettability, increasing the water permeability.

Based on Skauge & Ottesen [17], it is expected that the S_{or} will be reduced towards a neutral-wet state. This is illustrated in Figure 2.11. Based on S_{or} values in Table 5.9 and Table 5.10, only the aged rocks in the SW1 flood reduced its S_{or} values compared to the unaged core.

Comparing the relative oil permeability before and after aging may also give indications of wettability alteration [101]. As the core shifts towards a more intermediate-wet state it is expected that the oil permeability will be reduced due to the increased oil affinity of the rock. This is also the case in this experiment, as seen from Table 5.11.

Table 5.11: Permeabilities before and after aging

Core ID	Absolute Permeability [D]	K_{ro} (S_{wi}) Before aging	K_{ro} (S_{wi}) after aging
J1	414	1.16	0.94
J2	374	1.05	0.91
J3	376	1.17	0.74
J4	331	1.28	1.12

Based on these observations it is hard to conclude if any significant wettability alteration has occurred in J3 and J4 during aging. Although some parameters show an alteration of wettability, others show no different behavior than for the water-wet system. It is possible that some alteration towards oil-wet has occurred in J3 and J4, but not in a significant order. The cores J1 and J2 seems to have an alteration towards more oil-wet, as many of the parameters show a shift towards a more oil-wet behavior.

The most interesting and important observation in the secondary mode floods is the difference in oil recovery between SW1 and LSW. From literature (3.1) it was expected that LSW would give higher recoveries compared to SW1. One explanation to this could be that the SW1 waterflood was performed under more neutral-wet conditions. This would lead to an increased production compared to more water-wet conditions. The importance of the initial wettability state of the porous medium before LS injection has been stated by Shaker Shiran [92].

Table 5.12: Endpoint mobility ratios for secondary mode flooding

Core ID	M^0_{LSW}
J1	0.44
J2	0.56
J3	0.61
J4	0.83
C1	0.32
C2	0.36

The endpoint mobility ratios in Table 5.12 show that all the displacements are favorable and fingering is not expected to affect the displacing front. Although the values are low, there is some extent of deviation between the different cores. It is noteworthy that the cores flooded with low salinity brine has higher endpoint mobility ratios compared to the other cores. This may be the reason for the poor result with low salinity brine in secondary mode.

Assuming that the aging process has yielded equal intermediate wettability states for all the aged cores, it can be argued that the low salinity brine has induced a shift in wettability towards a more water-wet state. This has been reported by multiple authors [26, 29, 30, 35, 44, 64, 66, 67]. The composition of the connate water is equal to SW1 and injecting SW1 into the cores is not expected to change the wettability. This is due to cores already being in equilibrium with SW1. Cores flooded with SW1 will therefore maintain its intermediate wetting. In the cores injected with 10 % diluted SSW a change in wettability is possible, as the connate water and injection water is not initially in equilibrium. While equilibrium is achieved a change in wettability may occur. An alteration towards more water-wet, may explain the reduced production by LSW.

Observations of less recovery with LSW compared to SSW injection has been observed earlier. Hamouda et al. [102] performed secondary flooding experiments on aged Bentheimer sandstone cores at 70°C. In their experiments the effect of LSW (4 wt.% diluted SSW) showed a 9% OOIP less production compared to the SSW flood, resulting in a 22% OOIP total production.

Winoto et al. [38] also experienced reduced secondary production from outcrop sandstone cores injected with LSW compared to SSW. In the experiment the composition of the injected brine and the connate brine were the same, i.e. in the LSW flood the connate was low saline. Reduced production (2-5% OOIP) was observed in two of six injected sandstone cores.

The execution of the experiments of Hamouda et al. [102] and Winoto et al. [38] are not similar to the experiments in this thesis, comparison of the results should therefore be done with caution due the complexity of crude oil/brine/rock (COBR) interactions. In spite of this, results obtained in the secondary flood in this thesis and in the work of Winoto et al. [38] and Hamouda et al. [102] emphasizes the importance of studying the COBR interactions prior to field implementation.

5.4 Tertiary Low Salinity Waterflood

All cores, except for C2, were tested for LSE in tertiary mode. The procedure was in accordance with sequence 1, 2 and 3 in 4.2.6 for the respective cores. The LSW flood continued in tertiary mode in J3 and J4 with brines of different ion composition and salinity compared to the secondary mode. Cores J1, J2 and C1 had previously been injected with SW1 and were to be exposed to low salinity brine for the first time, injected at $S_{or,SW1}$.

5.4.1 Oil Recovery from LSW

Important experimental parameters are summarized in Table 5.13. The table shows the response to low salinity brine after all the tertiary low salinity floods. Response for tertiary mode LSW was observed in two of five cores.

Table 5.13: Experimental data from tertiary LSW

Core ID	LSW incremental Recovery [% ROIP]	Total Recovery after LSW [% OOIP]	$S_{or,LSW}$	$\Delta S_{or,LS}$ ($S_{ors,SW1}$ - $S_{or,LSW}$)	K_{rw} ($S_{or,LSW}$)
	± 1.0	± 2.0	± 1.0	± 0.1	0.01
J1	0	65.86	25.17	0	0.08
J2	4.81	64.06	28.03	1.42	0.25
J3	9.36	57.50	32.28	3.29	0.19
J4	0	58.72	31.31	0	0.32
C1	0	59.64	30.78	0	0.08

The effect of injecting low salinity brine in tertiary mode with different salinity and ion compositions is given in Table 5.14 . The flooding sequences for each core are given in Table 4.5.

Table 5.14: Experimental data from tertiary floods

	Incremental recovery (% ROIP)		
Core ID	1st flood	2nd flood	3rd flood
	± 0.50	± 0.50	
J1	0	0	0
J2	2.61	2.26	0
J3	6.78	2.66	-
J4	0	0	-
C1	0	-	-

5.4.2 Observations

The cores that showed a positive response to LSW injection in tertiary mode were the aged cores that had the least response to the secondary mode flooding (Table 5.9 and Table 5.10). For both cases, production in tertiary mode is observed for brine of two different ionic compositions and salinities.

The production in J2, as seen in Figure 5.3 and Figure 5.8, is experienced after changing the injection fluid from SW1 to SW2. Production of oil occurs in two stages during the flood, in the start, at 0.1 mL/min, and in the end of the flood. In the end, the production is observed when the rate is increased to 1 ml/min. Further reduction in salinity, injecting the 10 % diluted SSW, increases the production at low rates. Increasing rates and changing the injection brine to 3000 ppm NaCl does not further increase oil recovery. No pressure buildup or fines in the effluent were observed, indicating that microscopic flow diversion is not a key contributor to the increased oil recovery. This is in accordance with previous work done by Boussour et al. [103] and Cissokho et al. [104].

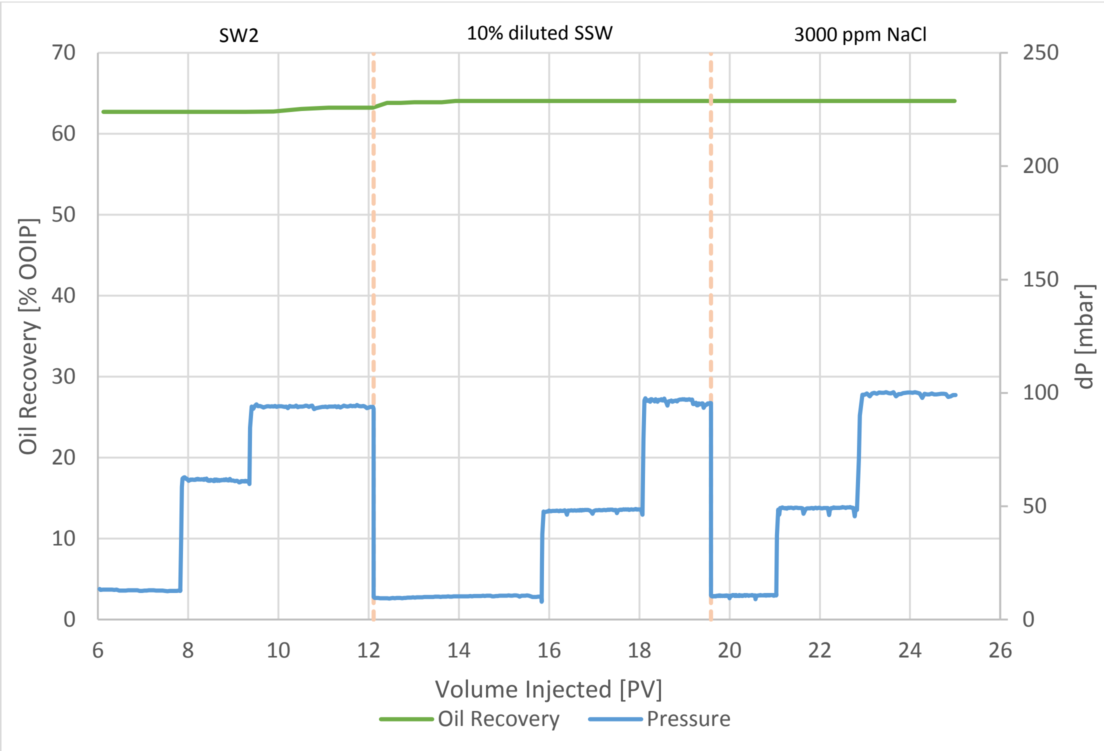

Figure 5.8: Tertiary mode production profile for J2

Incremental oil recovery in J3 also occurs in two stages, as observed in Figure 5.4 and Figure 5.9. The first increase in production is seen when injecting SW2. This flood goes up in salinity and ionic strength compared to the preceding 10 % diluted SSW injection. The production ceases fast, and no production is further observed for this flood. When changing to injection of 3000 ppm NaCl, a small incremental recovery is observed. As for J2, no pressure buildup or fines in the effluent were discovered.

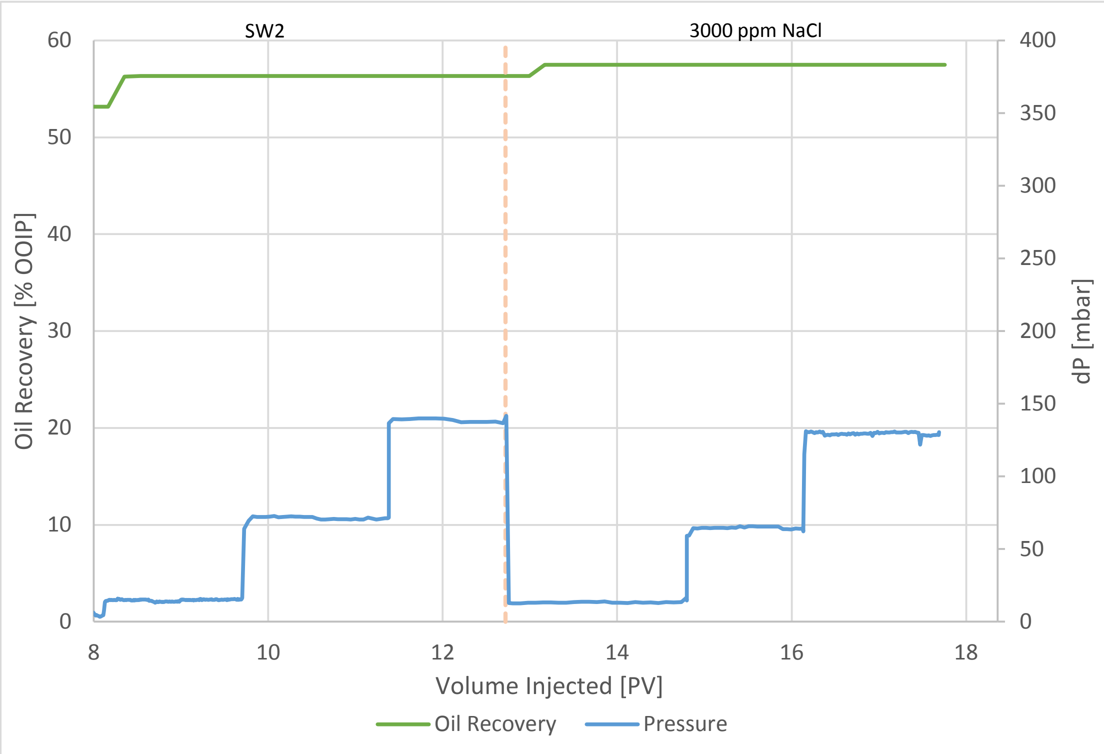

Figure 5.9: Tertiary mode production profile in J3

Observations of oil production when removing divalent ions from the injection water has been observed by Cissokho et al. [105], Ligthelm et al. [64], and Zhang et al. [30]. All experiments used NaCl brine of different salinities, experiencing increased production (10-13% OOIP) when reducing salinity of the injected brine. As Ligthelm et al. [64] and Zhang et al. [30] had preflushed the cores with a higher salinity NaCl brine, the cores only contained Na^{+}, and no cation exchange or stripping effects were expected to occur. Nevertheless, production was observed , which Ligthelm et al. [64] attributed to double layer expansion.

In the first tertiary flood in J2 the salinity is reduced compared to the preceding flood and no divalent ions reside in the injection water. In theory this will increase the double layer, inducing a possibility for wettability alteration. It may also induce an increase in production as sites containing divalent ions will be exchanged with monovalent ions in an effort to reach equilibrium, detaching oil adhering to these sites. In the next flood the salinity is further reduced and the double layer is expected to further expand, inducing higher recoveries. As there is no significant pressure increase or increase in pH, enhanced recovery by fines migration, clay swelling and/or pH increase is not expected to be the cause.

In the first tertiary flood (SW2) in J3 it is hard to determine the behavior of the double layer. As the salinity of the injected brine(SW2) is increased it is expected that the double layer will decrease, but simultaneously the divalent ions are removed which would have induced an expansion of the double layer. Without knowing which mechanism is prevailing, a conclusion on the behavior of the double layer is hard to determine. However, oil adhering to clay sites by cation binding may be removed, resulting in increased production. In the 3000 ppm NaCl flood, initial conditions are similar to those experienced by Ligthelm et al. [64] and Zhang et al.[30], where divalent ions are removed from the core. By reducing salinity of the injected brine compared to the residing water, it is expected that the double layer will expand. As all divalent ions are removed from the core, no cation exchange nor stripping effect are expected to occur. It is therefore possible to assume as Ligthelm et al. [64]; double layer expansion may be the cause of the increased production in the 3000 ppm NaCl flood.

Observed in Figure 5.1 and Figure 5.10, an increase in pressure occurs during the first tertiary flood on J1. When increasing the rate from 0.1 ml/min to 0.5 ml/min, a gradually increasing trend in the pressure is observed, but no oil is recovered. Since it was of interest to conduct comparable experiments, and no oil was produced for 2 PV, it was decided to increase the rate. This lead to a new gradually increasing trend in pressure that starts to stabilize after 2 PV of injection. As no oil was recovered in this step either, it was decided to continue the experiments by injecting the next brine.

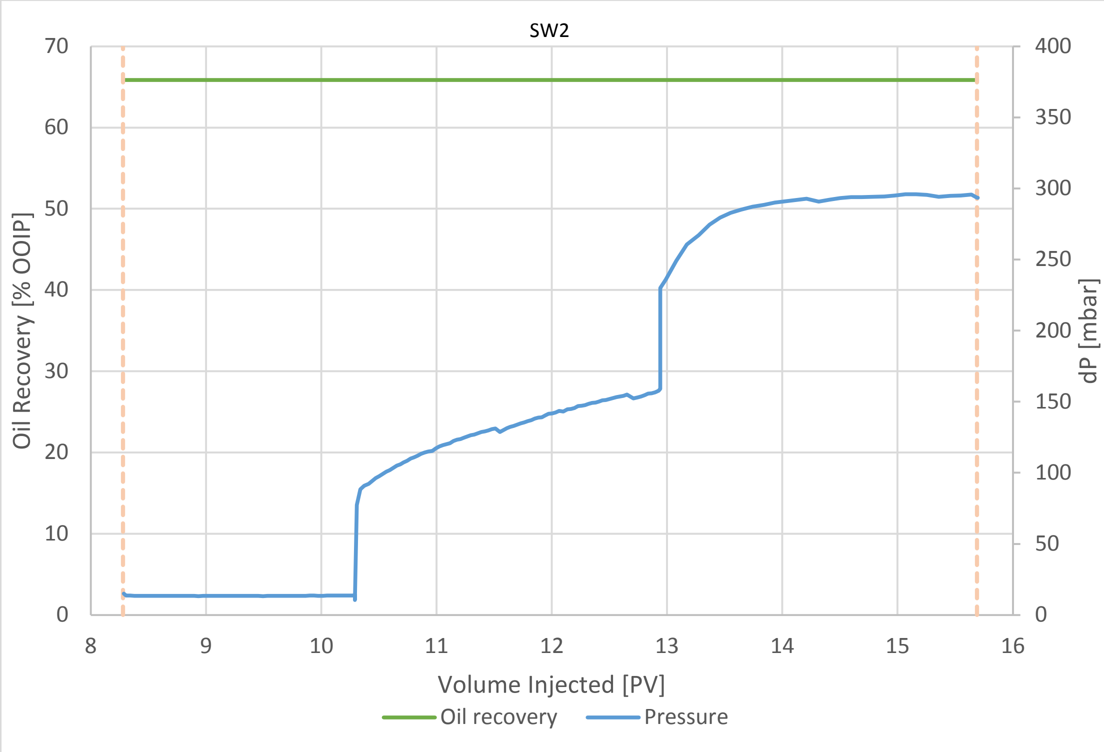

Figure 5.10: Production profile for SW2 in J1, with gradually increasing pressure. The oil recovery is expressed as % OOIP, no oil production is observed.

The pressure increase may have come as a result of fines migration or clay swelling in the core. This reaction is only seen during the flood that had the divalent ions (Ca^{2+} and Mg^{2+}) removed from the injection water. By removing the divalent ions from the injection water, destabilization of the clay may occur as Na^{+} ions intrude into the clay structure, releasing clay particles. From Figure 5.11, it is observed that endpoint permeability is reduced to half, as the differential pressure over the core has increased. This may indicate blockage of pores.

This phenomena has been reported by multiple authors [52, 106-111], where it is experienced that removal of divalent cations, as calcium and magnesium, from the injection water leads to a decrease in permeability. The decrease in permeability is suggested to be a result of fines migration or clay swelling blocking pore throats. This behavior is also experienced to occur when salinity contrast between the injected brine and the formation brine is high, resulting in a salinity shock through the porous medium [106, 112, 113].

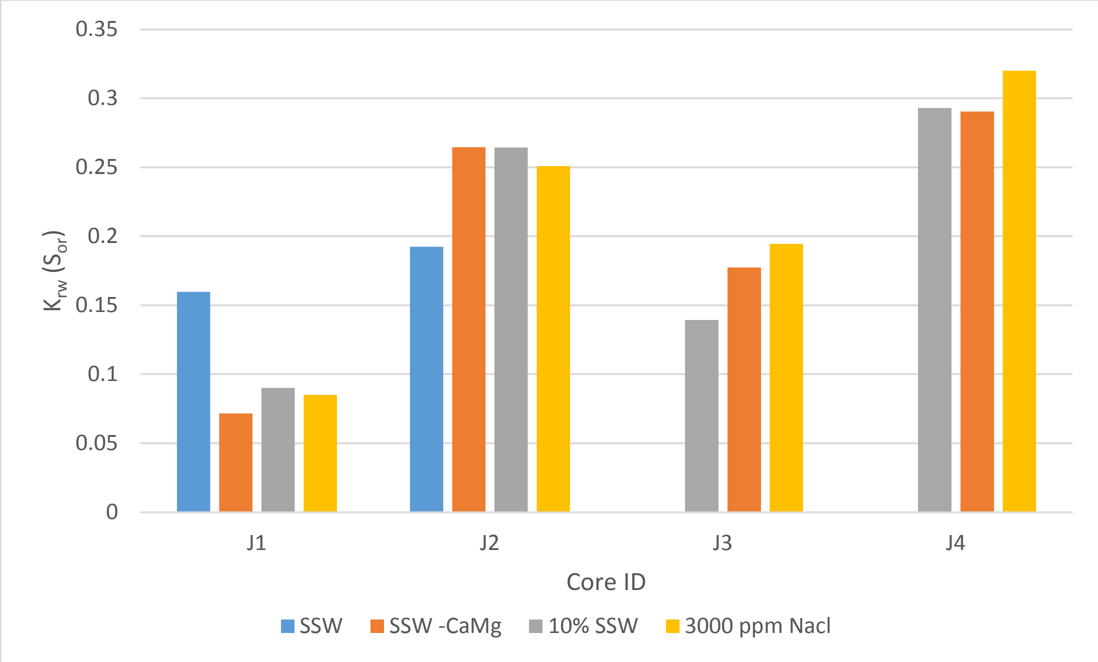

Figure 5.11: Endpoint water relative permeabilities after each coreflood, flooding sequences are from left to right

Zhang & Morrow [29] experienced a similar pressure increase when injecting distilled water into comparable Berea cores relative to those used in this experiment. No production of oil was observed, ascribing the pressure increase to permeability damage caused by salinity contrast. Boussour et al. [103] also experienced an increase in pressure when reducing the salinity of the injected brine on a reservoir core. The brine was free for divalent ions and no increase in production was observed. During the experiments fines production was observed, giving indication of migration being the reason for the increased pressure.

As Berea sandstone consist of little to no amount of expanding clays, like montmorillonite or bentonite [58, 114], the author believes that the pressure increase may be an effect of fines migration. Although this may be an explanation, no fines were observed in the effluent. Despite the fact that no oil was produced due to the pressure buildup, one may argue that the oil may have been redistributed in the core before being capillary trapped again.

In Figure 5.1, it is observed that the following floods for J1 exhibit stable pressures, indicating that possible fines migration have been stabilized. This happens when injecting 10 % diluted SSW that contains divalent ions. It is known that divalent ions stabilize clay by lowering the Zeta potential, resulting in lowering of the repulsive force [115, 116].

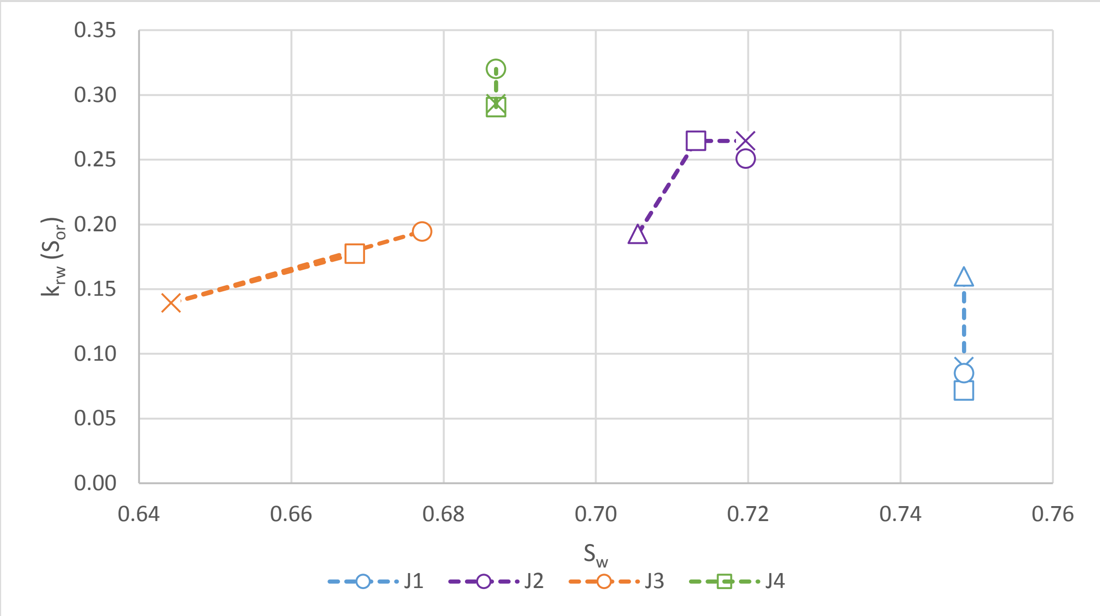

Figure 5.12: Relative water permeability as a function of water saturation. Figure description: Δ : SW1 flood ◻: SW2 flood x : 10 wt,% diluted SSW ○ : 3000 ppm NaCl

It is noteworthy that although no production is seen in J1, there is still an increase in endpoint relative water permeability, as seen in Figure 5.11 and Figure 5.12. This behavior may be attributed to redistribution of oil in the reservoir, could imply a change in wettability towards a more oil-wet system or it may be a result of the stabilization of fines. A change towards more oil-wet conditions may also happen as a consequence of stabilization of fines, as oil may adhere to the clay due to cation exchange.

An increase in endpoint relative water permeability is observed in J4, as the 3000 ppm NaCl flooding increases the permeability without reducing the S_{or}. This may indicate an alteration of wettability or redistribution of the oil, as for J1. Although J3 and J4 shows an increasing trend in endpoint relative water permeability, S_{or} is also reduced, making it difficult to conclude on any wettability alteration occurring.

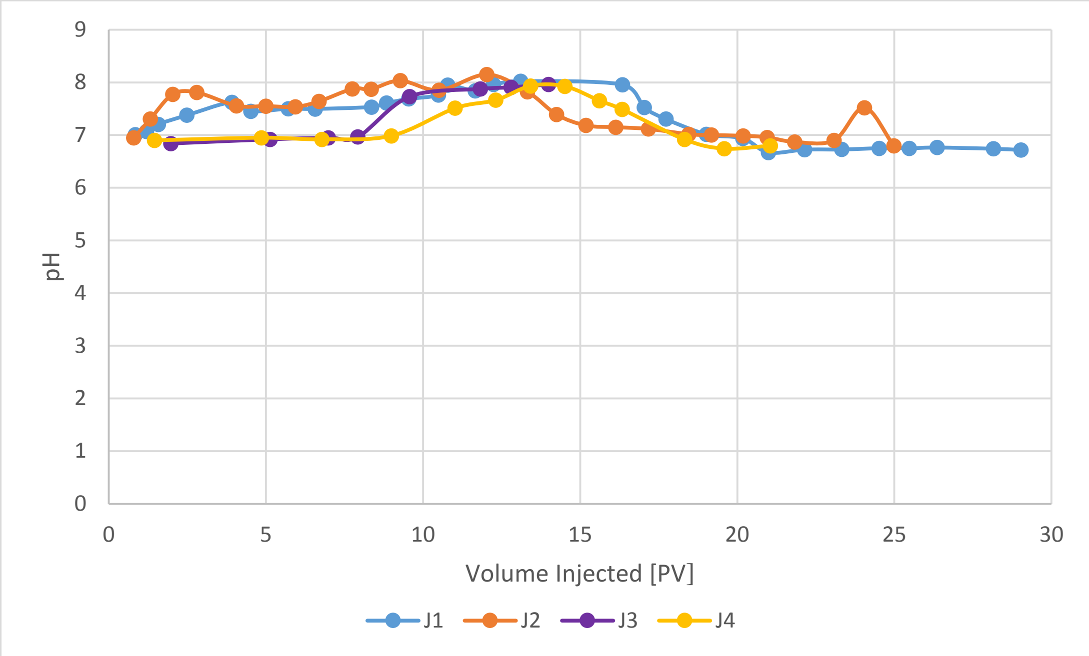

Figure 5.13: pH measurements of the effluent

The pH measurements were done post-experimental on cores J1-J4 (Figure 5.13). The pH varies between 6.5 and 8, thus no significant pH change is observed during flooding. Single pH curves are given for each core in Appendix A.5.

Lack of response to pH has been reported by multiple authors [39, 43, 48, 85]. It is also important to point out that the cores that produced under tertiary mode have same trends in pH as the cores that did not produce. As pH don't vary much and the acidity of the effluent is nearly neutral, pH is not seen as a factor for increased recovery in these experiments.

5.5 Low Salinity Surfactant Polymer flooding (LSSP)

Following the LSW injection, the cores were injected with a LSSP flood. The procedure was similar for all cores, given in 4.2.7. The production curve for each core is given in Appendix A.9. Summarized production data is given Table 5.15.

Table 5.15: Experimental results (LSSP)

Core ID	LSSP incremental Recovery [% ROIP]	LSSP incremental Recovery [% OOIP]	Total Recovery after LSSP [% OOIP]	$S_{or,LSSP}$	$\Delta S_{or,LS}$ ($S_{ors,SW1}$ - $S_{or,LSW}$)	K_{rw} ($S_{or,LSSP}$)
	± 2.0	± 2.0	± 3.0	± 1.0	± 0.1	± 0.01
J1	26.47	9.04	74.90	18.51	6.66	0.09
J2	30.52	10.97	75.04	19.48	8.56	0.08
J3	19.31	8.21	65.71	26.05	6.23	0.10
J4	19.06	7.87	66.59	25.35	5.97	0.17
C1	9.90	4.62	63.84	27.57	3.52	0.08
C2	31.86	13.10	71.98	21.63	10.12	0.13

Table 5.16: Capillary number after each chemical flood

Core ID	$N_{vc, surf}$	$N_{vc, 300 ppm HPAM}$	$N_{vc, 300 ppm HPAM}$
	± 0.3E-05	± 0.3E-05	± 0.3E-05
J1	5.78E-05	2.67E-04	5.98E-04
J2	5.79E-05	2.63E-04	5.83E-04
J3	5.80E-05	2.64E-04	5.86E-04
J4	5.79E-05	2.60E-04	5.71E-04
C1	5.90E-05	2.65E-04	5.84E-04
C2	5.37E-05	2.42E-04	5.33E-04

5.5.1 Observations

It is observed from Table 5.5 that combining a low salinity environment with chemical additives, such as surfactants and polymers, results in an enhanced oil recovery of 10-32% ROIP.

The general trend observed in the production curves is an increase in the differential pressure when injecting surfactants. This is due to the formation of an oil bank induced by the decreased interfacial tension between oil and water. The decrease in interfacial tension may influence the oil production by mobilizing oil that has been trapped, as mentioned in chapter 2.4, or by invading the smaller uncontacted pores due to more favorable capillary pressure. Little production is experienced during the first pore volume of injection. Further injection of polymer, i.e. increasing the viscous forces, enhances the differential pressure and production is detected in all cores. After one PV of injected polymers the core is flushed with a 3000 ppm NaCl solution until a stationary state of no more oil production is reached. The following polymer flood increases the differential pressure, and production is again seen from the cores. NaCl is then injected until no production is observed from the core. Previous studies [117] have shown production of fines during surfactant flooding. No fines were observed in these experiments, and fines migration or clay swelling is not seen as a cause for the pressure buildups experienced during LSSP. The slug sizes of the surfactant and polymer injection were decided to be one PV, as it is of economical interest to achieve highest possible recovery with least possible injection costs [118]. Slug optimization was not performed, as it was not part of this thesis.

Comparing the different recoveries divulges a higher total recovery for J2 and C2 compared to the other cores.

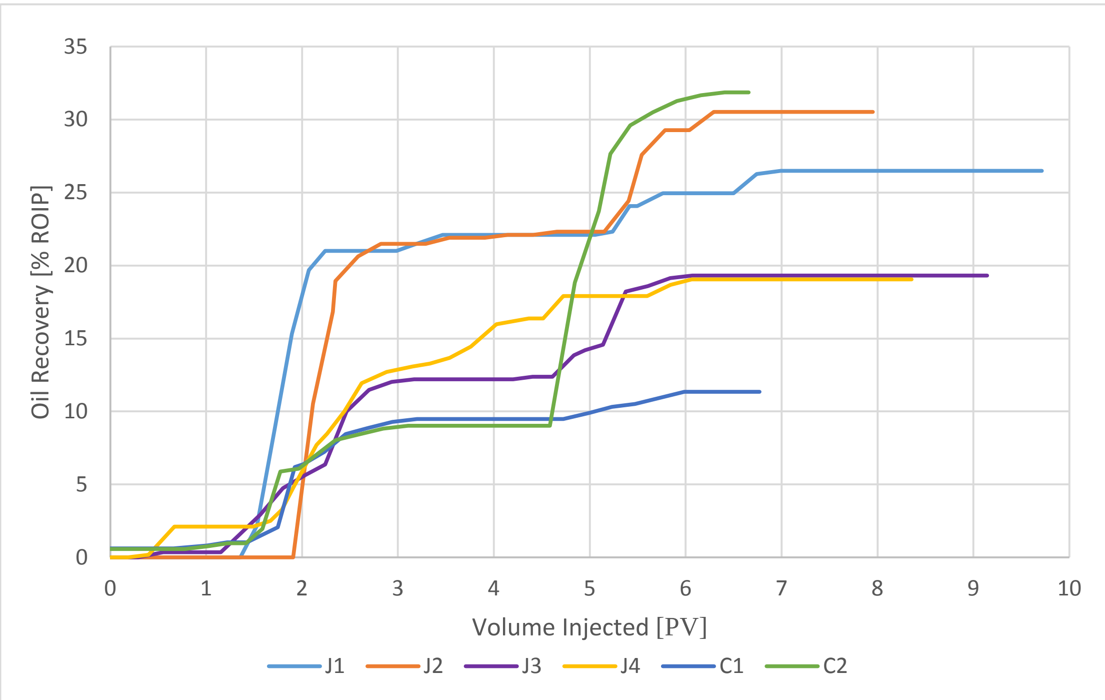

Figure 5.14: Incremental recovery of residual oil after LSW waterflood

Studying Figure 5.14, the effect of the LSSP flood is better understood. Figure 5.14 illustrates the incremental recovery of residual oil after the LSW waterfloods. Similar to previous floods, cores J1 and J2 responds well to the injected fluid, and has a high production of oil early in the flooding sequence.

The core that responded best to the LSSP flood was C2. From Figure 5.14, it is observed that the unaged cores, C1 and C2, have almost equal response to the injection fluid until the 600 ppm HPAM flood. In the latter flood, C2 experiences an increase in incremental production of 20% OOIP, resulting in the highest recovery of all tested cores. A reason for this behavior could be that the retention is satisfied after 300 ppm HPAM injection, leading to little retention during the 600 ppm HPAM injection.

Disregarding the effect of 600 ppm HPAM on C2, the cores that responds best to the LSSP are the aged cores. This has previously been reported for surfactants by Alagic [82] and Solbakken [117] . The behavior was explained by Alagic [82] to be due to less water-wet cores containing more unstable oil layers, with larger degree of continuous oil. The effect of using surfactants was therefore thought to be more an effect of avoiding re-trapping of oil at low capillary pressure, than oil mobilization due to higher capillary numbers.

From literature [119], the critical capillary number for water-wet and intermediate-wet Berea sandstone are ~10^{-5} and ~10^{-4}, respectively. From Table 5.16 it is observed that the capillary number for the surfactant flood is in the critical area of the capillary desaturation curve for Berea sandstone. This is also illustrated in Figure 5.15. This may be an explanation for the low response observed early in the LSSP. Another explanation may be that not sufficient amounts of surfactants were injected. In the work of Alagic [82] the majority of enhanced production by low salinity surfactant flooding was observed after 1 PV, it could therefore been beneficial to inject larger surfactant slugs. It is important to emphazise that optimization of the surfactants have not been done, and that the surfactant system chosen has only been chosen based on interfacial tension measurements. Optimization of the surfactant system could enhance the effect of the surfactant flood. Increasing the viscous forces, injecting 300 ppm HPAM, the capillary number gets more favorable, and increased production is observed in all cores. When adding polymers to the injection water, the efficiency of oil banking is improved as a result of more favorable mobility ratio, thereby increasing the displacement efficiency. It is assumed that the polymer does not influence the interfacial tension between the oil and brine. Further increase in the viscous forces increases the production from the cores.

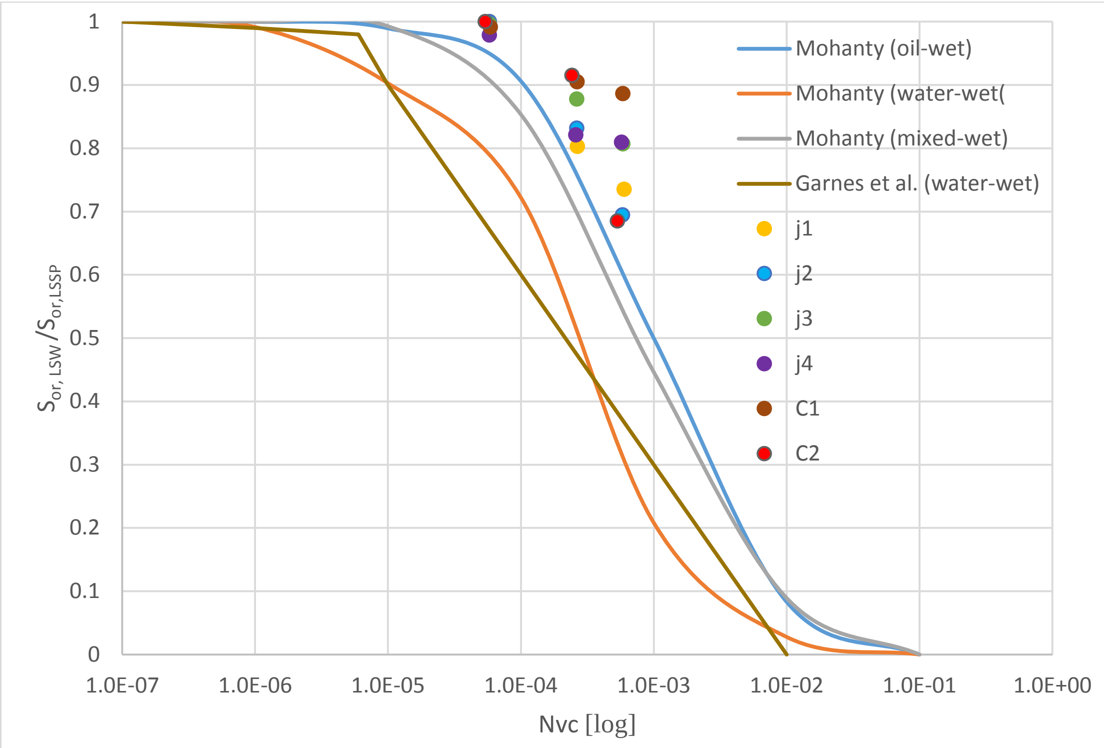

Figure 5.15: Comparison of the capillary numbers obtained in the experiments with literature values for Berea Sandstone [9, 119]

From Figure 5.15 it is possible to analyze the capillary numbers obtained in these experiments, showing some deviation compared to literature values. One explanation to this could be that the slug sizes chosen were too small. It is believed that bigger slug sizes, either of surfactants or polymers, could have given higher recovery, as production was still occurring when the slugs sizes ended. This would have given higher reduction in S_{or}, and give more correct values compared to literature. Unpublished work by Al-Ajmi [120] confirm this, observing increased recovery with increased surfactant slug sizes.

Retention of surfactants during flooding at residual oil saturation can be expected due to (i) adsorption onto the rock surface, (ii) trapping in immobile hydrocarbon phases and (iii) precipitation with divalent ions [73]. No precipitation is expected, as the cores are free for divalent ions. Presuming that cores J1 and J2 are more oil-wet compared to the cores J3, J4, C1 and C2, may explain the recovery behavior during LSSP. It is believed that anionic surfactant retention in water-wet systems are higher compared to more oil-wet systems. This is especially thought to be the case in a Winsor type I system, where the surfactants resides in the brine. As the surfactant is in the aqueous phase and is in less contact with the rock, due to the rock`s increased affinity for oil, the retention is believed to decrease. As less retention is experienced, the effect of the surfactant is believed to increase. Although the phase behavior in these experiments is not know, this may be an explanation for the better response in more oil-wet cores.

6 Conclusion

In literature, the potential for enhanced recovery with LSW has shown to be beneficial. Through this study, the potential for low salinity brine in secondary and tertiary mode, as well as in combination with a low salinity surfactant polymer (LSSP) waterflood, has been investigated.

The results of these experiments shows a lower production (1-12% OOIP) by injecting low salinity brine compared to injecting synthetic seawater in secondary mode. These results are in contradiction to most results reported in the literature. One possible explanation is that the results can be attributed to different wettability states in the cores. This can have been induced by poor wettability alteration during aging and/or wettability alteration during LSW flooding towards more water-wet state.

In tertiary mode enhanced production (5-9% ROIP) was observed in altering ion composition or reducing totalt salinity. The extra oil production was observed in some of the cores, but seems not to be reproduced in all parallel experiments. No significant change in pH was observed during the LSW injection and no fines were found in the effluent. These mechanisms are therefore not considered to cause increased recovery.

Flooding core J1 with water lacking divalent ions showed a pressure increase without enhancing the oil recovery. This is consistent with prior studies, and neglects fines migration or clay swelling being the primary mechanism for the low salinity effect. This is also supported by the previous mentioned enhanced oil recovery in tertiary mode.

A significant response to LSSP (11-32% ROIP) was observed in all cores. It is experienced that less water-wet systems respond better to LSSP than water-wet cores.

7 Further Work

Although the interest in low salinity waterflooding is increasing, there are still many aspects which needs to be further investigated.

Most importantly, it should be prioritized to understand the mechanisms prevailing during LSW floods. To achieve this, it would be beneficial to adapt a basic setup for research on COBR interactions, making it easier to compare the different results. Also, obtaining basic information about the cores and corefloods by using CT scanning, XRD diffraction, ICP analysis and electron micrographs would enhance the information available.

Another aspect which would be interesting to investigate is the impact of LSSP on reservoir cores. It has been observed that reservoir cores respond better to LSW than outcrop cores, and investigating if this also applies for LSSP would be beneficial. Additionally, this can be extended with studies of the effects of pH, wettability, pressure and temperature on LSSP.

It would be of interest to study the impact of LSW in secondary mode, especially to understand why there is observed different trends in results with respect to oil recovery. A lot of studies have been made on LSW in tertiary mode, and it would be beneficial to quantify the process improvements by LSW in secondary mode. This could be further extended to study the effects of LSW on different wettability systems in secondary mode.

References

1. Morrow, N. and Buckley, J., *Improved Oil Recovery by Low-Salinity Waterflooding.* Journal of Petroleum Technology, 2011. **63**(5): p. 112.SPE-129421-JPT
2. Alotaibi, M.B., Azmy, R., and Nasr-El-Din, H.A. *A Comprehensive EOR Study Using Low Salinity Water in Sandstone Reservoirs*. in *SPE Improved Oil Recovery Symposium*. 2010. Tulsa, Oklahoma, USA: Society of Petroleum Engineers.
3. Zolotukhin, A.B. and Ursin, J.R., *Introduction to Petroleum Reservoir Engineering*. 2000: Høyskoleforlaget, Norwegian Academic Press.
4. Anderson, W.G., *Wettability Literature Survey Part 5: The Effects of Wettability on Relative Permeability.* Journal of Petroleum Technology, 1987. **39**(11): p. 1 468.SPE-16323-PA
5. Skarestad, M. and Skauge, A., *Reservoarteknikk II , PTEK 213.* Fluid Properties and Recovery Methods, 2011
6. Atkins, P. and De Paula, J., *Physical Chemistry*. Vol. 9. 2010: W. H. Freeman.
7. Schramm, G. and Haake, G., *A practical approach to rheology and rheometry*. 1994: Haake Karlsruhe.
8. Holstein, E.D. and Lake, L.W., *Petroleum engineering handbook: Reservoir engineering and petrophysics*. Vol. 5. 2007, Richardson, TX: Society of Petroleum Engineers. viii, 1651 s. : ill. (some col.).
9. Garnes, J.M., Mathisen, A.M., Scheie, A., and Skauge, A. *Capillary Number Relations for Some North, Sea Reservoir Sandstones*. in *SPE/DOE Enhanced Oil Recovery Symposium*. 1990. Tulsa, Oklahoma, USA: Society of Petroleum Engineers.
10. Stegemeier, G.L. *Relationship of Trapped Oil Saturation to Petrophysical Properties of Porous Media*. in *SPE Improved Oil Recovery Symposium*. 1974. Tulsa, Oklahoma, USA: Society of Petroleum Engineers.
11. Lake, L.W., *Enhanced Oil Recovery*. 1989: Prentice Hall Incorporated.
12. Skauge, A., Spildo, K., Høiland, L., and Vik, B., *Theoretical and experimental evidence of different wettability classes.* Journal of Petroleum Science and Engineering, 2007. **57**(3–4): p. 321-333

13. Jerauld, G.R. and Rathmell, J.J., *Wettability and relative permeability of Prudhoe Bay: a case study in mixed-wet reservoirs.* SPE Reservoir Engineering, 1997. **12**(01): p. 65
14. Anderson, W.G., *Wettability Literature Survey-Part 6: The Effects of Wettability on Waterflooding.* Journal of Petroleum Technology, 1987. **39**(12): p. 1622.SPE-16471-PA
15. Raza, S.H., Treiber, L.E., and Archer, D.L., *Wettability of reservoir rocks and its evaluation.* Journal Name: Prod. Mon.; (United States); Journal Volume: 32:4, 1968. **32**(4): p. 2-4, 6-7
16. Agbalaka, C.C., Dandekar, A.Y., Patil, S.L., Khataniar, S., and Hemsath, J. *The Effect Of Wettability On Oil Recovery: A Review*. in *SPE Asia Pacific Oil and Gas Conference and Exhibition*. 2008. Perth, Australia: Society of Petroleum Engineers.
17. Skauge, A. and Ottesen, B. *A summary of experimentally derived relative permeability and residual saturation on North Sea reservoir cores*. in *International Symposium of the SCA*. 2002. Monterey, California, USA.
18. Craig, F.F., *The Reservoir Engineering Aspects of Waterflooding*. 1971, Dallas: Society of Petroleum Engineers of AIME.
19. Salathiel, R.A., *Oil Recovery by Surface Film Drainage In Mixed-Wettability Rocks.* Journal of Petroleum Technology, 1973. **25**(10): p. 1224.SPE-4104-PA
20. Yildiz, H.O., Valat, M., and Morrow, N.R., *Effect of Brine Composition On Wettability And Oil Recovery of a Prudhoe Bay Crude Oil.* Journal of Canadian Petroleum Technology, 1999. **38**(1).PETSOC-99-01-02
21. Buckley, J.S., Liu, Y., and Monsterleet, S., *Mechanisms of Wetting Alteration by Crude Oils.* SPE Journal, 1998. **3**(1): p. 61.SPE-37230-PA
22. Buckley, J.S. and Morrow, N.R. *Characterization of Crude Oil Wetting Behavior by Adhesion Tests*. in *SPE/DOE Enhanced Oil Recovery Symposium*. 1990. Tulsa, Oklahoma: Society of Petroleum Engineers.
23. Muskat, M., *Physical principles of oil production*. 1949: McGraw-Hill Book Co.

24. Bernard, G.G. *Effect of Floodwater Salinity on Recovery Of Oil from Cores Containing Clays*. in *SPE California Regional Meeting*. 1967. Los Angeles, California: Society of Petroleum Engineers.

25. Jadhunandan, P.P. and Morrow, N.R., *Effect of Wettability on Waterflood Recovery for Crude-Oil/Brine/Rock Systems.* SPE Reservoir Engineering, 1991. **10**(1): p. 46.SPE-22597-PA

26. Tang, G.Q. and Morrow, N.R., *Salinity, Temperature, Oil Composition, and Oil Recovery by Waterflooding.* SPE Reservoir Engineering, 1997. **12**(4): p. 276.SPE-36680-PA

27. Tang, G.Q. and Morrow, N.R., *Influence of brine composition and fines migration on crude oil/brine/rock interactions and oil recovery.* Journal of Petroleum Science and Engineering, 1999. **24**(2–4): p. 111

28. Yildiz, H.O. and Morrow, N.R., *Effect of brine composition on recovery of Moutray crude oil by waterflooding.* Journal of Petroleum Science and Engineering, 1996. **14**(3–4): p. 168

29. Zhang, Y. and Morrow, N.R. *Comparison of Secondary and Tertiary Recovery With Change in Injection Brine Composition for Crude-Oil/Sandstone Combinations*. in *SPE/DOE Symposium on Improved Oil Recovery*. 2006. Tulsa, Oklahoma, USA: Society of Petroleum Engineers.

30. Zhang, Y., Xie, X., and Morrow, N.R. *Waterflood Performance By Injection Of Brine With Different Salinity For Reservoir Cores*. in *SPE Annual Technical Conference and Exhibition*. 2007. Anaheim, California, USA: Society of Petroleum Engineers.

31. Zhou, X., Morrow, N.R., and Ma, S., *Interrelationship of Wettability, Initial Water Saturation, Aging Time, and Oil Recovery by Spontaneous Imbibition and Waterflooding.* SPE Journal, 2000. **5**(2): p. 207

32. Jadhunandan, P.P., *Effects of brine composition, crude oil and ageing conditions on wettability and oil recovery.* 1990: p. 284

33. Sharma, M.M. and Filoco, P.R., *Effect of Brine Salinity and Crude-Oil Properties on Oil Recovery and Residual Saturations.* SPE Journal, 2000. **5**(3): p. 300.SPE-65402-PA

34. Wickramathilaka, S., Morrow, N.R., and Howard, J. *Effect of Salinity on Oil Recovery by Spontaneous Imbibition*. in *International Symposium of Society*

of Core Analysts. 2010. Halifax, Nova Scotia, Canada: Society of Petroleum Engineers.

35. Al-Aulaqi, T., Fisher, Q., Grattoni, C., and Al-Hinai, S.M. *Wettability Alteration by Brine Salinity and Temperature in Reservoir Cores*. in *SPE Saudi Arabia Section Technical Symposium and Exhibition*. 2013. Khobar, Saudi Arabia: Society of Petroleum Engineers.
36. Nasralla, R.A., Alotaibi, M.B., and Nasr-El-Din, H.A. *Efficiency of Oil Recovery by Low Salinity Water Flooding in Sandstone Reservoirs*. in *SPE Western North American Region Meeting*. 2011. Anchorage, Alaska, USA.
37. Ashraf, A., Hadia, N., Torsaeter, O., and Tweheyo, M.T. *Laboratory Investigation of Low Salinity Waterflooding as Secondary Recovery Process: Effect of Wettability*. in *SPE Oil and Gas India Conference and Exhibition*. 2010. Mumbai, India: Society of Petroleum Engineers.
38. Winoto, W., Loahardjo, N., Xie, S.X., Yin, P., and Morrow, N.R. *Secondary and Tertiary Recovery of Crude Oil from Outcrop and Reservoir Rocks by Low Salinity Waterflooding*. in *SPE Improved Oil Recovery Symposium*. 2012. Tulsa, Oklahoma, USA: Society of Petroleum Engineers.
39. Lager, A., Webb, K.J., Black, C.J.J., Singleton, M., and Sorbie, K.S., *Low Salinity Oil Recovery - An Experimental Investigation.* Petrophysics, 2008. **49**(1)
40. McGuire, P.L., Chatham, J.R., Paskvan, F.K., Sommer, D.M., and Carini, F.H. *Low Salinity Oil Recovery: An Exciting New EOR Opportunity for Alaska's North Slope*. in *SPE Western Regional Meeting*. 2005. Irvine, California, USA: Society of Petroleum Engineers.
41. Siyambalagoda Gamage, P.H. and Thyne, G.D. *Comparison of Oil Recovery by Low Salinity Waterflooding in Secondary and Tertiary Recovery Modes*. in *SPE Annual Technical Conference and Exhibition*. 2011. Denver, Colorado, USA: Society of Petroleum Engineers.
42. Thyne, G.D. and Siyambalagoda Gamage, P.H. *Evaluation Of The Effect Of Low Salinity Waterflooding For 26 Fields In Wyoming*. in *SPE Annual Technical Conference and Exhibition*. 2011. Denver, Colorado, USA: Society of Petroleum Engineers.

43. Shaker Shiran, B. and Skauge, A. *Wettability and Oil Recovery by Low Salinity Injection*. in *SPE EOR Conference at Oil and Gas West Asia*. 2012. Muscat, Oman: Society of Petroleum Engineers.

44. Rivet, S., Lake, L.W., and Pope, G.A. *A Coreflood Investigation of Low-Salinity Enhanced Oil Recovery*. in *SPE Annual Technical Conference and Exhibition*. 2010. Florence, Italy: Society of Petroleum Engineers.

45. Loahardjo, N., Morrow, N.R., and Winoto, W. *Assessment of Oil Recovery by Low Salinity Waterflooding from Laboratory Tests*. in *SPE Improved Oil Recovery Symposium*. 2014. Tulsa, Oklahoma, USA: Society of Petroleum Engineers.

46. Webb, K.J., Black, C.J.J., and Al-Ajeel, H. *Low Salinity Oil Recovery - Log-Inject-Log*. in *SPE/DOE Symposium on Improved Oil Recovery*. 2004. Tulsa, Oklahoma, USA: Society of Petroleum Engineers.

47. Skrettingland, K., Holt, T., Tweheyo, M.T., and Skjevrak, I., *Snorre Low-Salinity-Water Injection--Coreflooding Experiments and Single-Well Field Pilot.* SPE Reservoir Evaluation & Engineering, 2011. **14**(2): p. 192

48. Lager, A., Webb, K.J., Collins, I.R., and Richmond, D.M. *LoSal Enhanced Oil Recovery: Evidence of Enhanced Oil Recovery at the Reservoir Scale*. in *SPE Symposium on Improved Oil Recovery*. 2008. Tulsa, Oklahoma, USA: Society of Petroleum Engineers.

49. Seccombe, J., Lager, A., Jerauld, G.R., Jhaveri, B., Buikema, T., Bassler, S., Denis, J., Webb, K.J., Cockin, A., and Fueg, E. *Demonstration of Low-Salinity EOR at Interwell Scale, Endicott Field, Alaska*. in *SPE Improved Oil Recovery Symposium*. 2010. Tulsa, Oklahoma, USA: Society of Petroleum Engineers.

50. Seccombe, J.C., Lager, A., Webb, K.J., Jerauld, G.R., and Fueg, E. *Improving Wateflood Recovery: LoSalTM EOR Field Evaluation*. in *SPE Symposium on Improved Oil Recovery*. 2008. Tulsa, Oklahoma, USA: Society of Petroleum Engineers.

51. Berg, J.C., *An Introduction to Interfaces & Colloids: The Bridge to Nanoscience*. 2010: World Scientific.

52. Nasralla, R.A. and Nasr-El-Din, H.A., *Double-Layer Expansion: Is It a Primary Mechanism of Improved Oil Recovery by Low-Salinity*

Waterflooding? SPE Reservoir Evaluation & Engineering, 2014. **17**(1): p. 59.SPE-154334-PA

53. Yousef, A.A., Al-Saleh, S., and Al-Jawfi, M.S. *Smart WaterFlooding for Carbonate Reservoirs: Salinity and Role of Ions*. in *SPE Middle East Oil and Gas Show and Conference*. 2011. Manama, Bahrain: Society of Petroleum Engineers.
54. Yousef, A.A., Al-Saleh, S., and Al-Jawfi, M.S. *The Impact of the Injection Water Chemistry on Oil Recovery from Carbonate Reservoirs*. in *SPE EOR Conference at Oil and Gas West Asia*. 2012. Muscat, Oman: Society of Petroleum Engineers.
55. Yousef, A.A., Al-Saleh, S., and Al-Jawfi, M.S. *Improved/Enhanced Oil Recovery from Carbonate Reservoirs by Tuning Injection Water Salinity and Ionic Content*. in *SPE Improved Oil Recovery Symposium*. 2012. Tulsa, Oklahoma, USA: Society of Petroleum Engineers.
56. Yousef, A.A., Al-Saleh, S., Al-Kaabi, A.U., and Al-Jawfi, M.S. *Laboratory Investigation of Novel Oil Recovery Method for Carbonate Reservoirs*. in *Canadian Unconventional Resources and International Petroleum Conference*. 2010. Calgary, Alberta, Canada: Society of Petroleum Engineers.
57. Yousef, A.A. and Ayirala, S.C. *A Novel Water Ionic Composition Optimization Technology for Smartwater Flooding Application in Carbonate Reservoirs*. in *SPE Improved Oil Recovery Symposium*. 2014. Tulsa, Oklahoma, USA: Society of Petroleum Engineers.
58. Sheng, J., *Modern Chemical Enhanced Oil Recovery: Theory and Practice*. 2010: Elsevier Science.
59. Ehrlich, R. and Wygal, R.J., *Interrelation of Crude Oil and Rock Properties With the Recovery of Oil by Caustic Waterflooding.* Society of Petroleum Engineers Journal, 1977. **17**(4): p. 270.SPE-5830-PA
60. Jerauld, G.R., Webb, K.J., Lin, C.Y., and Seccombe, J.C. *Modeling Low-Salinity Waterflooding*. in *SPE Annual Technical Conference and Exhibition*. 2006. San Antonio, Texas, USA: Society of Petroleum Engineers.
61. Sandengen, K., Tweheyo, M.T., Raphaug, M., Kjølhamar, A., Crescente, C., and Kippe, V. *Experimental Evidence of Low Salinity Water Flooding*

Yielding a More Oil-Wet Behaviour. in *Symposium of the Society of Core Analysts*. 2011. Austin, Texas, USA.

62. Fjelde, I., Asen, S., and Omekeh, A.V. *Low Salinity Water Flooding Experiments and Interpretation by Simulations*. in *SPE Improved Oil Recovery Symposium*. 2012. Tulsa, Oklahoma, USA: Society of Petroleum Engineers.
63. Morrow, N.R., *Wettability and Its Effect on Oil Recovery.* Journal of Petroleum Technology, 1990. **42**(12): p. 1484.SPE-21621-PA
64. Ligthelm, D.J., Gronsveld, J., Hofman, J., Brussee, N., Marcelis, F., and van der Linde, H. *Novel Waterflooding Strategy By Manipulation Of Injection Brine Composition*. in *EUROPEC/EAGE Conference and Exhibition*. 2009. Amsterdam, The Netherlands: Society of Petroleum Engineers.
65. Alotaibi, M.B., Nasralla, R.A., and Nasr-El-Din, H.A. *Wettability Studies Using Low-Salinity Water in Sandstone Reservoirs*. in *Offshore Technology Conference*. 2011. Houston, Texas, USA: Society of Petroleum Engineers.
66. Agbalaka, C.C., Dandekar, A.Y., Patil, S.L., Khataniar, S., and Hemsath, J.R., *Coreflooding studies to evaluate the impact of salinity and wettability on oil recovery efficiency.* Transport in Porous Media, 2009. **76**(1): p. 94
67. Vledder, P., Gonzalez, I.E., Carrera Fonseca, J.C., Wells, T., and Ligthelm, D.J. *Low Salinity Water Flooding: Proof Of Wettability Alteration On A Field Wide Scale*. in *SPE Improved Oil Recovery Symposium*. 2010. Tulsa, Oklahoma, USA: Society of Petroleum Engineers.
68. Appelo, C.A.J. and Postma, D., *Geochemistry, groundwater and pollution*. 2005: CRC Press.
69. Valocchi, A.J., Street, R.L., and Roberts, P.V., *Transport of ion-exchanging solutes in groundwater: Chromatographic theory and field simulation.* Water Resources Research, 1981. **17**(5): p. 1527
70. Arnarson, T.S. and Keil, R.G., *Mechanisms of pore water organic matter adsorption to montmorillonite.* Marine Chemistry, 2000. **71**(3): p. 320
71. Sposito, G., *The chemistry of soils*. 2008: Oxford university press.
72. Lee, S.Y., Webb, K.J., Collins, I.R., Lager, A., Clarke, S., Sullivan, M., Routh, A., and Wang, X. *Low Salinity Oil Recovery: Increasing Understanding of the*

Underlying Mechanisms. in *SPE Improved Oil Recovery Symposium*. 2010. Tulsa, Oklahoma, USA: Society of Petroleum Engineers.

73. Alagic, E. and Skauge, A., *Combined Low Salinity Brine Injection and Surfactant Flooding in Mixed−Wet Sandstone Cores.* Energy & Fuels, 2010. **24**(6): p. 3551-3559
74. Elworthy, P.H., ., Florence, A.T., and Macfarlane, C.B., *Solubilization by surface-active agents and its applications in chemistry and the biological sciences*. 1968: Chapman & Hall.
75. Mukerjee, P. and Mysels, K.J., *Critical micelle concentrations of aqueous surfactant systems*. 1971: U.S. National Bureau of Standards; for sale by the Supt. of Docs., U.S. Govt. Print. Off.
76. Burk, R.E. and Grummitt, O., *Frontiers in colloid chemistry*. Vol. 8. 1950, New York: Interscience Publishers.
77. Evans, D.F. and Wennerström, H., *The Colloidal Domain: Where Physics, Chemistry, Biology, and Technology Meet*. 1999: Wiley.
78. Israelachvilli, J., Mitchell, J., and Ninham, B., *Theory of self-assembly of hydrocarbon amphiphiles into micelles and bilayers.* Journal of the Chemical Society, Faraday Transactions 2: Molecular and Chemical Physics, 1976. **72**(9)
79. Winsor, P.A., *Solvent properties of amphiphilic compounds*. 1954: Butterworths Scientific Publications.
80. Nelson, R.C. and Pope, G.A., *Phase Relationships in Chemical Flooding.* Society of Petroleum Engineers Journal, 1978. **18**(5): p. 338.SPE-6773-PA
81. Healy, R.N., Reed, R.L., and Stenmark, D.G., *Multiphase Microemulsion Systems.* Society of Petroleum Engineers Journal, 1976. **16**(3): p. 160.SPE-5565-PA
82. Alagic, E., Spildo, K., Skauge, A., and Solbakken, J., *Effect of crude oil ageing on low salinity and low salinity surfactant flooding.* Journal of Petroleum Science and Engineering, 2011. **78**(2): p. 220-227
83. Spildo, K., Johannessen, A.M., and Skauge, A. *Low Salinity Waterflood at Reduced Capillarity*. in *SPE Improved Oil Recovery Symposium*. 2012. Tulsa, Oklahoma, USA: Society of Petroleum Engineers.

84. Johannessen, A.M. and Spildo, K., *Enhanced Oil Recovery (EOR) by Combining Surfactant with Low Salinity Injection.* Energy & Fuels, 2013. **27**(10): p. 5749
85. Riisøen, S., *Effect of combined low salinity and surfactant injection on oil recovery in aged Bentheimer sandstones at different temperatures*. 2012, Bergen: Department of Chemistry, University of Bergen. XIV, 99 s. : ill.
86. Kolnes, J., *Improved Oil Recovery*. 1993.
87. Chauveteau, G. and Zaitoun, A. *Basic rheological behavior of xanthan polysaccharide solutions in porous media: effects of pore size and polymer concentration*. in *First European Symposium on Enhanced Oil Recovery*. 1981. Bournemouth, England,: Society of Petroleum Engineers.
88. Stavland, A., Jonsbraten, H., Lohne, A., Moen, A., and Giske, N.H. *Polymer Flooding - Flow Properties in Porous Media versus Rheological Parameters*. in *SPE EUROPEC/EAGE Annual Conference and Exhibition*. 2010. Barcelona, Spain: Society of Petroleum Engineers.
89. Ayirala, S.C., Uehara-Nagamine, E., Matzakos, A.N., Chin, R.W., Doe, P.H., and van den Hoek, P.J. *A Designer Water Process for Offshore Low Salinity and Polymer Flooding Applications*. in *SPE Improved Oil Recovery Symposium*. 2010. Tulsa, Oklahoma, USA: Society of Petroleum Engineers.
90. Kozaki, C., *Efficiency of low salinity polymer flooding in sandstone cores.* 2012
91. Mohammadi, H. and Jerauld, G.R. *Mechanistic Modeling of the Benefit of Combining Polymer with Low Salinity Water for Enhanced Oil Recovery*. in *SPE Improved Oil Recovery Symposium*. 2012. Tulsa, Oklahoma, USA: Society of Petroleum Engineers.
92. Shaker Shiran, B. and Skauge, A., *Enhanced Oil Recovery (EOR) by Combined Low Salinity Water/Polymer Flooding.* Energy & Fuels, 2013. **27**(3): p. 1223-1235
93. Churcher, P.L., French, P.R., Shaw, J.C., and Schramm, L.L. *Rock Properties of Berea Sandstone, Baker Dolomite, and Indiana Limestone*. in *SPE International Symposium on Oilfield Chemistry*. 1991. Anaheim, California: Society of Petroleum Engineers.

94. Bøe, S.O., *Syre/base eigenskaper til råolje og deira innverknad på fukting i vann-olje-kvarts system.* 1998
95. Buckley, J.S., *Wetting Alteration of Solid Surfaces by Crude Oils and Their Asphaltenes.* Oil & Gas Science and Technology - Rev. IFP, 1998. **53**(3): p. 312
96. Zhao, P., Jackson, A., Britton, C., Kim, D.H., Britton, L.N., Levitt, D., and Pope, G.A. *Development of High-Performance Surfactants for Difficult Oils*. in *SPE Symposium on Improved Oil Recovery*. 2008. Tulsa, Oklahoma, USA: Society of Petroleum Engineers.
97. Mezger, T.G., *The Rheology Handbook: For Users of Rotational and Oscillatory Rheometers*. 2011: Vincentz Network.
98. Vonnegut, B., *Rotating Bubble Method for the Determination of Surface and Interfacial Tensions.* Review of Scientific Instruments, 1942. **13**(1): p. 9
99. Princen, H.M., Zia, I.Y.Z., and Mason, S.G., *Measurement of interfacial tension from the shape of a rotating drop.* Journal of colloid and interface science, 1967. **23**(1): p. 99-107
100. Bier, A., *Electrochemistry : Theory and Practice*. 2010: Hach Company.
101. Anderson, W.G., *Wettability Literature Survey- Part 1: Rock/Oil/Brine Interactions and the Effects of Core Handling on Wettability.* Journal of Petroleum Technology, 1986. **38**(10): p. 1144.SPE-13932-PA
102. Hamouda, A.A., Valderhaug, O.M., Munaev, R., and Stangeland, H. *Possible Mechanisms for Oil Recovery from Chalk and Sandstone Rocks by Low Salinity Water (LSW)*. in *SPE Improved Oil Recovery Symposium*. 2014. Tulsa, Oklahoma, USA: Society of Petroleum Engineers.
103. Boussour, S., Cissokho, M., Cordier, P., Bertin, H.J., and Hamon, G. *Oil Recovery by Low-Salinity Brine Injection: Laboratory Results on Outcrop and Reservoir Cores*. in *SPE Annual Technical Conference and Exhibition*. 2009. New Orleans, Louisiana, USA: Society of Petroleum Engineers.
104. Cissokho, M., Ahmadi, A., Bertin, H., Omari, A., and Hamon, G. *Some investigations on the role of microparticles on the low salinity process*. in *International Symposium of the Society of Core Analysts*. 2012. Aberdeen, Scotland, UK.

105. Cissokho, M., Bertin, H., Boussour, S., Cordier, P., and Hamon, G., *Low Salinity Oil Recovery On Clayey Sandstone: Experimental Study.* Petrophysics, 2010. **51**(5).SPWLA-2010-v51n5a2
106. Jones, F.O., Jr., *Influence of Chemical Composition of Water on Clay Blocking of Permeability.* Journal of Petroleum Technology, 1964. **16**(4): p. 446.SPE-631-PA
107. Mungan, N., *Permeability Reduction Through Changes in pH and Salinity.* Journal of Petroleum Technology, 1965. **17**(12): p. 1453.SPE-1283-PA
108. Cerda, C.M., *Mobilization of kaolinite fines in porous media.* Colloids and Surfaces, 1987. **27**(1–3): p. 219-241
109. Omar, A.E., *Effect of brine composition and clay content on the permeability damage of sandstone cores.* Journal of Petroleum Science and Engineering, 1990. **4**(3): p. 245-256
110. Gray, D.H. and Rex, R.W., *Formation Damage in Sandstones caused by clay dispersion and migration.* Formation Damage, SPE Reprint Series, 1990(29): p. 82-95
111. Khilar, K.C. and Fogler, H.S., *Water Sensitivity of Sandstones.* Society of Petroleum Engineers Journal, 1983. **23**(01): p. 64.SPE-10103-PA
112. Galliano, G., Federici, M., and Cavallaro, A., *Formation Damage Control: Selecting Optimum Salinity in a Waterflooding Pilot.* Journal of Canadian Petroleum Technology, 2002. **41**(2).PETSOC-02-02-04
113. Vaidya, R.N. and Fogler, H.S., *Formation damage due to colloidally induced fines migration.* Colloids and Surfaces, 1990. **50**(0): p. 215-229
114. Holm, L.W. and Robertson, S.D., *Improved Micellar/Polymer Flooding With High-pH Chemicals.* Journal of Petroleum Technology, 1981. **33**(1): p. 161 - 172.SPE-7583-PA
115. Kia, S.F., Fogler, H.S., Reed, M.G., and Vaidya, R.N., *Effect of Salt Composition on Clay Release in Berea Sandstones.* SPE Production Engineering, 1987. **2**(4): p. 283.SPE-15318-PA
116. Khilar, K.C., Vaidya, R.N., and Fogler, H.S., *Colloidally-induced fines release in porous media.* Journal of Petroleum Science and Engineering, 1990. **4**(3): p. 221

117. Solbakken, J., *An experimental study of low salinity surfactant flooding in low permeability berea sandstone*, in *Department of Chemistry*. 2010, University of Bergen: Centre for Integrated Petroleum Research (Uni CIPR).
118. Reed, R.L. and Healy, R.N., *Some physicochemical aspects of microemulsion flooding: a review.* Improved Oil Recovery by Surfactant and Polymer Flooding, 1977: p. 437
119. Mohanty, K.K. *Multiphase Flow in Porous Media: III. Oil Mobilization, Transverse Dispersion, and Wettability*. in *SPE Annual Technical Conference and Exhibition*. 1983. San Francisco, California, USA: Society of Petroleum Engineers.
120. Al-Ajmi, A., *Low Salinity Waterflood in Combination with Surfactant/Polymer; Effect of Surfactant Slug Size*, in *Department of Physics*. 2014, University of Bergen: UNI Research CIPR.

A Appendix

A.1 Fluid Properties

Table A.1: Summary of fluid properties at ambient temperature

Fluid	Density [g/cm^3]	Viscosity [cp]	pH
SSW (SW1)	1.02	1.01	7.70
3000 ppm NaCl	1.00	0.92	5.90
1/10 SSW	-	1.04	6.96
1/22 SSW	-	-	-
SW w/o Ca^{2+} & Mg^{2+} (SW2)	-	0.99	7.97
North Sea Crude oil	0.90	31.5	-
North Sea Crude + 40% octane*	0.81	3.31	-
North Sea Crude + 40% octane**	0.81	2.71	-
Marcol 152	-	63.3	-
XOF 25S	0.99	1.38	9.34
XOF 26S	0.99	1.16	4.66
1000 ppm HPAM	-	11.2	6.42
600 ppm HPAM	-	6.92	6.30
300 ppm HPAM	-	3.58	6.18
100 ppm HPAM	-	1.77	6.14

A.2 Measured rock properties

	Length [cm]	Average length [cm]	Diameter [cm]	Average diameter [cm]
J1	6.38	6.38 ± 0.01	3.835	3.8325 ± 0.01
	6.38		3.835	
	6.38		3.83	
	6.385		3.83	
J2	6.345	6.34 ± 0.01	3.83	3.82875 ± 0.01
	6.345		3.825	
	6.34		3.83	
	6.345		3.83	
J3	6.32	6.33 ± 0.01	3.825	3.825 ± 0.01
	6.325		3.825	
	6.33		3.83	
	6.325		3.82	
J4	6.25	6.3 ± 0.01	3.83	3.238 ± 0.01
	6.30		3.825	
	6.30		3.83	
	6.35		3.83	
C1	6.29	6.29 ± 0.01	3.79	3.79 ± 0.01
	6.295		3.80	
	6.30		3.79	
	6.29		3.79	
C2	6.47	6.48 ± 0.01	3.79	3.80 ± 0.01
	6.48		3.8	
	6.48		3.8	
	4.48		3.79	

A.3 Salts

Table A.2: Salt manufacturers

Salt	Manufacturer
$NaCl$	Sigma-Aldrich
Na_2SO_4	Sigma-Aldrich
$NaHCO_3$	Fluka-Chemika
KCl	Fluka-Chemika
$CaCl_2$ * $2H_2O$	Sigma-Aldrich
$MgCl_2$ * 6 H_2O	Fluka-Chemika

A.4 Density Measurements

Table A.3: Density measurements, with uncertainty ± 0.001

T (°C)	ρ_{NSCO} [g/ml]	$\rho_{diluted\ NSC}$ [g/ml]	ρ_{SW1} [g/ml]	$\rho_{3000\ ppm\ NaCL}$ [g/ml]
21	-	0.8227	1.042	-
23	0.8999	0.8115	1.024	0.9986
25	0.8982	0.8084	1.021	0.9984
27	0.8977	-	-	0.9976
29	0.8963	-	-	0.9964

Table A.4: Density measurements of surfactant and oil in equilibrium, uncertainty ± 0.001

T (°C)	$\rho_{diluted\ NSC}$ [g/ml]	XOF 25S [g/ml]	$\rho_{diluted\ NSC}$ [g/ml]	XOF 26S [g/ml]
23	0.8087	0.9987	0.8098	0.9961

A.5 pH measurements

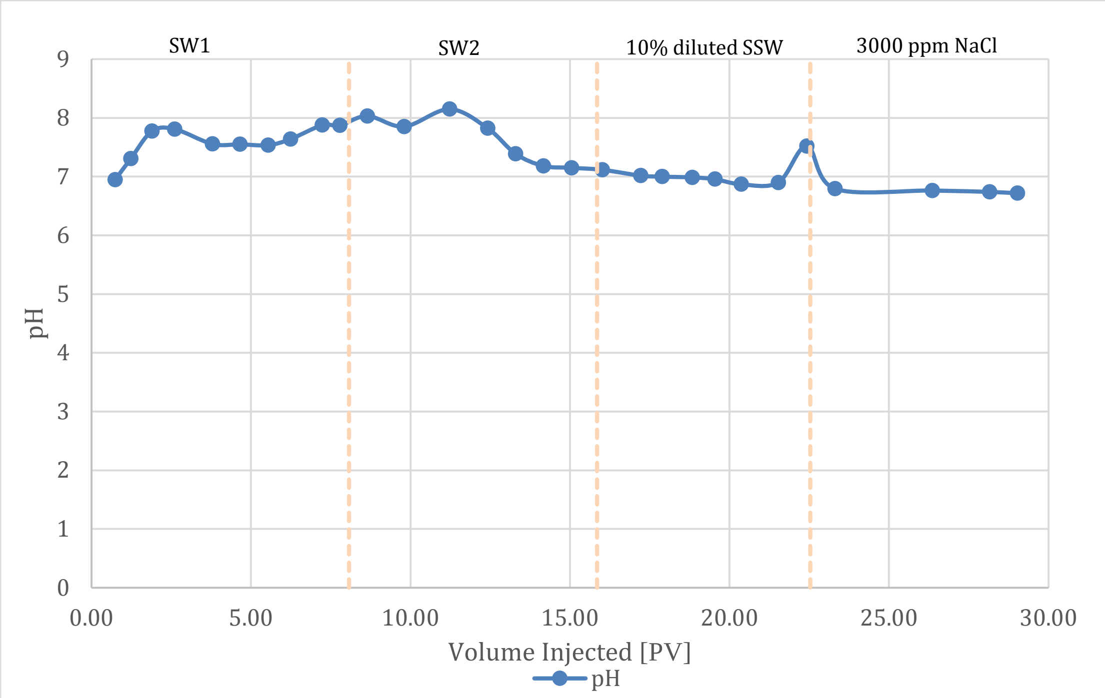

Figure A.1: pH measurements on J1 waterfloods

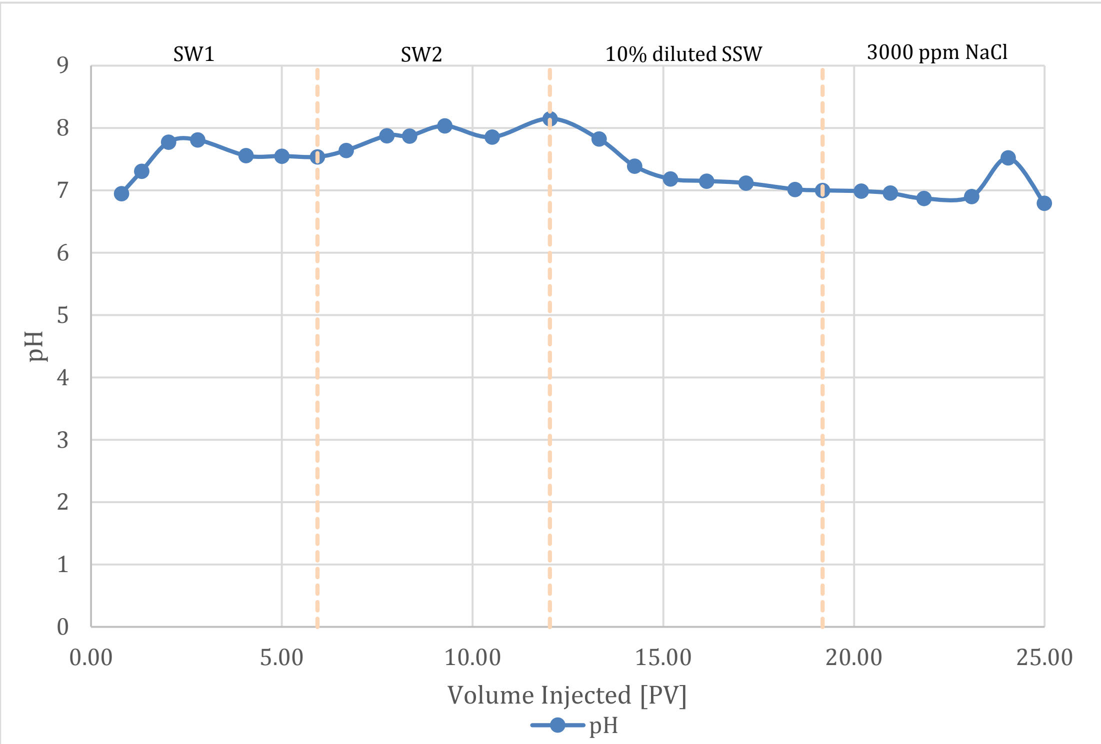

Figure A.2 pH measurements for J2 waterfloods

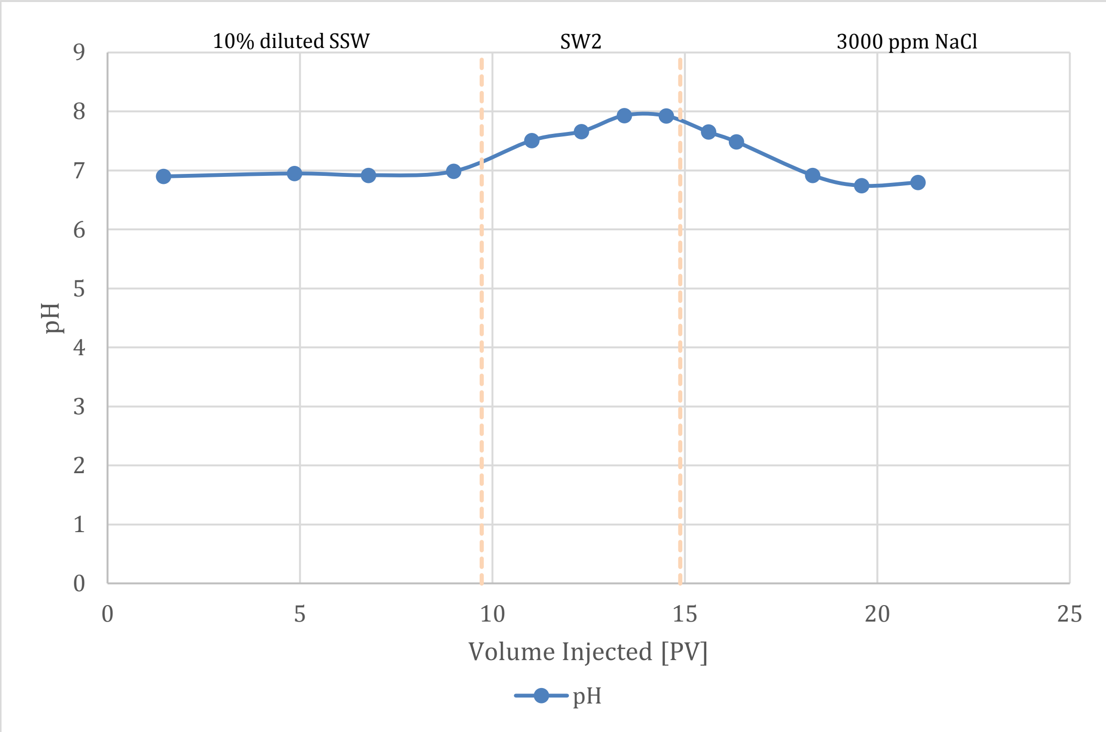

Figure A.3: pH measurements for J3 waterfloods

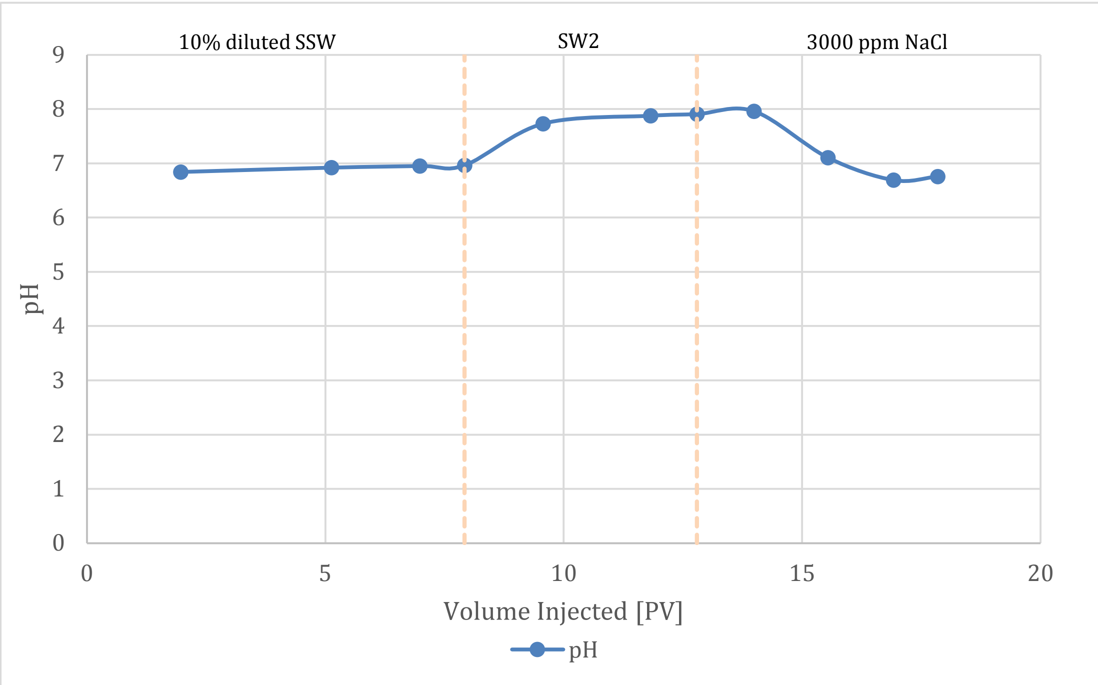

Figure A.4: pH measurements for J4 waterfloods

A.6 Viscosity Data

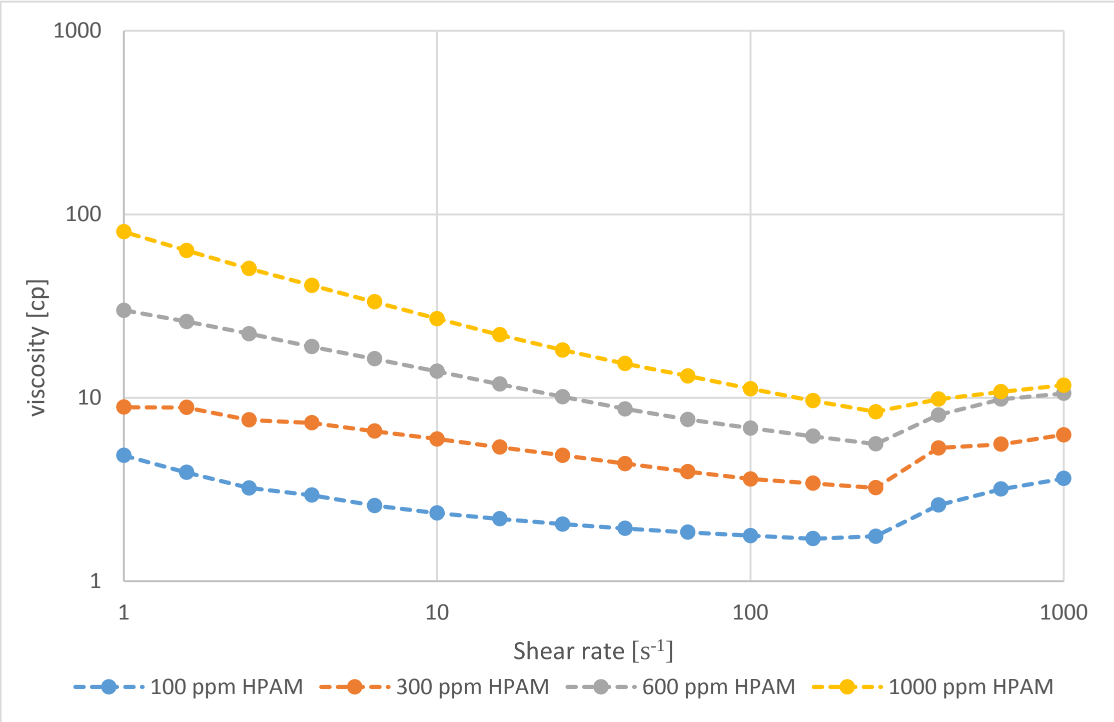

Figure A.5: Shear dependency of HPAM solutions

Table A.5: Viscosity of HPAM solutions at different shear rates

HPAM Concentration [ppm]	Shear rates [s^{-1}]			
	1	10	100	1000
100	4.85 ± 0.24	2.35 ± 0.12	1.77 ± 0.09	3.62 ± 0.18
300	8.89 ± 0.44	5.97 ± 0.30	3.61 ± 0.18	6.29 ± 0.31
600	29.96 ± 1.50	13.96 ± 0.70	6.29 ± 0.31	10.56 ± 0.53
1000	80.35 ± 4.202	26.99 ± 1.35	11.2 ± 0.56	11.71 ± 0.59

A.7 Interfacial tension

Table A.6: Interfacial tension measurements for XOF 25S

T [°C]	Rotational velocity [RPM]	$\sigma_{o/w}$ [mN/m]	$\sigma_{o/w,\ average}$ [mN/m]
23	2400	0.05859	0.04746 ± 0.009
23	3400	0.04457	
23	3900	0.04097	
23	5600	0.04572	
Pure Sample			
23	5600	0.05831	0.05831 ± 0.009

Table A.7: Interfacial tension measurements for XOF 26S

T [°C]	Rotational velocity [RPM]	$\sigma_{o/w}$ [mN/m]	$\sigma_{o/w,\ average}$ [mN/m]
23	2400	0.01487	0.01554 ± 0.002
23	2800	0.01348	
23	3400	0.01828	
Pure Sample			
23	4000	0.02931	0.02931 ± 0.002

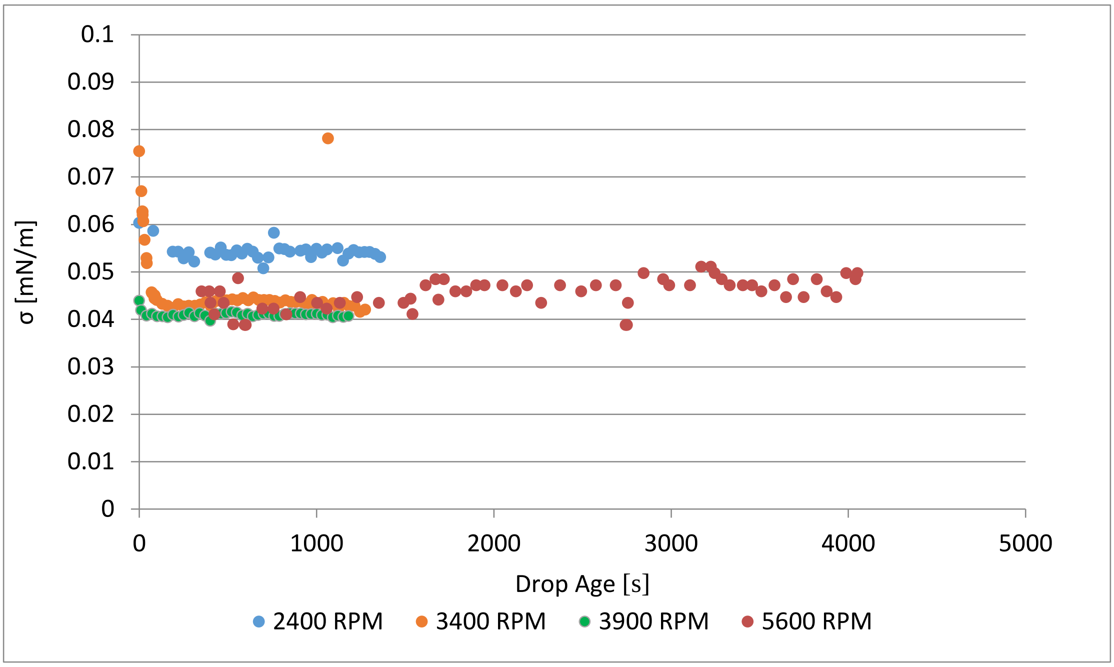

Figure A.6: Interfacial tension measurements for different rotational velocities on equilibrated XOF 25S

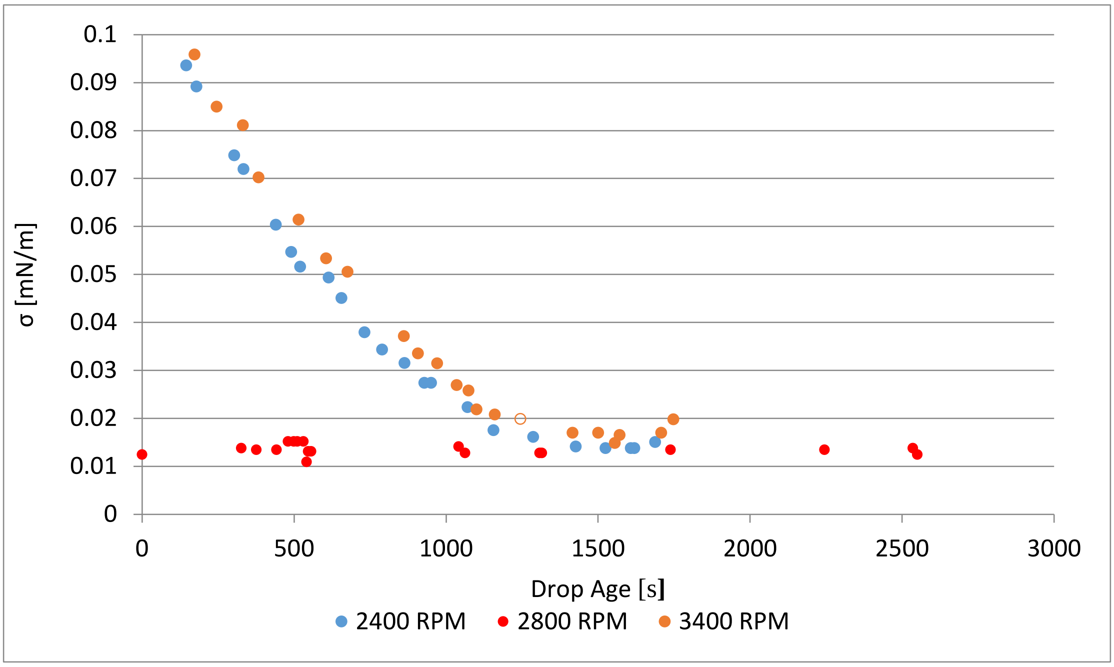

Figure A.7: Interfacial tension measurements for different rotational velocities on equilibrated XOF 26S

A.8 Experimental Production data

Table A.8: Experimental data obtained during waterfloods in J1

Rate [ml/min]	Total Injected brine [PV]	Produced Oil volumes from core [mL]	Oil Recovery [% OOIP]	Comments
	± 0.1	± 0.1	± 2.0	
SW1				
0.1	0.655	8.085	60.40	WBT
0.1	3.040	8.435	63.02	
0.5	6.570	8.775	65.56	
1	8.355	8.815	65.86	
SW2				
0.1	10.49	8.815	65.86	
0.5	13.1	8.815	65.86	
1	15.86	8.81	65.86	
10 % dilution SSW				
0.1	17.84	8.815	65.86	
0.5	20.99	8.815	65.86	
1	23.32	8.815	65.86	
3000 ppm NaCL				
0.1	25.47	8.815	65.86	
0.5	27.59	8.815	65.86	
1	29.6	8.815	65.86	
LSSP				
0.1	39.31	10.015	74.90	

Table A.9: Experimental data obtained during waterfloods in J2

Rate [ml/min]	Total Injected brine [PV]	Produced Oil volumes from core [mL]	Oil Recovery [% OOIP]	Comments
	± 0.1	± 0.1	± 2.0	
SW1				
0.1	0.61	7.72	58.39	WBT
0.1	2.79	8.16	61.72	
0.5	4.68	8.23	62.25	
1	5.93	8.23	62.25	
SW2				
0.1	7.75	8.29	62.70	
0.5	9.27	8.29	62.70	
1	12.03	8.36	63.23	
10 % dilution SSW				
0.1	15.89	8.47	64.06	
0.5	18.13	8.47	64.06	
1	19.67	8.47	64.06	
3000 ppm NaCL				
0.1	21.20	8.47	64.06	
0.5	23.08	8.47	64.06	
1	25.25	8.47	64.06	
LSSP				
0.1	33.20	9.92	75.03	

Table A.10: Experimental data obtained during waterfloods in J3

Rate [ml/min]	Total Injected brine [PV]	Produced Oil volumes from core [mL]	Oil Recovery [% OOIP]	Comments
	± 0.1	± 0.1	± 2.0	
10 % dilution SSW				
0.1	0.41	5.62	43.49	WBT
0.1	3.89	6.87	53.16	
0.5	6.25	6.87	53.16	
1	7.92	6.87	53.16	
SW2				
0.1	9.76	7.28	56.34	
0.5	11.44	7.28	56.34	
1	12.80	7.28	56.34	
3000 ppm NaCL				
0.1	14.83	7.43	57.50	
0.5	16.18	7.43	57.50	
1	17.85	7.43	57.50	
LSSP				
0.1	26.99	8.49	65.61	

Table A.11: Experimental data obtained during waterfloods in J4

Rate [ml/min]	Total Injected brine [PV]	Produced Oil volumes from core [mL]	Oil Recovery [% OOIP]	Comments
	± 0.1	± 0.1	± 2.0	
10 % dilution SSW				
0.1	0.62	7.04	55.89	WBT
0.1	4.51	7.30	57.97	
0.5	8.05	7.39	58.72	
1	9.76	7.39	58.72	
SW2				
0.1	11.74	7.39	58.72	
0.5	13.41	7.39	58.72	
1	14.88	7.39	58.72	
3000 ppm NaCL				
0.1	17.05	7.39	58.72	
0.5	19.05	7.39	58.72	
1	21.05	7.39	58.72	
LSSP				
0.1	29.40	8.38	66.59	

Table A.12: Experimental data obtained during waterfloods in C1

Rate [ml/min]	Total Injected brine [PV]	Produced Oil volumes from core [mL]	Oil Recovery [% OOIP]	Comments
	± 0.1	± 0.1	± 2.0	
SW1				
0.1	0.55	6.7	55.90	WBT
0.1	4.04	7.1	59.64	
0.5	6.92	7.1	59.64	
1	9.81	7.1	59.64	
4.5 % dilution SSW				
0.1	13.59	7.1	59.64	
0.5	16.76	7.1	59.64	
1	18.98	7.1	59.64	
LSSP (inc. NaCl preflush)				
0.1	28.44	7.65	63.85	

Table A.13: Experimental data obtained during waterfloods in C2

Rate [ml/min]	Total Injected brine [PV]	Produced Oil volumes from core [mL]	Oil Recovery [% OOIP]	Comments
	± 0.1	± 0.1	± 2.0	
4.5% diluted SSW				
0.1	0.75	7.1	57.27	WBT
0.1	3.78	7.2	58.07	
0.5	6.09	7.2	58.07	
1	9.56	7.3	58.88	
LSSP (inc. NaCl preflush)				
0.1	18.07	8.93	71.98	

A.9 LSSP Production Curves

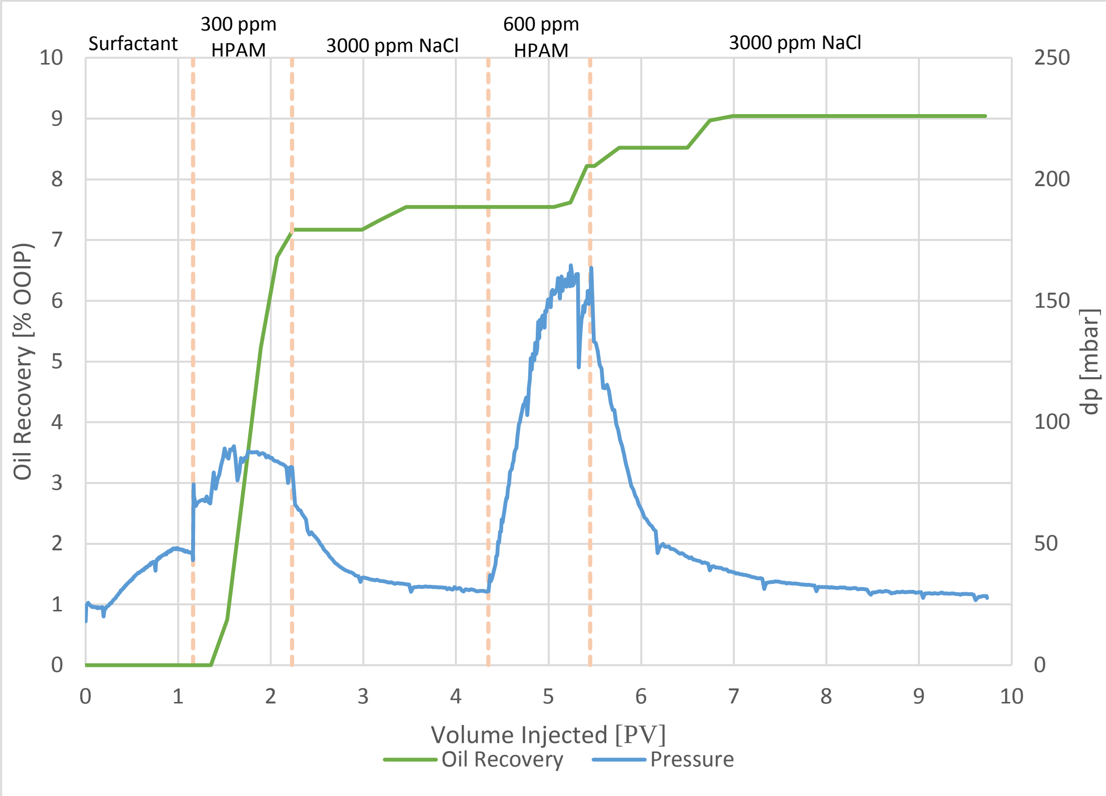

Figure A.8: LSSP waterflood J1

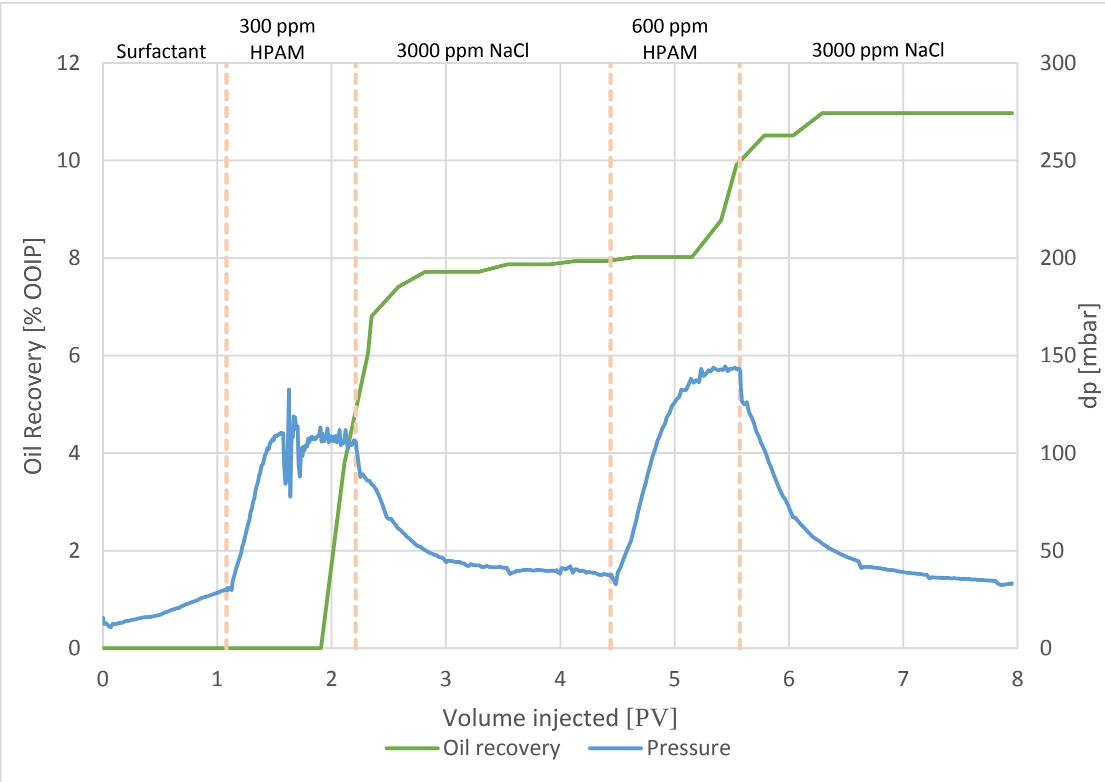

Figure A.9: LSSP waterflood J2

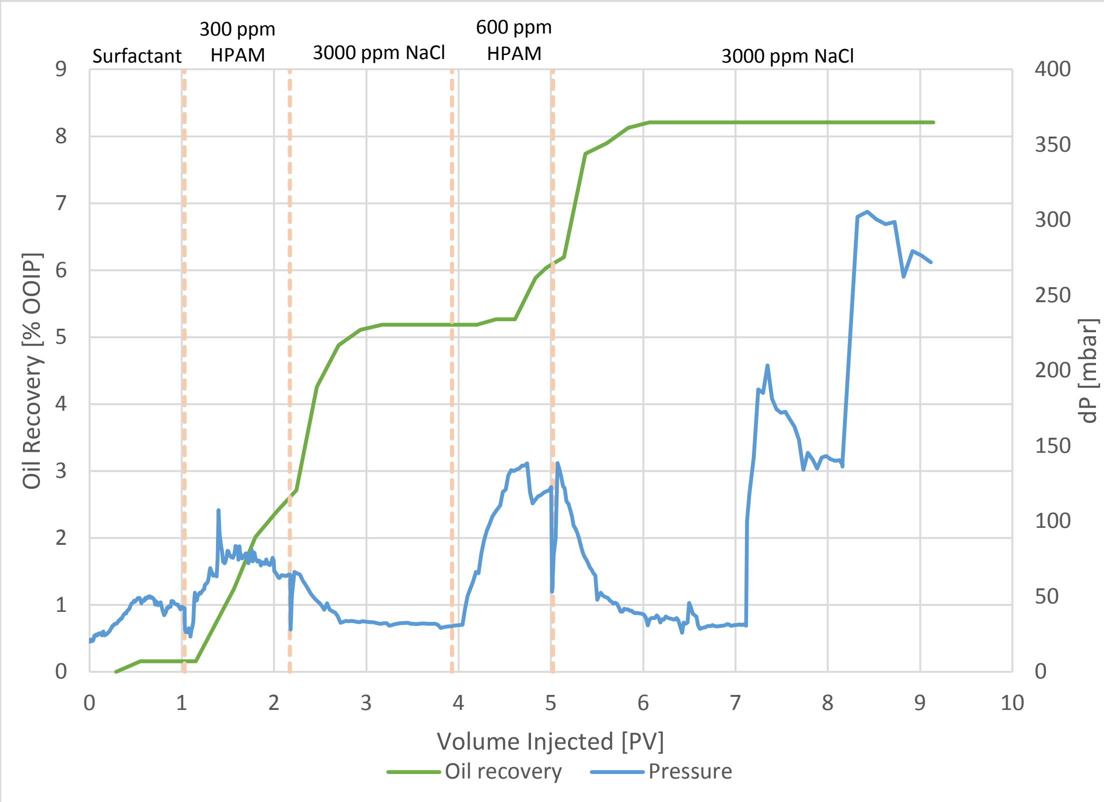

Figure A.10: LSSP waterflood in J3

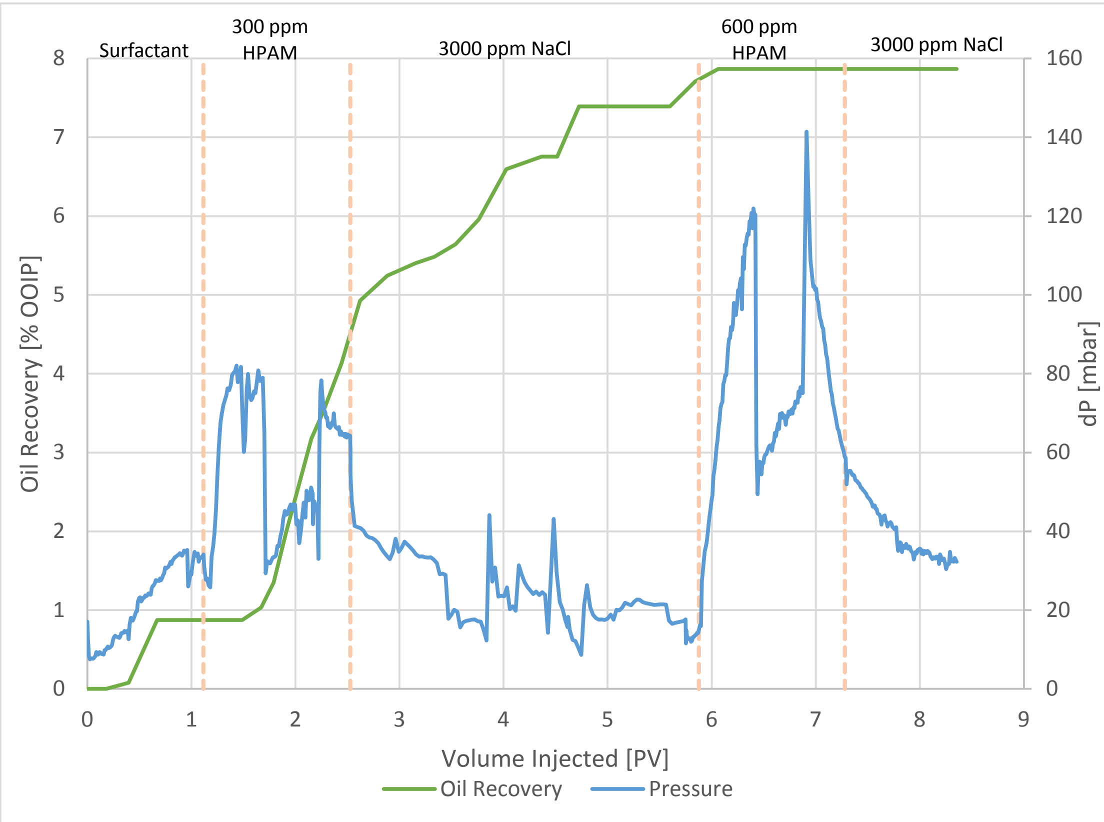

Figure A.11: LSSP waterflood in J4

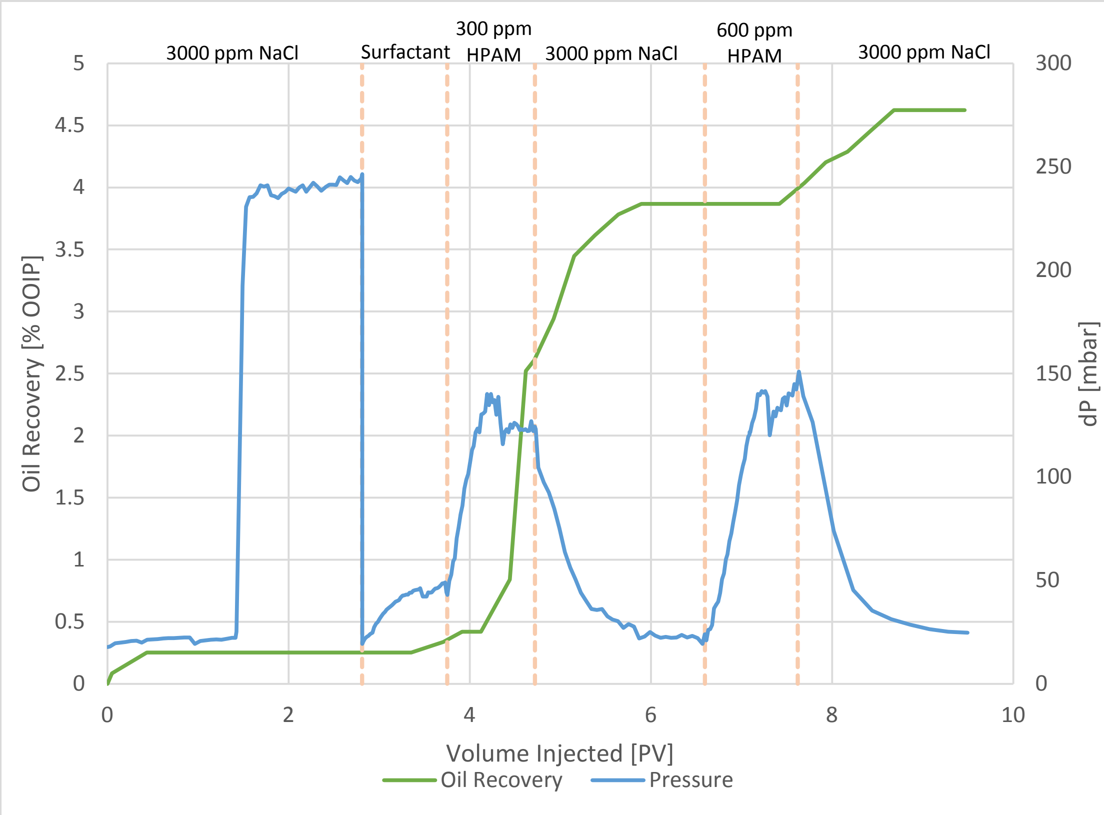

Figure A.12: LSSP Flood for C1 including NaCl preflush

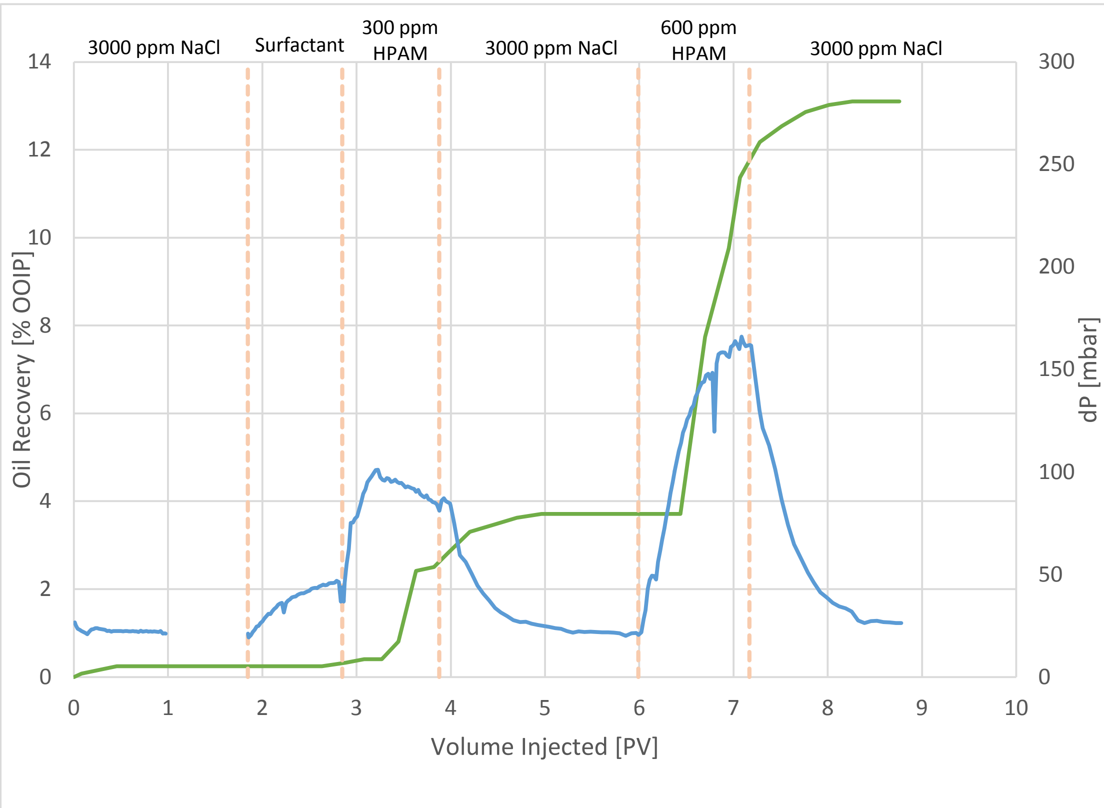

Figure A.13: LSSP Flood for C2 including NaCl preflush

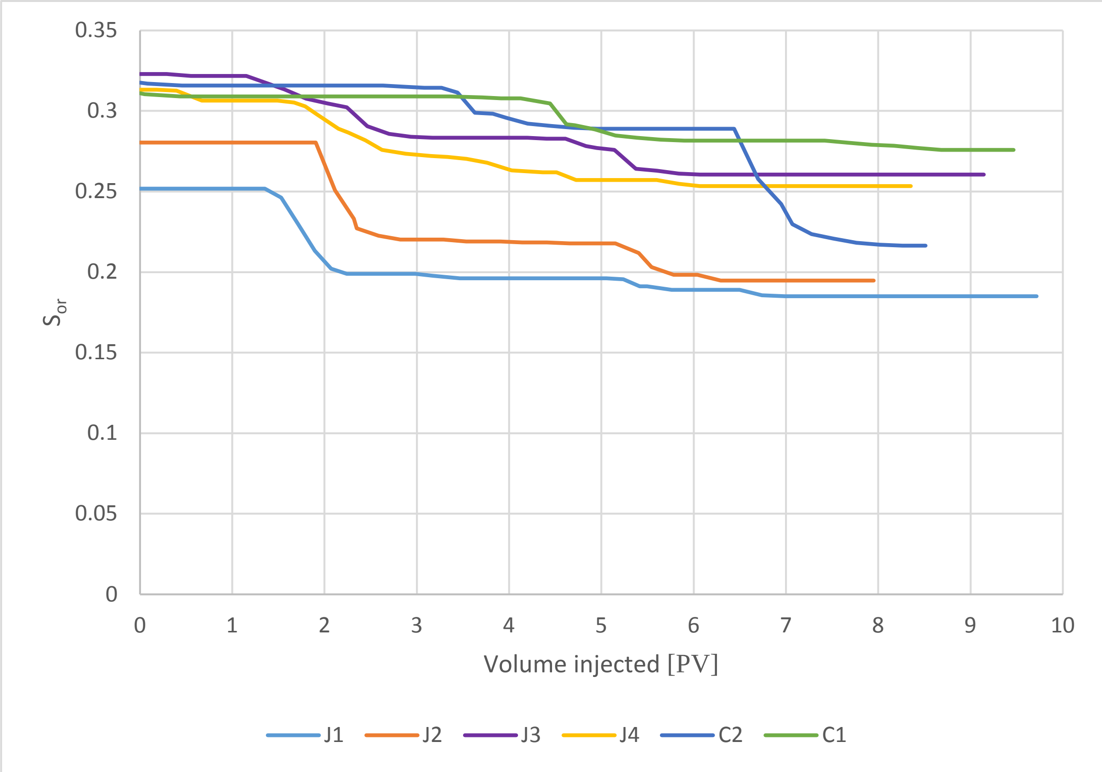

Figure A.14: Residual oil saturations during LSSP